JPRS L/10557

1 June 1982

USSR Report

PHYSICS AND MATHEMATICS

(FOUO 4/82)

FBIS FOREIGN BROADCAST INFORMATION SERVICE

FOR OFFICIAL USE ONLY

APPROVED FOR RELEASE: 2007/02/09: CIA-RDP82-00850R000500070003-6

NOTE

JPRS publications contain information primarily from foreign newspapers, periodicals and books, but also from news agency transmissions and broadcasts. Materials from foreign-language sources are translated; those from English-language sources are transcribed or reprinted, with the original phrasing and other characteristics retained.

Headlines, editorial reports, and material enclosed in brackets [] are supplied by JPRS. Processing indicators such as [Text] or [Excerpt] in the first line of each item, or following the last line of a brief, indicate how the original information was processed. Where no processing indicator is given, the information was summarized or extracted.

Unfamiliar names rendered phonetically or transliterated are enclosed in parentheses. Words or names preceded by a question mark and enclosed in parentheses were not clear in the original but have been supplied as appropriate in context. Other unattributed parenthetical notes within the body of an item originate with the source. Times within items are as given by source.

The contents of this publication in no way represent the policies, views or attitudes of the U.S. Government.

APPROVED FOR RELEASE: 2007/02/09: CIA-RDP82-00850R000500070003-6

JPRS L/10557

1 June 1982

USSR REPORT

PHYSICS AND MATHEMATICS

(FOUO 4/82)

CONTENTS

FLUID DYNAMICS

UDC 532

HEAVY LIQUID WAVES

Leningrad TEORIYA VOLN NA POVERKHNOSTI TYAZHELOY ZHIDKOSTI in Russian 1981 (signed to press 8 Apr 81) pp 2-4, 195-196

[Annotation, preface and table of contents from book "Theory of Waves on the Surface of a Heavy Liquid", by Yuriy Zosimovich Aleshkov, Izdatel'stvo Leningradskogo universiteta, 2623 copies, 196 pages]

[Text] The textbook elucidates topics of the theory of waves on the surface of a heavy liquid, and interaction between such waves and solid surfaces. Cases are examined with high-amplitude waves in the presence of depth-variable currents, with waves in shallow water from the standpoint of the nonlinear-dispersion approximation, and also questions of wave propagation on the surface of a liquid of variable depth.

For advanced university students in mechanics and mathematics courses majoring in applied mathematics and mechanics of liquids, gases and plasma.

Preface

The study of motion of a liquid with free surface and its interaction with a solid body is of considerable interest for such fields of knowledge as hydraulic engineering, geophysics and ship navigation. With this in mind, our book takes up questions of the theory of waves on the surface of a heavy liquid and their interaction with solid surfaces that may be either stationary or in arbitrary motion.

As to the nature of the liquid, it is taken as ideal and incompressible, and motion is assumed to be irrotational. In this case, quantitative evaluation of the interaction between the liquid and a solid surface is determined from solving the appropriate nonlinear boundary value problem of potential theory. Such an approach to problems of mathematical modeling of some physical effects caused by wave motion of liquid enables theoretical determination of the parameters of motion of the liquid and its force action on different obstacles.

The first chapter is introductory. It gives various forms of equations of motion of liquid, and formulates principal boundary conditions inherent in wave motions of liquid.

The second chapter is devoted to investigation of the properties of free progressive waves of finite amplitude. This topic is presented with maximum completeness for practical calculation of the parameters of such waves.

Next, the third chapter examines problems of the theory of forced traveling waves of finite amplitude. The exposition is limited to the case where steady-state waves occur on the free surface. An investigation is made of the important case of resonance of the free surface in the nonlinear approximation.

The fourth chapter outlines problems of the theory of both free and forced waves on a current that varies with depth. Conditions of existence of potential waves with such a current are explained. The solution of the problem is given with third-approximation accuracy.

The fifth chapter offers material on quantitative evaluation of the force action of high-amplitude waves on a vertical wall in the case of frontal approach of waves. This problem is generalized to the case of approach of waves of finite amplitude toward a vertical wall at an arbitrary angle in the sixth chapter.

The seventh chapter gives the derivation of equations of the theory of long waves in the three-dimensional case of a liquid of variable depth.

Problems of wave propagation in a liquid of variable depth are especially important for problems of marine hydraulic engineering. At the same time, they are very difficult in the sense of explicit construction of a solution. The eighth chapter gives an asymptotic solution of the linear problem of wave propagation on the surface of a liquid of variable depth, and also offers a solution for the problem of wave passage from one depth to another, and wave passage over a vertical barrier.

The ninth chapter examines problems of wave diffraction by vertical cylindrical surfaces. The case of wave diffraction by two arbitrarily oriented vertical walls is of particular interest for applications.

The tenth chapter presents the theory of interaction of a moving solid with a liquid of finite depth. Final results are found for the case of a slender body.

The eleventh and last chapter is devoted to questions of interaction of irregular waves with solid surfaces. The state of the sea due to wind action must as a rule be described by random functions that are solutions of the corresponding hydromechanical problems. Such an approach enables accounting for the action of wind waves on various obstacles.

The list of problems arising from interaction of waves with solid surfaces requires a number of approaches for solution. This book uses the method of the small parameter for constructing the solution of nonlinear boundary value problems, the Lyapunov-Schmidt method for studying nonlinear integral equations, the method of separation of variables, conformal mapping techniques,

the method of reducing a linear boundary value problem of elliptical type to an integral equation by the fundamental formula of the theory of harmonic functions, methods of the theory of random functions.

On the whole, the book uses analytical methods both for direct construction of a solution for the external problem of potential theory and for reducing this problem to a form convenient for using numerical methods and computers.

In accordance with the above, this book deals with the field of applied mathematics on problems of fluid dynamics. It examines deterministic and stochastic models of wave motions of a heavy liquid.

Formation of the scientific interests of the author has been considerably influenced by the works of A. I. Nekrasov, N. Ye. Kochin, L. N. Sretenskiy, Ya. I. Sekerzh-Zen'kovich and Yu. M. Krylov, who have contributed prominently to the development of wave theory. The study of their works has opened up possibilities for solving new problems of both theoretical and practical interest.

Many points of the book have been discussed directly with Professor Ya. I. Sekerzh-Zen'kovich, to whom the author is sincerely grateful for useful advice.

Contents

6610
CSO: 1862/95

UDC 621.371.255

PHASE FLUCTUATIONS OF MULTIMODE LASER FIELD IN TURBULENT ATMOSPHERE

Moscow KVANTOVAYA ELEKTRONIKA in Russian Vol 9, No 1(115), Jan 82 (manuscript received 13 Feb 81) pp 9-13

[Article by M. S. Belen'kiy and V. L. Mironov, Institute of Optics of the Atmosphere, Siberian Department, USSR Academy of Sciences, Tomsk]

[Text] A method is proposed for calculating the phase fluctuations of multimode radiation in a medium with random inhomogeneities, using the concept of average diffraction rays. An investigation is made of the influence that the initial coherence of the source field and diffraction conditions have on the radiating aperture, and the effect that turbulent conditions of propagation have on spatial structure of the phase function and on the variance of tremor of the source image. The results of theory are compared with experimental data obtained in the actual atmosphere.

Phase fluctuations of waves propagating in the atmosphere considerably limit the capabilities of various practical laser systems [Ref. 1, 2]. However, despite the fact that many sources used in systems of this kind have finite temporal and spatial scales of field coherence, phase fluctuations of partly coherent radiation in a turbulent atmosphere have not yet been calculated. This paper proposes a method of calculating phase fluctuations of a multimode laser beam in a medium with random inhomogeneities, and investigates the way that the structure function of the phase and associated variance of image tremor depend on initial source field coherence, conditions of diffraction by the radiating aperture, and turbulent conditions of propagation.

The initial distribution of the field in the plane of the radiating aperture ($x = 0$) is given in the form [Ref. 2]

$$u_0(\rho)=\exp[-\rho^2(1/2a^2+ik/2F)+iS_1(\rho)], \quad (1)$$

where a is effective beam radius, k is the wave number, F is focal length of the transmitter, $S_1(\rho)$ is random phase distributed by a normal law. The average value of phase $S_1(\rho)$ is zero, and the structure function takes the form $\frac{1}{2}D_{S_1}(\rho) = \rho^2/4\rho_k^2$. Here $2\rho_k$ is the initial spatial coherence radius of the field. Phase fluctuations of the wave in the plane of observation ($x = X$) in a turbulent atmosphere are described by the relation

$$S(X, \rho)=S_i(X, \rho)+S_t(X, \rho), \tag{2}$$

where $S_i(X, \rho)$ are random phase distortions in a homogeneous medium due to fluctuations of the field on the radiating aperture, $S_t(X, \rho)$ is random phase advance caused by turbulent inhomogeneities of the atmosphere. Formula (2) is implied by the stochastic wave equation with random boundary condition (1) when it is solved either by the method of geometric optics or by the method of smooth perturbations. As a consequence of the statistical independence of quantities S_i and S_t, the structure function of overall phase fluctuations in accordance with (2) takes the form

$$D_s(X, \rho)=D_{si}(X, \rho)+D_{st}(X, \rho). \tag{3}$$

When calculating $D_{si}(X, \rho)$ in a homogeneous field, we take consideration of the fact that for a beam with initial field distribution (1), disregarding amplitude fluctuations the relation $\Gamma_2(X, \rho)/\Gamma_2(X, 0)=\exp[-\frac{1}{2}D_{si}(X, \rho)]$ is satisfied, where Γ_2 is the mutual coherence function of the second-order field. Then as the coherence radius of the unbounded plane wave $\rho_0 \to \infty$ [$\rho_0=(1.45k^2 \times C_n^2X)^{-3/5}$, C_n^2 is the structure characteristic of fluctuations of the index of refraction], we have from the results of Ref. 3

$$^1/_2D_{si}(X, \rho)=\rho^2/4[\rho_k^2(1-X/F)^2+(X/ka)^2(1+\rho_k^2/a^2)]. \tag{4}$$

Formula (4) defines the change in structure function of the phase of a multimode laser beam in a homogeneous medium due to field diffraction by the radiating aperture.

To calculate random phase advance of the wave $S_t(X, \rho)$ due to atmospheric turbulence, we use the concept of average diffraction rays [Ref. 4, 5]. In accordance with Ref. 4, 5:

$$S_t(X, \rho_1)=\frac{1}{2}k\int_0^X \varepsilon_1(x, \rho(x))\,dx;\ \rho(X)=\rho_1, \tag{5}$$

where the ε_1 are fluctuations of permittivity of the medium at points lying on the average diffraction ray arriving at the observation point (X, ρ_1). The trajectories of rays of a multimode beam in a medium with random inhomogeneities are determined analogously [Ref. 4, 5]. In accordance with Ref. 4, 5, the solution of the nonlinear differential equation that describes the trajectories of average diffraction rays in the paraxial approximation $(\rho_1/X \ll 1)$ with accuracy to terms of order $(\rho_1/X)^2$ coincides with the expression

$$\rho(x)=\rho_1\exp\left[-\int_x^X \nu(\xi, \Omega, q, \alpha)\,d\xi\right], \tag{6}$$

where x is the instantaneous distance along the path,

$$\nu(\xi, \Omega, q, \alpha)=\frac{\xi(\alpha+2\Omega q\xi^{6/5}}{|\Omega^2+\xi^2[\alpha+^4/_3\Omega q\xi^{6/5}]|}$$

is the curvature of the average phase front of the collimated (X/F = 0) beam, $\Omega = ka_0^2/X$ is the Fresnel parameter of the radiating aperture, $q = X/k\rho_0^2$ is a parameter that characterizes turbulence intensity on the path, $\alpha = 1 + a^2/\rho_k^2$. According to Ref. 6, parameter α at the output of a laser with spherical cavity in the case of a large number of transverse modes of oscillations (N>1) can be evaluated by the formula $\alpha \cong N$.

The average diffraction rays found from relation (6) for a multimode beam under conditions of weak ($q \ll 1$) at $\Omega \ll q^{-1}$ and strong ($q \gg 1$) at $\Omega \ll \min(q, \alpha)$ intensity fluctuations are defined by the expressions

$$\rho(x) = \rho_1 \frac{[\Omega^2 + \alpha (x/X)^2]^{1/2}}{[\Omega^2 + \alpha]} \tag{7}$$

and

$$\rho(x) = \rho_1 \left[1 - \frac{\alpha}{\alpha + {}^4/_3 \Omega q x/X}\right]\left[1 - \frac{\alpha}{\alpha + {}^4/_3 \Omega q}\right]^{-1} \times \times [\alpha + {}^4/_3 \Omega q (x/X)^{6/5}]^{5/4} [\alpha + {}^4/_3 \Omega q]^{-5/4} \tag{8}$$

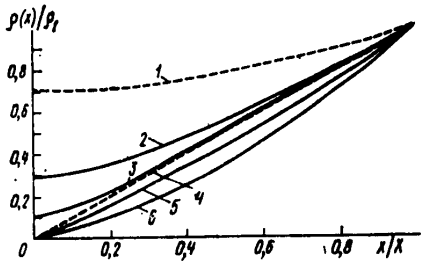

Fig. 1. Average diffraction rays of multimode laser beam (X/F = 0, Ω = 1) in turbulent atmosphere: 1--α = 1, q = 0; 2--α = 10, q = 0; 3--$\alpha = 10^2$, q = 0; 4--$\alpha = 10^4$, q = 1-10^2 or α = 1, Ω = 0; 5--α = 10, q = 10; 6--α = 1-10, $q = 10^3$

respectively. The trajectories of these rays at different parameters q, α and Ω are shown in Fig. 1. It can be seen that the spatial position and shape of the average diffraction rays of a restricted collimated beam depend on the coherent properties of the source and turbulent conditions of propagation. In particular, with increasing parameter α at $\alpha \gg \Omega q$ the beams of the multimode laser approach the rays of a spherical wave ($\rho(x) = \rho_1(x/X)$, curve 4), while under conditions of strong intensity fluctuations ($q \gg 1$), with the additional condition $\alpha q^{-1} \ll \Omega \ll q$ they become close to the limiting position of rays of a single-mode ($\alpha = 1$) beam ($\rho(x) = \rho_1(x/X^{3/2}$, curve 6). In this case, the rays of a multimode laser are situated closer to the axis of the beam even in comparison with the rays of a spherical wave.

Relations (5)-(8) enable us to calculate the spatial statistical characteristics of phase fluctuations of optical waves. To calculate time characteristics we should use the expression for random phase advance at time delayed by τ as written using the hypothesis of frozen turbulence [Ref. 1]:

$$S_1(X, \rho, \tau) = \frac{k}{2} \int_0^X \varepsilon_1 (x, \rho(x) - v_\perp(x)\tau)\, dx,$$

where $v_\perp(x)$ is the component of wind velocity across the path.

The spatial structure of the phase function of a multimode beam in a medium with Kolmogorov turbulence spectrum takes the form

$$D_{st}(X, \Omega, q, \alpha, \rho)=\gamma(\Omega, q, \alpha)D^0_{st}(X, \rho), \tag{9}$$

where $D_{st}(X, \rho)$ is the structure function of the phase of a plane wave,

$$\gamma(\Omega, q, \alpha)=\int_0^1 \exp\left[-\frac{5}{3}\int_x^X \nu(\xi, \Omega, q, \alpha)\,d\xi\right]dx. \tag{10}$$

At the special values $\Omega \to 0$, $\Omega \to \infty$, formulas (9), (10) imply known results [Ref. 1, 2] for an unbounded plane wave ($\gamma = 1$) and a spherical wave ($\gamma = 3/8$) respectively, and at $\alpha = 1$ these formulas coincide with the corresponding expressions for a single-mode beam obtained in Ref. 5, 7. In particular, it was shown in these papers that in the case of a single-mode spatially restricted beam ($\alpha = 1$, $\Omega \cong 1$) under conditions of strong intensity fluctuations ($q \gg 1$) the parameter $\gamma = 2/7$, whereas in the region of weak fluctuations ($q \ll 1$), $\gamma = 2/5$. In the case of a multimode laser $\alpha \gg 1$ at $q \gg 1$ and $\alpha q^{-1} \ll \Omega \ll q$, formula (10) also implies $\gamma = 2/7$, and when $q \ll 1$ we have

$$\gamma(\Omega, q, \alpha)=[1+\alpha\Omega^{-2}]^{-5/6}F_1(-5/6, 1/2; 3/2; -\alpha\Omega^2).$$

From this we see that with the same scatter of observation points ($\rho = \text{const}$) the structure function of the phase of a spatially limited beam in the region of strong intensity fluctuations ($q \gg 1$) is less than this quantity for both plane and spherical waves. According to Ref. 4, 5, this is due to the approach of average diffraction rays (see Fig. 1), which reduces the average phase difference at observation points.

Phase fluctuations of a wave received by an optical system cause image tremor [Ref. 1]. Using the results found above, we calculate the variance of the tremor σ^2_α which from Ref. 1 when $\rho_b \gg a_L$ (ρ_b is the average beam size in the plane of the receiver, a_L is the radius of the reception lens) is uniquely determined by the structure function of the incident wave phase. Taking our lead from Ref. 1, we get from formulas (3), (9)

$$\sigma^2_\alpha = \sigma^2_{\alpha i} + \gamma(\Omega, q, \alpha)\,\sigma^2_{\alpha 0}, \tag{11}$$

where $\sigma^2_{\alpha i}$ is variance of the tremor of the image of a fluctuating source in a homogeneous medium, $\sigma^2_{\alpha 0} = 2 \cdot 0.97/[k^2 (2a_t)^{1/3} \rho_0^{5/3}]$ is the variance of image tremor for reception of an initially coherent infinite plane wave in turbulent atmosphere. When $\alpha \gg 1$ and $\Omega \ll \alpha^2$, formula (4) is considerably simplified and takes the form $D_{si}(X, \rho) = \rho^2/2(X/ka)^2$. Here $\sigma^2_{\alpha i} = (a/X)^2/2$, where a/X is the angular size of the source.

Thus with increasing path length X, the variance of image tremor for a partly coherent source in turbulent atmosphere on the one hand decreases since $\sigma^2_{\alpha i} \sim X^{-2}$, and on the other hand increases since $\sigma^2_{\alpha 0} \sim X$. Differentiating formula (11) with respect to x, we can determine from the condition $d\sigma^2_\alpha/dx = 0$ the position of the plane of minimum termor of the image on the path. However,

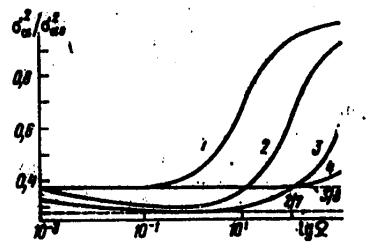

Fig. 2. Image tremor variance as a function of parameter Ω at fixed parameters q and q_k: 1--$q_k = 10$, $q = 0.1$; 2--$q_k = 0$-10, $q = 10^2$; 3--$q_k = 0$-10, $q = 10^3$; 4--$q_k = 10^4$, $q = 0.1$-10^3

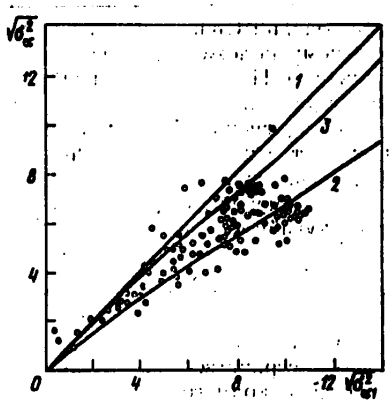

Fig. 3. Experimental data from Ref. 10 (points), straight line $\sqrt{\sigma_\alpha^2} = \sqrt{\sigma_{\alpha_1}^2}$ (1) and calculation by formulas (10-(12) at $L_0 = 1.4$ m (2) and ∞ (3)

when these results are used in practice, it should be borne in mind that formula (11) is derived without consideration [Ref. 8] of the finiteness of coherence time τ_c of the source or the response time T of the receiver. If we consider the fact that for many sources and receivers of optical radiation $\tau_c \ll T$, then the phase fluctuations $S_i(x, \rho)$ of the source will be averaged out by the receiver, and formula (11) will take the form

$$\sigma_\alpha^2 = \gamma(\Omega, q, \alpha)\,\sigma_{\alpha 0}^2. \qquad (12)$$

Relation (12) defines the variance of image tremor at arbitrary values of the parameters α, q and Ω. The special case of image tremor in reception of a single-mode beam ($\alpha = 1$) using results found in Ref. 4, 5 was considered in Ref. 9. The results of that paper follow from formula (12) at $\alpha = 1$.

Fig. 2 shows the dependence of the ratio $\sigma_\alpha^2/\sigma_{\alpha 0}^2$ on parameter Ω at different values of q and $q_k = (\alpha - 1)/\Omega$. We can see that for fixed turbulence conditions of propagation ($q \leqslant 1$) the variance of image tremor of an appreciably incoherent source (curve 4) is 2.7 times less than for a source of the same size with larger coherence radius (curve 1). Besides, we can see that under conditions of strong intensity fluctuations ($q \gg 1$), the image tremor variance in reception of spatially limited beams ($\Omega \cong 1$) is less than for either a plane wave ($\gamma = 1$) or a spherical wave ($\gamma = 3/8$). Let us note that this result cannot be obtained by the ordinary method of geometric optics (without the use of average diffraction rays) or by the method of smooth perturbations [Ref. 1, 2].

Tremor of the image of a partly coherent source in a turbulent atmosphere was experimentally studied in Ref. 10. The measurements were made with a thermal source of diameter $2r = 0.3$ mm and wavelength $\lambda = 0.5$ μm placed in the focal plane of a radiating lens with focal length $F_L = 250$ mm and angular size

of the aperture at distance X equal to $2a_L/X = 5''$. The optical measurements were accompanied by gradient measurements of parameter C_n^2 on an average height of beam propagation h = 2 m.

The measured values of $\sqrt{\sigma_\alpha^2}$ and the rms deviations $\sqrt{\sigma_{\alpha_1}^2}$ calculated from data for C_n^2 by formula (12) at the special value $\gamma = 3/8$ for path of X = 1750 m taken from Ref. 10 are shown on Fig. 3 together with theoretical curves $\sqrt{\sigma_\alpha^2} = f(\sqrt{\sigma_{\alpha_1}^2})$ computer-calculated by formulas (10), (12) at values of the parameters Ω, q and α corresponding to conditions of experiment [Ref. 10]. Curve 2 corresponds to the Kolmogorov spectrum of turbulence, curve 3 corresponds to the spectral density of fluctuations of the index of refraction of form $\Phi_n(\kappa) = 0.033C_n^2\kappa^{-11/3} \times [1 - \exp(-\kappa^2/\kappa_0^2)]$ that accounts for finiteness of the external turbulence scale L_0 ($\kappa_0 = 2\pi/L_0$).

Under the conditions of experiment [Ref. 10], $\Omega = 4$, $\alpha = 1.6 \cdot 10^3$, $1 \leqslant q \leqslant 3.0 \cdot 10^2$. The scale of ρ_k was determined from the formula $\rho_k = 0.61\lambda F_L/r$. The estimate $L_0 = 0.7h$ [Ref. 2] was used for the external turbulence scale.

It can be seen from Fig. 3 that the proposed method of calculation enables quantitative description of variance of the tremor of the image of a partly coherent source in turbulent atmosphere. The reduction of measured rms deviations of image tremor $\sqrt{\sigma_\alpha^2}$ observed in Ref. 10 as compared with the values calculated by the formula for an unbounded spherical wave (straight line *1*, $\sqrt{\sigma_\alpha^2} = \sqrt{\sigma_{\alpha_1}^2}$) is due both to the influence of the external scale of turbulence and to the curvature of the average phase front of the beam and of the associated average diffraction rays that is caused by the medium [Ref. 4, 5]. Let us note that for a single-mode laser this effect was experimentally observed in the atmosphere in Ref. 11.

REFERENCES

1. Tatarskiy, V. I., "Rasprostraneniye voln v turbulentnoy atmosfere" [Wave Propagation in Turbulent Atmosphere], Moscow, Nauka, 1967.

2. Gurvich, A. S., Kon, A. I., Mironov, V. L., Khmelevtsov, S. S., "Lazernoye izlucheniye v turbulentnoy atmosfere" [Laser Radiation in Turbulent Atmosphere], Moscow, Nauka, 1976.

3. Belen'kiy, M. S., Kon, A. I., Mironov, V. L., KVANTOVAYA ELEKTRONIKA, Vol 4, 1977, p 517.

4. Belen'kiy, M. S., Mironov, V. L., "Tezisy dokladov. Pervoye Vsesoyuznoye soveshchaniye po atmosfernoy optike" [Abstracts of Papers. First All-Union Conference on Atmospheric Optics], Part 1, Tomsk, 1976, pp 138-142.

5. Belen'kiy, M. S., Mironov, V. L., J. OPT. SOC. AMER., Vol 70, 1980, p 159.

6. Arutyunyan, A. G., Akhmanov, S. A., Golyayev, Yu. D., Tunkin, V. G., Chirkin, A. S., PIS'MA V ZHURNAL EKSPERIMENTAL'NOY I TEORETICHESKOY FIZIKI, Vol 64, 1973, p 1511.

7. Buldakov, V. M., Belen'kiy, M. S., "Tezisy dokladov. Chetvertyy Vsesoyuznyy simpozium po rasprostraneniyu lazernogo izlucheniya v atmosfere" [Abstracts of Papers. Fourth All-Union Symposium on Propagation of Laser Emission in Atmosphere], Tomsk, 1977, pp 183-187.

8. Fante, R. L., RADIO SCIENCE, Vol 12, 1977, p 223.

9. Mironov, V. L., Nosov, V. V., Chen, B. N., IZVESTIYA VYSSHIKH UCHEBNYKH ZAVEDENIY: RADIOFIZIKA, Vol 23, 1980, p 461.

10. Gurvich, A. S., Kallistratova, M. A., IZVESTIYA VYSSHIKH UCHEBNYKH ZAVEDENIY: RADIOFIZIKA, Vol 11, 1968, p 66.

11. Belen'kiy, M. S., Boronoyev, V. V., Gomboyev, N. Ts., Mironov, V. L., Trubachev, E. A., OPTIKA I SPEKTROSKOPIYA, Vol 49, 1980, p 595.

6610
CSO: 1862/114

UDC 621.375.826

CHARACTERISTICS OF THREE-PASS AMPLIFIER USING NEODYMIUM GLASS PLATE

Moscow KVANTOVAYA ELEKTRONIKA in Russian Vol 9, No 1(115), Jan 82 (manuscript received 10 Jun 81) pp 121-125

[Article by M. Ye. Brodov, V. P. Degtyareva, A. V. Ivanov, P. I. Ivashkin, V. V. Korobkin, P. P. Pashinin, A. M. Prokhorov and R. V. Serov, Physics Institute imeni P. N. Lebedev, USSR Academy of Sciences, Moscow]

[Text] An experimental study is done on the enrgy characteristics of a three-pass telescopic amplifier with neodymium glass active element. The paper gives the results of a simplified model calculation of the process of amplification of a short laser pulse in such an amplifier with compound optical arrangement. The high levels of output energy (300 J) and gain that are achieved show the promise for the use of such amplifiers in the output stages of powerful laser systems.

One of the most important problems for powerful laser systems is to improve the efficiency of using stored inversion. One of the ways to handle this problem is to use multipass amplifiers, particularly in the output stages of such systems. The advantages of multipass telescopic amplifiers make them feasible as the basis for effective amplifiers with large volume of active medium [Ref. 1, 2]. The outlook for using such amplifiers in the quasisteady state has been rather well confirmed by theory and experiment [Ref. 3-5]. Far less research has been devoted to the possibilities of telescopic amplifiers operating in a follow-up mode (for amplifying short laser pulses) [Ref. 2, 6], and more theoretical and experimental research is needed on the question of the efficacy and advisability of using them for powerful laser facilities.

The theoretical study of energy characteristics of telescopic amplifiers in the follow-up mode is a rather complicated matter as the calculation of amplification of an active medium with several intersecting and interfering waves requires simultaneous solution of equations for the electromagnetic field and the active medium. Simplifications and model approximations that are natural in such a situation require thorough substantiation and experimental verification. For example, careless calculation and selection of the parameters of a quasisteady-state telescopic amplifier is quite detrimental to its energy capabilities [Ref. 3, 5].

This paper is a report on an experimental study of the energy characteristics of a three-pass telescopic amplifier with neodymium glass active element that is the base amplifier in the powerful UMI-35 multichannel facility. The paper also gives a simplified energy model for such an amplifier, enabling optimization of some amplifier parameters.

Optical System of the Amplifier

A diagram of the base amplifier of the UMI-35 facility is shown in Fig. 1. The amplifier consists of active element 1 measuring 40 x 240 x 720 mm and a three-pass cylindrical telescope. Beam dimensions are magnified from 30 x 40 mm at the input to 210 x 40 mm at the output of the amplifier. The input beam passes the first time through active element 1 and is reflected from total-reflection cover prism 3. The front side of prism 3 has cylindrical curvature, and therefore on the second and third pass the reflected beam has cylindrical divergence along the 240-mm side of the active element. Two wedges 2 split the initial beam in two and prevent the radiation to be amplified from entering the input aperture of the amplifier. After reflection by two cover prisms 4, the now separated beam passes a third time through the amplifying medium, and then after the two cylindrical half-lenses 5 it leaves the amplifier. These half-lenses compensate for the divergence of the beams, and two parallel beams are produced at the output of the amplifier with plane phase front having dimensions of 40 x 105 mm each. The use of divergence in the amplifier makes it possible to keep the radiation flux density below the level of destruction of the glass while increasing the total beam power by amplification. On the other hand, the radiation energy density can be great enough to ensure more complete extraction of the stored inversion.

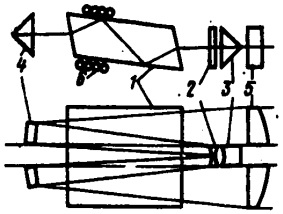

Fig. 1. Optical diagram of amplifier in side view (a) and top view (b): 1--active element; 2--wedges; 3--total-reflection cover prism with cylindrical surface; 4--cover prisms; 5--cylindrical half-lenses; 6--pumping lamps

To increase the efficiency of the amplifier and get uniform amplification along the 40-mm side, an arrangement was used with two reflections from the side surface of the active element made of GLS22 glass. The optical path of the rays in the side view and the pumping geometry are shown in Fig. 1a. pumping was by 36 IFP-8000-1 lamps (18 each on top and bottom) through the 240 x 720-mm surface of the active element. Incident on the input of the three-pass amplifier was a beam with plane phase front and uniform intensity distribution of the cross section obtained after the preamplification system of the UMI-35 facility. The laser pulse was single-frequency and had a duration of 60 ns.

Results of the Experiments

Two series of experiments were done. The energy after the first pass through the amplifier (in the first series) and after three passes (in the second series) was measured as a function of the input energy. The measurements

were done by a system of calorimeters. The relative error was reduced to ~5% by using mutual calibration of the calorimeters during the experiment. The pumping energy per lamp was 3.6 and 4.9 kJ. Let us note that in the second series of experiments, a photochromic filter with initial transmission of 30% was placed in front of prisms 4 to prevent self-excitation of the amplifier with 4.9 J pumping.

The gain K_1 on the first pass, and K on three passes were taken as the ratios Q_1/Q_0 and Q_3/Q_0, where Q_0 is input energy, Q_1 and Q_3 are the energies after one and three passes respectively.

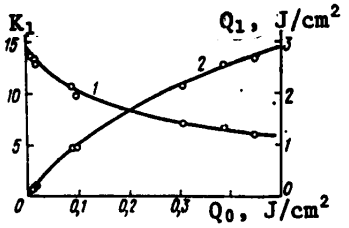

Fig. 2. Gain (1) and energy density (2) after first pass in amplifier as functions of input energy density with pumping at 3.6 kJ per lamp; experiment (points) and calculation for $\sigma = 5 \cdot 10^{-20}$ cm^2 (solid curves)

Results of measurements of gain after the first pass with 3.6 kJ pumping are shown in Fig. 2. It can be seen that gain falls from ~14.5 in a weak field to ~6 at input energy density of 0.5 J/cm^2. The results of energy density measurements after three passes as a function of the input energy density are shown in Fig. 3 for the same pumping. The total gain is $K \approx 3000$ in a weak field, and ~45 at input energy density of 0.5 J/cm^2.

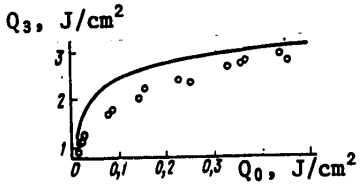

Fig. 3. Experimental (points) and theoretical (solid curve) plots of energy density at the amplifier output as a function of input energy at pumping of 3.6 kJ per lamp

At input energy of 4.5 J and pumping of 3.6 J per lamp, the output energy of the amplifier was 200 J. When pumping was increased to 4.9 kJ per lamp and a photochromic filter was included (as mentioned above), an output energy of 3000 J was obtained at the same input energy.

It is important for further optimization of multipass telescopic amplifiers, including for selecting the optimum telescope magnification, type of glass and so on, to develop methods of calculating such amplifiers that would give good agreement with experiment.

Method of Calculating Amplifier

As can be seen from the optical diagram shown in Fig. 1, exact calculation of the amplifier is a complicated problem because of the presence of three-dimensional regions with intersection of two and four diverging beams. To describe the process of radiation amplification in a three-pass optical arrangement we use certain simplifications that reduce the equations to one-dimensional equations.

The process of amplification of a light pulse that is short compared with the time of pumping and relaxation of the upper laser level when passing through the active medium in the simplest case is described by equation [from Ref. 8]

$$\frac{d\Phi}{dx} = \Delta(x)[1-\exp(-\sigma\Phi)]-\beta\Phi, \qquad (1)$$

where $\Phi(x)$ is the number of photons passing through a unit of area with coordinate x during the pulse; $\Delta(x)$ is initial inversion; σ is the induced radiation cross section; β is the coefficient of inactive absorption. Using the results of Ref. 9 and assuming that the amplitudes of two waves are equal for regions of intersection of two beams, we get the following equation with consideration of their interference:

$$\frac{d\Phi}{dx} = \frac{\Delta(x)}{2}\left[1-I_0(2\sigma\Phi)\exp(-2\sigma\Phi)\right]-\beta\Phi, \qquad (2)$$

where $I_0(2\sigma\Phi)$ is a Bessel function.

If we disregard interference in equation (2), we can write it as

$$\frac{d\Phi}{dx} = \frac{\Delta(x)}{2}[1-\exp(-2\sigma\Phi)]-\beta\Phi. \qquad (3)$$

Calculations show that equation (2) by comparison with (3) gives a correction in the gain on the first pass of approximately 5% at energy densities typical of our experiments.

In theoretical calculations of the first pass of the pulse, equations (1) and (2) were used for regions without intersection and with intersection waves respectively. In numerical integration, technical data for β were used, and consideration was taken of the transverse distribution of inversion in the active element as previously measured in independent experiments [Ref. 7].

Generalization of equations (1) and (2) with transition from one pass to a three-pass arrangement of an amplifier with cylindrical divergence reduces to the necessity of accounting for two factors: the divergence on the second and third pass, and the presence of regions where four beams intersect in a complicated three-dimensional configuration.

Divergence can be simply accounted for by adding another term to the second member of equations (1) and (2) $[-\Phi/(x_0+x)]$ that describes cylindrical divergence:

$$\frac{d\Phi}{dx} = \Delta[1-\exp(-\sigma\Phi)]-\beta\Phi-\frac{\Phi}{x_0+x}; \qquad (4)$$

$$\frac{d\Phi}{dx} = \frac{\Delta}{2}[1-I_0(2\sigma\Phi)\exp(-2\sigma\Phi)]-\beta\Phi-\frac{\Phi}{x_0+x}, \qquad (5)$$

where x_0+x is the radius of the cylindrical wavefront in the amplifying medium, and x_0 is determined by the parameters of the optical cavity.

In regions where four waves intersect, we can write an equation analogous to (5) for two waves:

$$\frac{d\Phi}{dx} = \frac{\Delta}{4}[1 - I_0^2(2\sigma\Phi)\exp(-4\sigma\Phi)] - \beta\Phi - \frac{\Phi}{x_0 + x}. \qquad (6)$$

Here we have made the simplifying assumption that only two pairs of waves are interfering. The formalism of accounting for the complex configuration of three-dimensional regions of intersection reduces to the following simplification in our calculations. A single calculation is done for the second and third passes by equations (4) and (5) without considering the intersection of these passes. Then another calculation is done by equations (5) and (6), assuming total overlap of the second and third passes. The final output energy density q_3 is obtained by averaging these results with specific weight proportional to the volume of the regions with and without intersection. (Such a simplification seems feasible since the regions of intersection of four waves occupy a small part of the volume of the amplifying medium, and besides the beams intersect at small angles.)

Discussion of the Results

Specific calculation of the first pass in the amplifier was done by formulas (1) and (2) where the free parameter was the cross section of the induced transition. Best agreement with experiment is obtained for $\sigma = 5 \cdot 10^{-20}$ cm^2 (see Fig. 2). We were prompted to vary σ in matching experimental data with calculated results by some scatter of the results of measurements of the cross section of indu ed transition by different methods [Ref. 10-12]. Besides, we did our calculations of the first pass by using the model of variable σ proposed in Ref. 10:

$$\sigma = \ln(1 + \sigma_0\Phi)/\Phi. \qquad (7)$$

By varying σ_0 in this case, we were also able to get agreement between experiment and calculation at $\sigma_0 = 3.5 \cdot 10^{-20}$ cm^2, which differs from the $\sigma_0 = 5 \cdot 10^{-20}$ cm^2 obtained for glass of the same grade (GLS22) in Ref. 10 by the method of measuring the luminescence with depopulation of inversion by a laser pulse.

The problem of the cross section for the stimulated transition is very important from the standpoint of determining the energy stored in the amplifying medium. Therefore to get this quantity more exactly, and consequently determine the maximum energy that can be taken from the laser amplifier, more experimental and theoretical research is needed.

Summing up, we can say that for the first pass of our amplifier at an input energy of 1 J/cm^2 the output energy undergoes saturation, i. e. a considerable fraction of the stored energy is converted to radiation.

A second consequence of this stage of measurements and calculations can be taken as their satisfactory agreement, which justifies the chosen computational scheme and enables complete calculation of a three-pass amplifier. The results of such calculation with the use of equations (4)-(6) are given together with experimental results on Fig. 3. Agreement can be considered

satisfactory. Some difference between experimental and calculated plots can be attributed to approximation in accounting for interference and the induced transition cross section, as well as to possible reduction of inversion due to amplification of luminescence. The results show the good outlook for using telescopic amplifiers in powerful laser systems with short radiation pulse.

In conclusion, the authors are sincerely grateful to V. V. Ravdin, Yu. N. Sidorenkov and V. I. Chernomyrdin for assisting with the experiments.

REFERENCES

1. Anan'yev, Yu. A., KVANTOVAYA ELEKTRONIKA, Vol 6, 1971, p 3.

2. Zverev, V. A., Kulikov, V. Ya., Ovchinnikov, V. M., Shagal, A. M., OPTIKO-MEKHANICHESKAYA PROMYSHLENNOST', No 6, 1978, p 25.

3. Gorlanov, A. V., Kalinina, A. A., Lyubimov, V. V., Orlova, I. B., Petrov, V. F., ZHURNAL PRIKLADNOY SPEKTROSKOPII, Vol 17, 1972, p 617.

4. Anan'yev, Yu. A., Sherstobitov, V. Ye., ZHURNAL TEKHNICHESKOY FIZIKI, Vol 43, 1973, p 1014.

5. Anan'yev, Yu. A., Koval'chuk, L. V., Sherstobitov, V. Ye., KVANTOVAYA ELEKTRONIKA, Vol 3, 1976, p 1412.

6. Vartapetov, S. K., Vovchenko, V. I., Krasyuk, I. K., Pashinin, P. P., "Tezisy dokladov. Pervaya Vsesoyuznaya konferentsiya 'Optika lazerov'" [Abstracts of Papers. First All-Union Conference on Laser Optics], Leningrad, 1977.

7. Brodov, M. Ye., Gavrilov, N. I., Ivashkin, P. I., Korobkin, V. V., Nikolayevskiy, V. G., Serov, R. V., KVANTOVAYA ELEKTRONIKA, Vol 5, 1978, p 1072.

8. Mikayelyan, A. A., Ter-Mikayelyan, M. L., Turkov, Yu. G., "Opticheskiye generatory na tverdom tele" [Solid-State Lasers], Moscow, Sov. radio, ±967.

9. Arutyunyan, V. M., ZHURNAL EKSPERIMENTAL'NOY I TEORETICHESKOY FIZIKI, Vol 536, 1967, p 183.

10. Rudnitskiy, Yu. P., Smirnov, R. V., Sokolov, V. I., Preprint IAE-3094, Institute of Atomic Energy imeni I. V. Kurchatov.

11. Dianov, Ye. M., Karasik, A. Ya., Korniyenko, A. S., Prokhorov, A. M., Shcherbakov, I. A., KVANTOVAYA ELEKTRONIKA, Vol 2, 1975, p 1665.

12. Avakyants, L. I., Buzhinskiy, I. M., Koryagina, Ye. I., Surkova, V. F., KVANTOVAYA ELEKTRONIKA, Vol 5, 1978, p 725.

6610
CSO: 1862/114

UDC 658.328.2:621.3.038.8.004.1

SAFE OPERATION OF LASER INSTALLATIONS

Moscow BEZOPASNOST' PRI EKSPLUATATSII LAZERNYKH USTANOVOK in Russian 1981 (signed to press 30 Apr 81) pp 2-5, 113

[Annotation, foreword and table of contents from book "Safe Operation of Laser Installations", by Boris Nikolayevich Rakhmanov and Yevgeniy Dmitriyevich Chistov, Izdatel'stvo "Mashinostroyeniye", 7000 copies, 113 pages]

[Text] ANNOTATION

The results of investigations on the problem of safe operation of lasers are systematized for the first time in Soviet literature. The specific applications of lasers in industry, the biological effect of laser emission and protection from this type of radiation are considered. The characteristics of reflected laser emission and air-dispersed systems are presented. Data are presented on the personal protection system of personnel engaged in operating lasers. The book is intended for a wide range of specialists involved in operation of laser installations and also workers of safety services of industrial enterprises and the state sanitary inspection.

FOREWORD

During the past few years production processes based on local heating of material to be treated by laser emission* have gained considerable development. According to the estimate of specialists, laser technology will become one of the leading technologies in the future.

Continuous expansion of the application of laser installations in different areas of human activity is related to recruitment of a large number of personnel for servicing them. Along with the unique properties and advantages over other equipment used for similar purposes, laser installations represent a specific hazard to the health of maintenance personnel.

---

*The term "laser" means "light amplification using stimulated emission." The word consists of the initial letters of the English phrase Light Amplification by Stimulated Emission of Radiation--Laser. This term is now accepted in Soviet and foreign literature.

Laser emission is a new physical factor which does not at present represent such a hazard as air pollution by chemical and radioactive substances or high- and superhigh frequency radio wave generation. This circumstance is related to localization of beams of laser emission in limited spaces. However, medical and biological research carried out in the USSR and abroad indicates the potential hazard of direct and reflected laser emission to the human organism and primarily to the eyes. Accompanying hazardous and harmful production factors--radiation of pumping lamps, electromagnetic fields, noise, noxious chemical substances released from laser installations and targets, X-radiation, plasma phenomena and so on--occur during operation of laser installations. Thus, one can be subjected to the combined effects of various hazardous and harmful production factors which, together with laser emission, comprise a hygienic background under which laser operation occurs.

The problem of laser safety was first posed in 1968 in [38], where the complex approach to study of hazardous and harmful production factors was indicated and this problem was then supplemented considerably and developed in [27].

Laser production installations generate non-ionizing radiation with energy below 10 keV, which has a different nature of interaction with materials than ionizing radiation. At the same time, the operation of powerful and superpowerful lasers may be accompanied by the development of ionizing radiation. A special working group was assigned the task of analyzing the status of protection against nonionizing radiation (including that from laser emission) at the Third International Congress on Radiation Protection (Washington, D. C., 1973), organized by the International Radiation Protection Association (IRPA). The conclusions on the work of the group of specialists were outlined at the European Congress of IRPA (1975), which can be formulated in the following manner: use of apparatus that generates non-ionizing radiation leads to increased hazard of workers being irradiated; the effect of this type of radiation on the health of personnel has been little studied; the requirements on protection and practical safety guidelines are frequently based on criteria differing considerably in different countries; international cooperation similar to that existing in the field of protection against ionizing radiation is required.

The need to work out universal principles of protection against non-ionizing radiation and also criteria, standards, definitions of basic concepts and the maximum permissible levels of non-ionizing (laser) radiation was pointed out at the Fourth International Congress of IRPA (Paris, 1977). Similar problems were discussed in our country (Odessa, 1977).

The rapid rates of introducing laser installations into the national economy contributed to intensive research being conducted in the field of safe operation of these installations.

A special-purpose study of hazardous sources when using research and industrial laser installations was required to solve the problems that arose. The basic requirements of safety on installation and operation were formulated during development of the first industrial lasers. Therefore, introduction of production processes using laser installations was developed on the basis that included aspects of laser safety.

It should be noted that the use of lasers in new production processes is characterized by the initial phase in development of laser technology. During the next few years the sphere of influence of lasers will be expanded continuously and new designs of laser installations will be developed. Therefore, it is quite natural to expect both the appearance of additional hazardous and harmful production factors and the manifestation to a greater degree of already existing factors, which represent no hazard at present.

There are no special papers devoted to the problem of laser safety in Soviet and foreign literature. However, today's requirements indicate a need for such a publication. In this regard the authors of this book have taken on themselves the labor of generalizing and systematizing the results of Soviet and foreign research and of characterizing the current state of the problem of providing safe working conditions when working with lasers.

The authors will be grateful to all who express their opinion of the given book, they will be grateful for comments and wishes and will take them into account in their further work on this problem. It is requested that comments and wishes be sent to Izdatel'stvo "Mashinostroyeniye" at the address: 107076, Moscow, B-76, Stromynskiy pereulok, 4.

CONTENTS

6521
CSO: 1862/104

UDC 628.371+535.05

INVESTIGATION OF He-Xe PLASMA RECOMBINATION LASER STIMULATED BY LASER PULSES WITH $\lambda = 10.6$ μm

Moscow KVANTOVAYA ELEKTRONIKA in Russian Vol 9, No 1(115), Jan 82 (manuscript received 29 Apr 81) pp 92-98

[Article by V. A. Danilychev, V. D. Zvorykin, I. V. Kholin and A. Yu. Chugunov, Physics Institute imeni P. N. Lebedev, USSR Academy of Sciences, Moscow]

[Text] An experimental study is done on the IR lasing characteristics of a recombination laser in which the working mixture is the plasma produced in optical breakdown of a mixture of helium and xenon by CO_2 pulsed laser emission. Lasing was observed on four transitions of Xe I ($\lambda = 2.03$, 2.65, 3.43 and 3.65 μm) when it is contained in the mixture in amounts of 0.005-1.3% at a total pressure of 20-760 mm Hg. It is shown that population inversion arises due to heating of the gas in the wave of absorption of laser emission and subsequent rapid adiabatic cooling of the resultant plasma during expansion. An investigation is made of the way that the lasing parameters depend on concurrent gasdynamic processes.

Introduction

Population inversion in a nonequilibrium intensely recombining plasma is of considerable interest for developing new types of lasers that emit in the XUV and x-ray bands, lasers with nuclear pumping, enabling conversion of the energy released in a reactor to coherent emission, powerful lasers with excitation by electron beam or hard ionizing radiation and the like [Ref. 1]. One of the methods of getting a dense nonequilibrium plasma is to heat a vaporized solid or gas by a powerful laser pulse followed by rapid cooling of the resultant plasma as it expands into a vacuum or into the ambient gas [Ref. 2, 3]. Induced emission in such a supercooled plasma upon recombination of singly ionized ions and electrons has been observed in mixtures of gases Ar, Kr and Xe with He [Ref. 4] and also in Cd vapor [Ref. 5]. However, many important relations of the output parameters of the recombination laser, and in particular the way that these parameters depend on plasma heating conditions and on the gasdynamic processes taking place in the gas have not been duly explained.

In this paper a detailed investigation is made of the emission characteristics of a recombination laser in which the active medium is the plasma produced in optical breakdown of He-Xe mixture close to the surface of an aluminum target by radiation of a powerful pulsed CO_2 laser [Ref. 6].

Lasing in a recombination arrangement on infrared transitions between the upper states of the Xe atom has been achieved recently in a different experimental facility upon excitation of the He-Xe mixture at high pressure (up to several atmospheres) by a rapid transverse electric discharge [Ref. 7], upon nuclear pumping by ^{235}U fission fragments [Ref. 8, 9] and by products of the reaction $^{3}He(n, p)^{3}H$ [Ref. 10, 11], and also upon expansion of plasmoids produced in a hypocycloidal pinch [Ref. 12].

2. Experimental Facility

A diagram of the experiments is shown in Fig. 1. The emission pulse of an electron-beam-controlled CO_2 laser with energy of $E \leqslant 30$ J and half-amplitude duration of $\tau \cong 150$ ns (~250 ns on the base) (see Fig. 2a) was focused by cylindrical NaCl lens 1 ($F = 150$ mm) on the surface of aluminum target 2 in a strip 1.5 mm wide with length $l \leqslant 95$ mm. The target was accommodated in a hermetically sealed chamber (not shown on the diagram) filled with He-Xe mixture with concentration ratio from 19000:1 to 76:1 and total pressure from 10 to 760 mm Hg. The emission of the plasma arising near the target was coupled out along its axis through LiF side windows in the chamber set at the Brewster's angle. The optical cavity of the plasma laser 0.8 m long was formed by opaque spherical mirror 3 with radius of curvature of 3 m and semitransparent dielectric mirror 4 with reflectivity of ~90% in the near infrared region of the spectrum, sputtered on a lithium fluoride backing. The energy and shape of the lasing pulse were measured by a sensitive calorimeter and FD9E-111 gremanium photodiode with time resolution of ~0.1 μs. The lasing spectrum was studied by an MDR-2 monochromator with diffraction grating of 100 lines/mm and by calorimeter. The absolute error of wavelength measurement was no more than ±0.01 μm.

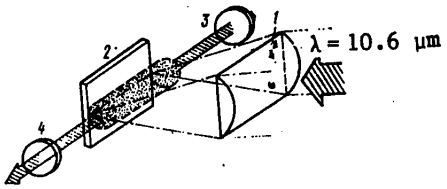

Fig. 1. Diagram of the experiments: 1--cylindrical NaCl lens; 2--aluminum target; 3--opaque mirror of the plasma laser cavity; 4--semitransparent cavity mirror

3. Results of Experiments

Fig. 2 shows oscillograms of the laser pulse on $\lambda = 10.6$ μm that heats the plasma (pulse shape was registered by a gremanium detector with time resolution of ~1 ns), the pulse of plasma self-radiation in a broad spectral range of 0.4-2 μm determined by the sensitivity range of the photodiode, and the pulse of induced plasma radiation on $\lambda = 2.03$ μm. To isolate this last pulse from the wide-band thermal radiation of the plasma, the photodiode was covered with germanium foil transparent to

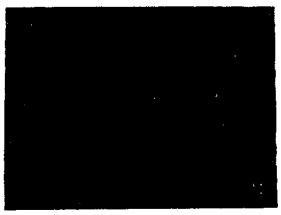

Fig. 2. Oscillograms of CO_2 laser pulse (*а*), 0.4-2 μm thermal emission of plasma (*б*), 2.03 μm plasma emission (*в*); 1 μs/div

radiation with $\lambda \geqslant 1.8$ μm. Induced plasma radiation was observed in a tuned optical cavity in which the output mirror had minimum losses at $\lambda \cong 2$ μm. When the opaque mirror of the cavity was covered, this emission disappeared, unlike the thermal self-radiation of the plasma, which showed almost no change in amplitude when this was done. Comparison of the oscillograms shows that lasing in the plasma developed after termination of the CO_2 laser pulse, attaining its greatest value only after ~1 μs, whereas the maximum thermal radiation corresponds to the stage of plasma heating by laser emission with $\lambda = 10.6$ μm.

The measured lasing wavelength $\lambda = 2.03$ μm is identified with transition $5d[3/2]_1^0$-$6p[1/2]_0$ in atomic Xe [Ref. 13]. When another cavity output mirror was used with approximately the same reflectivity of ~90% in the 2.5-3.7 μm region, lasing arose simultaneously on several transitions between excited states of Xe I: $5d[3/2]_1^0$-$6p[1/2]_0$ ($\lambda = 2.65$ μm), $7p[5/2]_2$-$7s[3/2]_1^0$ (3.43 μm), $7p[1/2]_1$-$7s[3/2]_2^0$ (3.65 μm). Fig. 3 shows the dependence of total lasing energy

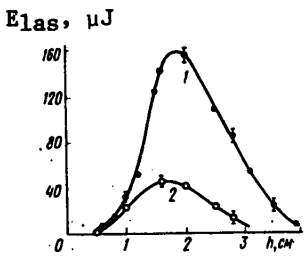

Fig. 3. Dependence of lasing energy E_{las} in plasma ($\lambda = 2.65$, 3.43, 3.65 μm) on distance between the optical axis of the cavity and target surface h for mixture He:Xe = 760:1 at pressure p = 200 mm Hg (1) and 760 mm Hg (2); pulse energy of CO_2 laser E = 25 J

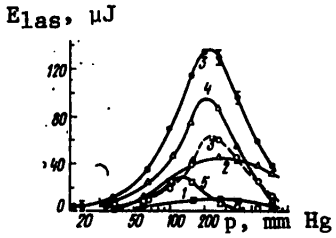

Fig. 4. Dependence of lasing energy E_{las} at $\lambda = 2.03$ μm (broken line) and 2.65, 3.43, 3.65 μm (solid line) on pressure p for mixtures of He:Xe = 19000:1 (1), 3800:1 (2), 760:1 (3), 380:1 (4) and 76:1 (5); E = 25 J, h = 1.8 cm

E_{las} in these three lines on the position of the optical axis of the cavity relative to the target surface h. The best conditions are realized at a distance of 1.6-2.0 cm from the target, the maximum of the curve for $E_{las}(h)$ moving away from the target somewhat as the gas mixture pressure decreases from 760 to 200 mm Hg.

Fig. 4 shows the lasing energy E_{las} at the optimum position of the cavity axis relative to the target as a function of the composition of the mixture and its total pressure p. The greatest lasing energy (~0.06 and ~0.15 mJ) is reached for a mixture with Xe content of about 0.13% (He:Xe = 760:1) at overall pressure $p \cong 200$ mm Hg. A reduction in the percent content of Xe in the mixture, just like an increase, reduces the lasing energy throughout the pressure range. For any mixture, the curve $E_{las}(p)$ has a maximum with position that is comparatively weakly dependent on mixture composition: an increase in the precentage of Xe by a factor of 250 shifts the maximum from ~250 mm Hg

(He:Xe = 19000:1) to 125 mm Hg (76:1). However, the lasing energy in the high-pressure region falls off much more steeply.

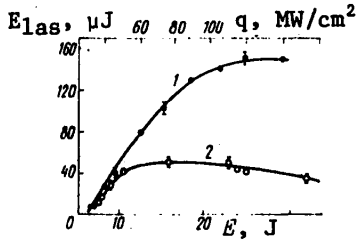

Fig. 5. Lasing energy E_{las} ($\lambda = 2.65$, 3.43, 3.65 μm) as a function of CO_2 laser pulse energy E or flux density q for mixture He:Xe = 760:1 at p = 200 mm Hg (1) and 760 mm Hg (2); h = 1.8 cm

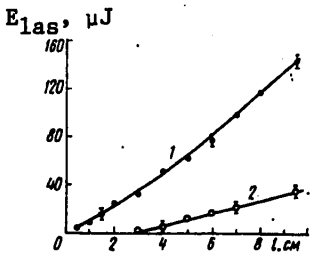

Fig. 6. Lasing pulse energy E_{las} as function of plasma length l for mixture He:Xe = 760:1 at p = 200 mm Hg (1) and 760 mm Hg (2); E = 25 J

Fig. 5 shows E_{las} as a function of CO_2 laser pulse energy E or the corresponding flux density q of laser emission with $\lambda = 10.6$ μm for mixture He:Xe = 760:1 at different pressures. At p = 200 mm Hg, lasing energy increases monotonically with increasing energy of the stimulating pulse; at values of $E \cong 25$-30 J ($q \cong (1.2\text{-}2.4)\cdot 10^8$ W/cm^2) saturation is observed. This effect is more strongly pronounced at high pressure of the mixture p = 760 mm Hg, where there is even some reduction of lasing energy at $E \gtrsim 16$ J ($q \gtrsim 8\cdot 10^7$ W/cm^2).

Fig. 6 shows the dependence of E_{las} on length l of the active region, obtained by reducing the longitudinal dimension of the focusing spot on the target (with a corresponding reduction in the length of the resultant plasma) by using diaphragms to restrict the cross section of the laser beam. Since the radiation density distribution over the cross section of the CO_2 laser beam was rather uniform (within ~20%), the energy per unit of length of the plasma $E/l = 2.5$ J/cm remained unchanged. The dependence $E(l)$ measured in this way was close to linear. The shortest plasma length l_{thr} at which lasing still takes place in a mixture of He:Xe = 760:1 is $l_{thr} \cong 0.5$ cm at p = 200 mm Hg, and $l_{thr} \cong 3.0$ cm at p = 760 mm Hg. Assuming that losses in the optical cavity are determined only by its transparency, we find the average gain for lines with $\lambda = 2.65$, 3.43, 3.65 μm in the plasma: $\kappa = \frac{1}{2} l_{thr}^{-1} \ln (R_1 R_2)^{-1} = 0.1$ cm^{-1} (p = 200 mm Hg) and $\kappa = 0.016$ cm^{-1} (760 mm Hg), where the reflectivities of the mirrors in the cavity are $R_1 = 1.0$ and $R_2 = 0.9$.

4. Discussion of Results

To interpret the relations found above, let us turn to results of investigation of gasdynamic processes that develop in a gas under the action of powerful CO_2 laser pulses [Ref. 6, 14, 15]. After the first instant of initiation associated with vaporization of the target, subsequent plasma formation takes place due to heating of the gas adjacent to the target in the laser emission

absorption wave [Ref. 14]. At the optimum pressure for development of lasing in the plasma p = 200 mm Hg and $q \approx 1.5 \cdot 10^8$ W/cm^2 corresponding to pulse energy E ≈ 25 J at which the principal measurements were made (see Fig. 3, 4, 6), the absorption wave in He propagates in the light-detonation mode [Ref. 15].

To evaluate the velocity $v_{сд}$, pressure $p_{сд}$, and specific internal energy $\varepsilon_{сд}$ of the light-detonation wave, and the degree of compression θ of the gas that is heated in the wave, we use the following relations [Ref. 16]:

$$v_{сд}=[2(\gamma^2-1)]^{1/3}(q/\rho_0)^{1/3}; \quad (1)$$

$$p_{сд}=\rho_0 v_{сд}^2/(\gamma+1)=[2(\gamma^2-1)]^{2/3}\rho_0^{1/3}q^{2/3}/(\gamma+1); \quad (2)$$

$$\varepsilon_{сд}=\frac{\gamma v_{сд}^2}{(\gamma^2-1)(\gamma+1)}=\frac{\gamma}{\gamma+1}\left(\frac{4}{\gamma^2-1}\right)^{1/3}\left(\frac{q}{\rho_0}\right)^{2/3}; \quad (3)$$

$$\theta=\rho/\rho_0=(\gamma+1)/\gamma, \quad (4)$$

where γ is the effective adiabatic exponent; ρ_0 and ρ are the initial and final gas densities. Setting $\gamma = 1.3$, $\rho_0 = 4.4 \cdot 10^{-5}$ g/cm^3, we get for He at $q = 1.15 \times 10^8$ W/cm^2 and p = 200 mm Hg: $v_{сд} = 3.3 \cdot 10^6$ cm/s, $p_{сд} = 2.1 \cdot 10^8$ dynes/cm^2, $\varepsilon_{сд} = 8.85 \cdot 10^{12}$ ergs/g = 36.6 eV/atom, $\theta = 1.77$. During the laser pulse, the wave front propagates to a distance $h \approx v_{сд}\tau \approx 0.5$ cm from the surface of the target.

The temperature T of the resultant plasma as found by the interpolation formula of Ref. 17

$$\varepsilon = 2{,}5\, A^{1/6}(T \cdot 10^{-4})^{5/3}(\rho_a/\rho)^{0{,}12} \text{ eV/atom} \quad (5)$$

(where $\rho_a = 1.79 \cdot 10^{-4}$ g/cm^3 is the density of He under normal conditions, A = 4 is its atomic weight), is 41 kK. The equilibrium degree of ionization obtained on the basis of the Saha equation [Ref. 18]

$$\frac{\alpha^2}{1-\alpha}=\frac{u_1}{u_0}\frac{1{,}797 \cdot 10^{-4}T^{3/2}}{\delta}\exp(-I/kT) \quad (6)$$

(where I = 24.6 eV = $3.92 \cdot 10^{-11}$ ergs is the ionization potential of He; $u_0 \approx 1$, $u_1 \approx 2$ are the statistical sums of the atom and ion; $\delta = \rho/\rho_a = \rho_0\theta/\rho_a$ is relative density) in this case is $\alpha \approx 0.87$, which corresponds to an electron concentration in the plasma of $N_e \approx 10^{19}$ cm^{-3}.

Thus by the instant of completion of the laser pulse, an extended, hot, dense plasma has been set up near the target with high energy concentration. As a consequence of the high rate of collisions between particles, thermodynamic conditions in such a plasma should be close to equilibrium; in particular, the processes of recombination of ions and electrons are compensated by reverse processes of ionization of atoms. A reduction in temperature and density of the plasma upon subsequent adiabatic expansion should result in a situation where, beginning at a certain instant the degree of ionization present in the plasma is greater than the equilibrium value corresponding to the new conditions. This is due to the fact that the rate constant of recombination in triple collisions of ions with electrons (the principal mechanism at high particle density and not too low temperature) [Ref. 18] $\beta = 5.2 \cdot 10^{-28}/T^{9/2}$

changes with falling temperature more slowly than the equilibrium degree of ionization $\alpha \sim \delta^{-\frac{1}{2}} \exp(-I/2kT)$ in the cooled plasma ($\alpha \ll 1$). The determining process in such a supercooled plasma becomes recombination, whereas the probability of the reverse process falls off exponentially with decreasing temperature.

With the exception of photorecombination, which plays an insignificant part at high electron density, all other processes of recombination in triple collisions or with the participation of molecular ions lead to preferred formation of atoms in upper energy states [Ref. 18]. In subsequent relaxation of excitation downward through energy levels with favorable ratio of probabilities of transitions, population inversion may be formed between certain pairs of levels [Ref. 1]. The rate of formation of excited atoms of Xe* on the upper laser level, assuming that all particles formed as a result of recombination relax through this level, is determined by the equation

$$\frac{d[Xe^*]}{dt} = \beta [Xe^+] N_e^2 - \nu [Xe^*], \qquad (7)$$

where [Xe*], [Xe^+] are the concentrations of atoms and ions in the plasma, $\nu = \alpha_{im} Ne + Arad$ is a constant that determines the loss of Xe* from the upper laser level due to inelastic electron impacts and radiative transitions. The resultant inversion is proportional to the concentration of excited atoms Xe* on the upper laser level, and thus depends on the concentration of particles in the plasma and the cooling rate ($\beta \sim T^{-9/2}$).

To describe the gasdynamic processes that accompany expansion of the dense hot plasma initially heated by the laser pulse into the ambient cool gas, a theoretical model of a strong cylindrical explosion is used with instantaneous energy release occurring along the axis of symmetry [Ref. 19]. The validity of such an approach corroborated by experiments of Ref. 6 in plane geometry, is justified by the short duration of the CO_2 laser pulse and the small initial dimensions of the plasma formed close to the target as compared with the lasing time of ~1 μs (see Fig. 2*в*) and plasma dimensions of ~1.6-2.0 cm (see Fig. 3) that are typical of lasing development.

The change in plasma temperature in the process of adiabatic cooling is evaluated by the equation of the adiabat

$$T_{cn} p_{cA}^{(\gamma-1)/\gamma} = T(t) p(t)^{(\gamma-1)/\gamma}, \qquad (8)$$

Assuming that the pressure of the gas superheated in the light-detonation wave after a fairly long time $t \gg \tau$ becomes equal to the pressure in the central region of a strong cylindrical explosion with linear energy release E/l [Ref. 19]:

$$p(t) = k_2 (E\rho_0 / l\xi)^{1/2} t^{-1}, \qquad (9)$$

where the coefficients k_2 and ξ depend on the adiabatic exponent γ. If we disregard energy release in the recombination process and do not account for the change in the internal energy of atoms during cooling, then, assuming

$\gamma = 1.67$ ($\xi = 0.58$, $k_2 = 0.06$) and $E/l = 2.5$ J/cm, we get for $t = 1$ μs the temperature estimate $T \cong 7$ kK. Accounting for the mentioned circumstances by introducing an effective adiabatic exponent $\gamma = 1.3$ ($\xi = 1.3$, $k_2 = 0.086$) gives $T \cong 14$ kK. The plasma density in the expansion process up to this instant falls by a factor of 15-30. The reduction of density and the associated slowdown of recombination rate are apparently factors that limit the power and time of lasing in the given arrangement.

The reduction of particle concentration in the plasma also explains the reduction of lasing energy at low gas pressures on Fig. 4. On the other hand, with increasing pressure $p \cong 200$ mm Hg one also observes a reduction of lasing energy, which in this case is due to transition to the supersonic radiative mode of laser emission absorption wave propagation with $\lambda = 10.6$ μm in He [Ref. 15]. Such a transition is accompanied by a sharp rise in wave velocity and a corresponding reduction of temperature and degree of ionization of the heated plasma. Besides, the lower energy concentration in greater plasma volume should reduce the efficiency of subsequent adiabatic cooling. These same factors explain the reduction of lasing energy with an increase in the energy of the stimulating pulse $E \geqslant 16$ J on Fig. 5; the corresponding $q \cong 8 \cdot 10^7$ W/cm^2 precisely coincides with the threshold of transition from the light-detonation to the supersonic radiative wave in He at pressure of $p = 760$ mm Hg as measured in Ref. 15.

In the estimates given above, no consideration was taken of the influence of small additives of Xe to He on the concurrent gasdynamic processes and the parameters of the heated plasma. Preliminary experiments have shown that even a small amount (~0.1%) of Ar or Xe appreciably alters the pattern of gasdynamic processes in He, considerably lowering the threshold of establishment of the ultrasonic radiation wave. It is this circumstance that apparently explains the reduction of lasing energy observed on Fig. 4 when the Xe content is increased above 0.13% in the mixture rather than the occurrence of a relaxation channel that is parasitic for the given laser arrangement due to the formation of dimer molecules of Xe_2^* as suggested in Ref. 4. At Xe concentrations typical of the given experiments and rate constants of the reactions

$$Xe^* + Xe + He \xrightarrow{\beta_{He}} Xe_2^* + He,$$

$$Xe^* + Xe + Xe \xrightarrow{\beta_{Xe}} Xe_2^* + Xe,$$

$\beta_{He} = 1.4 \cdot 10^{-32}$ cm^6/s [Ref. 20], $\beta_{Xe} = 2.5 \cdot 10^{-32}$ cm^6/s [Ref. 21] (these constants are given for gas temperature $T = 300$ K, and decrease with increasing T) the time of formation of Xe_2^* molecules is several orders of magnitude longer than the characteristic time of lasing development (~1 μs). However, such a mechanism can occur at a higher pressure of the mixture [Ref. 7], and also in experiments with nuclear pumping [Ref. 8-11], where the duration of the lasing pulse is several hundreds of microseconds.

In conclusion we note that with more detailed consideration of elementary processes in the cooled plasma it is necessary to account for a number of plasma-chemical reactions that may appreciably influence the rate of recombination and formation of inverse population.

5. Conclusions

Thus as a result of experiments that were done an investigation was made of the way that emission parameters of a plasma recombination laser using a mixture of He-Xe depend on conditions of plasma heating by powerful CO_2 laser pulses and on the concurrent gasdynamic processes. Despite the fact that the efficiency of the laser arrangement considered in this research was quite low, the method itself of producing a dense supercooled plasma by a pulsed CO_2 laser is quite promising for studying the mechanism of formation of inverse population in recombination lasers.

The principal results of this research were reported at the Fourth International Conference on Lasers and Their Applications" [Ref. 22].

REFERENCES

1. Gudzenko, L. I., Yakovlenko, S. I., "Plazmennyye lazery" [Plasma Lasers], Moscow, Atomizdat, 1978.

2. Kuznetsov, I. M., Rayzer, Yu. P., ZHURNAL PRIKLADNOY MEKHANIKI I TEKHNICHESKOY FIZIKI, No 4, 1965, p 10.

3. Gudzenko, L. I., Filippov, S. S., Shelepin, L. A., ZHURNAL EKSPERIMENTAL'NOY I TEORETICHESKOY FIZIKI, Vol 51, 1966, p 115.

4. Silfvast, W. T., Szeto, L. H., Wood, O. R. Jr., APPL. PHYS. LETTS, Vol 31, 1977, p 335.

5. Silfvast, W. T., Szeto, L. H., Wood, O. R. Jr., OPTICS LETTS, Vol 4, 1979, p 271.

6. Boyko, V. A., Danilychev, V. A., Zvorykin, V. D., Kholin, I. V., Chugunov, A. Yu., KVANTOVAYA ELEKTRONIKA, Vol 3, 1976, p 1955.

7. Chapovsky, P. L., Lisitsyn, V. N., Sorokin, A. R., OPTICS COMMS, Vol 16, 1976, p 33.

8. Helmick, H. H., Fuller, J. L., Shneider, R. T., APPL. PHYS. LETTS, Vol 26, 1975, p 327.

9. Voinov, A. M., Dovbysh, L. Ye., Krivonosov, V. N., Mel'nikov, S. P., Kazakevich, A. T., Podmoshenskiy, I. V., Sinyanskiy, A. A., PIS'MA V ZHURNAL TEKHNICHESKOY FIZIKI, Vol 5. 1979, p 422.

10. De Young, R. J., Jalufka, N. N., Hohl, F., APPL. PHYS. LETTS, Vol 30, 1977, p 19.

11. Mansfield, C. R., Bird, P. F., Davis, J. F., Wimett, T. F., Helmick, H. H., APPL. PHYS. LETTS, Vol 30, 1977, p 640.

12. Lee, Ja. H., McFarland, D. R., Hohl, F., APPL. OPTICS, Vol 19, 1980, p 3343.

13. Prokhorov, A. M., ed., "Spravochnik po lazeram" [Laser Handbook], Moscow, Sov. radio, Vol 1, 1978.

14. Danilychev, V. A., Zvorykin, V. D., Kholin, I. V., Chugunov, A. Yu., KVANTOVAYA ELEKTRONIKA, Vol 7, 1980, p 2599.

15. Boyko, V. A., Vladimirov, V. V., Danilychev, V. A., Duvanov, B. N., Zvorykin, V. D., Kholin, I. V., PIS'MA V ZHURNAL TEKHNICHESKOY FIZIKI, Vol 4, 1978, p 1373.

16. Rayzer, Yu. P., "Lazernaya iskra i rasprostraneniye razryadov" [Laser Spark and Discharge Propagation], Moscow, Nauka, 1974.

17. Tsikulin, M. A., Popov, Ye. G., "Izluchatel'nyye svoystva udranykh voln v gazakh" [Radiative Properties of Shock Waves in Gases], Moscow, Nauka, 1977.

18. Zel'dovich, Ya. B., Rayzer, Yu. P., "Fizika udarnykh voln i vysokotemperaturnykh gidrodinamicheskikh yavleniy" [Physics of Shock Waves and High-Temperature Thermodynamic Phenomena], Moscow, Nauka, 1966.

19. Sedov, L. I., "Metody podobiya i razmernosti v mekhanike" [Methods of Dimensional Analysis in Mechanics], Moscow, Nauka, 1977.

20. Pice, J. K., Johnson, A. W., J. CHEM. PHYS., Vol 63, 1975, p 5235.

21. Werner, C. W., George, E. V., Hoff, P. W., Rhodes, C. K., IEEE J., Vol QE-13, 1977, p 769.

22. Danilychev, V. A., Zvorykin, V. D., Kholin, I. V., Chugunov, A. Yu., "Fourth International Conference on Lasers and Their Applications", Leipzig, 1981, p 75.

6610
CSO: 1862/114

UDC 621.375

VIBRATIONAL ENERGY EXCHANGE IN SYSTEMS WITH OPTICAL FEEDBACK

Moscow KVANTOVAYA ELEKTRONIKA in Russian Vol 9, No 1(115), Jan 82 (manuscript received 3 Mar 81) pp 36-43

[Article by A. S. Biryukov, R. I. Serikov and A. M. Starik, Physics Institute imeni P. N. Lebedev, USSR Academy of Sciences, Moscow]

[Text] A theoretical analysis is made of a CO_2 gasdynamic laser aditionally pumped by self-radiation. It is shown that using optical-channel feedback brings about a 5-15% improvement in efficiency of converting thermal energy to radiation.

There has recently been an upsurge of interest in phenomena that take place when laser radiation flows through gases. The presence of absorbing dopants in gas may lead for example to population inversion of levels. The action of nearly all optically pumped gas lasers is based on this effect. In some cases the absorption of radiation is accompanied by a temporary drop in temperature. This is the so-called "kinetic cooling effect" experimentally observed in Ref. 1. Additional optical pumping may also improve the energy characteristics of gasdynamic lasers [Ref. 2].

The gasdynamic laser has the distinguishing feature that the medium is at appreciably different levels of deviation from thermodynamic equilibrium in each cross section along the flow. Excitation of the upper working state and extraction of the luminous energy may be considerably separated in space and time. Because of this, by using the difference between relaxation rates of levels and taking advantage of the resonant properties of the system it is possible to increase imbalance by using "positive feedback" through the optical channel. Additional pumping for gasdynamic lasers was considered in Ref. 2, where it was shown that increasing the vibrational energy of a system of anharmonic oscillators under the action of radiation can improve working efficiency of a CO laser. At the same time, in the opinion of the authors of Ref. 2, efficiency should not be improved for steady-state CO_2 gasdynamic lasers with feedback.

Our paper analyzes the feasibility of improving the working efficiency of CO_2 gasdynamic lasers under conditions of additional pumping by self-emission. The principal conclusions of the research were reached in 1974; here these

conclusions are re-examined quantitatively in the light of recent data on the rate constants of elementary relaxation processes.

The working principle of the gasdynamic laser is that some of the enthalpy stored in internal degrees of freedom of the gas molecules is converted to luminous energy of coherent radiation when it is heated and subsequently rapidly cooled by expansion. In typical CO_2 lasers, the enthalpy of vibrational degrees of freedom is ~10% (at initial temperature of ~2 kK) of the total enthalpy, and only a small fraction of this amount can be transformed to radiation. This is due to the comparatively low (41%) quantum efficiency of conversion, relaxation losses and entrainment of a certain amount of the vibrationally excited donor gas (N_2) out of the optical cavity, so that the overall efficiency as a rule does not exceed ~1%. The major losses of vibrational energy are determined by relaxation processes in the small ($\lesssim$1 cm) near-critical zone of the nozzle where gas temperature and density are high. Nearly all the flux of lost energy goes to vibrational degrees of freedom via CO_2 molecules. Subsequently the vibrational energy is mainly "frozen." If a process that is free to compete with vibrational relaxation is introduced artificially into the region of the critical cross section of the nozzle, this will reduce losses considerably. Since in this region the medium is in the nonequilibrium state but far from inversion, so that the populations of the lower working levels of the CO_2 are high, such a process may be the absorption of CO_2 laser emission coming from the optical cavity of the same gasdynamic laser. Conversion of particles from the rapidly relaxing lower level to the slowly relaxing upper level increases the effective temperature of population of vibrational states of N_2 and asymmetric levels of CO_2 coupled by quasi-resonant exchange by comparison with a gasdynamic laser without feedback. As a result, the nonequilibrium of the medium is greater when it enters the optical cavity. It would seem that the increment in energy coupled by the cavity out of the flow in the steady state should correspond to the absorbed energy, and that efficiency should not increase. And this would actually be the case if the relaxation rate of the lower level over the entire extent of the nozzle were so high that its population would be determined by the gas temperature. However, if we take consideration of the finite rate of interaction of this level with translational degrees of freedom, then the reduction of its population upon absorption of resonant radiation may lead to an additional increase of energy in the cavity. At the same time, an artificial reduction of population of the lower level in the rapid relaxation zone is accompanied by local disruption of quasi-equilibrium between the corresponding vibrational and gas temperatures, and as a consequence by conversion of some of the energy of translational degrees of freedom to energy of deformation vibrations (kinetic cooling effect), and then via radiation to asymmetric vibrations, which also is conducive to an improvement of laser efficiency.

On the basis of the simplest arguments, let us estimate the increase in energy of a CO_2 gasdynamic laser when feedback is included.

Beyond the output mirror of the gasdynamic laser cavity we place a rotating optical system, and direct radiation into the near-critical part of the nozzle, as shown in Fig. 1. We will take the physical conditions in the gas stream

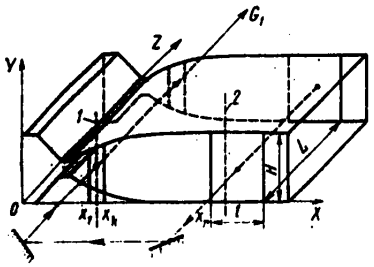

Fig. 1. Diagram of gasdynamic laser with feedback

in the absorption and cavity regions as identical with the conditions in certain average cross sections 1 and 2 of these regions respectively. We make the following simplifying assumptions: the energies of vibrational quanta of N_2 and asymmetric vibrations of CO_2 coincide; due to rapid intermolecular VV' exchange of quanta, the temperatures of population of the energy levels of these modes of vibrations are the same and equal to $T_3(x)$, where x is the coordinate along the nozzle; for the same reason of strong interaction we assume that the temperatures of symmetric and deformation vibrations of CO_2 also are the same and equal to $T_2(x)$, and that the gas temperature of the expanding flow behaves as in an ordinary gasdynamic laser without feedback (we disregard kinetic cooling). We will consider a CO_2-N_2-H_2O gas mixture with small mole fraction of water vapor $\gamma_{H_2O} < 5\%$, so that with good accuracy we can assume $\gamma_{H_2O} + \gamma_{N_2} = 1$. We will further assume that the upper level in cross section 1 is "frozen" ($T_3 = \text{const}$ at $x > x_1$), while the lower level on section 1-2 loses the α-th part of its population as a consequence of relaxation.

Maximum energy in the optical cavity is reached upon transillumination of the working transition in section 1. Let us find the amplitude of this maximum and the energy necessary for saturation; then their difference will give the output energy of the laser with feedback.

Let the average number of vibrational quanta per molecule of CO_2 or N_2 in cross section 1 before interaction with the saturating radiation be equal to ε_3^0, and for symmetric vibrations of CO_2 -- to ε_1^0. After absorption of light the populations of the upper and lower working levels of CO_2 (with consideration of rapid exchange with N_2) become equal and take on the value

$$N\varepsilon' = N\,(\varepsilon_3^0 + \varepsilon_1^0\gamma_{CO_2})/(1 + \gamma_{CO_2}),$$

where N is the total number of particles in a unit of mass of the mixture (here it is also assumed that absorption occurs at a rate appreciably exceeding the rate of VT-relaxation of the lower level, but more slowly than rotational relaxation). The energy necessary for transillumination of the working transition in cross section 1 will be

$$E_S = (\varepsilon_1^0 - \varepsilon_3^0)\frac{\gamma_{CO_2}}{1 + \gamma_{CO_2}} Nh\nu, \qquad (1)$$

where $h\nu$ is a quantum of laser emission.

In cross section 2 we get $\varepsilon_3^{(2)} = \varepsilon'$ and $\varepsilon_1^{(2)} = \varepsilon'(1-\alpha)$ and the maximum energy extracted by the cavity from a unit of mass of the gas is

$$E_{max} = \frac{\left|(\varepsilon_3^0 + \varepsilon_1^0\gamma_{CO_2})\,\alpha - \Delta^{(2)}(1+\gamma_{CO_2})\right|(1+\gamma_{CO_2})\,Nh\nu\beta}{\left[1 + \gamma_{CO_2} + (\varepsilon_3^0 + \varepsilon_1^0\gamma_{CO_2})(1-\alpha)\right](1+\gamma_{CO_2} + \varepsilon_3^0 + \varepsilon_1^0\gamma_{CO_2})\,Q^{(2)}}, \qquad (2)$$

where β is the efficiency of the cavity; $Q^{(2)}$ and $\Delta^{(2)}$ are the vibrational stat-sum and relative threshold inversion of populations in cross section 2.

In order for the output energy of the system with additional self-pumping to be greater than that of a conventional gasdynamic laser with the same stagnation parameters, the condition

$$\delta = (E_{max} - E_s)/E_0 - 1 > 0 \qquad (3)$$

must be met, $E_0 = [\varepsilon_3^0 - \varepsilon_1^0(1-\alpha) - \Delta]\, Nh\nu\beta / [(1+\varepsilon_1^0 - \varepsilon_1^0\alpha)(1+\varepsilon_3^0)\, Q]$ is the output energy of the gasdynamic laser without feedback; Q and Δ are the vibrational stat-sum and relative threshold inversion respectively in cross section 2.

Substituting (1) and (2) in (3), and setting $Q^{(2)} \approx Q$, $\Delta^{(2)} \approx \Delta$ we get with accuracy to terms of the second order of smallness with respect to ε_3^0, ε_1^0, Δ,

$$\delta = \frac{\varepsilon_1^0 - \varepsilon_1^0}{\varepsilon_3^0 - \varepsilon_1^0(1-\alpha) - \Delta} \cdot \frac{\beta(1-\alpha) - \gamma_{CO_2}(Q-\beta)}{\beta(1+\gamma_{CO_2})}. \qquad (4)$$

Estimates show that $\delta > 0$ over a fairly wide range of α, β, γ_{CO_2}, although the gain is low in absolute magnitude, being ~5-15%.

We can come to an analogous conclusion if we do not assume that the working transition in cross section 1 is transilluminated. In this case, condition (3) takes the form

$$\delta = q(1-\alpha)/[1 - q(2-\alpha)] > 0 \text{ for } q < (2-\alpha)^{-1}, \qquad (5)$$

where q is the fraction of energy absorbed in cross section 1.

These have not been rigorous arguments, and they only confirm the possibility in principle of improvement of CO_2 gasdynamic laser efficiency in the presence of feedback. Accounting for the positive contribution of the kinetic cooling effect is more complicated since it requires simultaneous consideration of the population kinetics of levels and gasdynamic equations.

Since the radiation produced by feedback passes through the near-critical part of the nozzle where the gas density gradients are rather high (and consequently so is the index of refraction), the luminous flux at the output becomes divergent due to refraction and the finite dimensions of the zone of absorption along the flow since the various components of the light beam emerge at different angles to the initial direction of propagation. Estimates show that for typical pressures, temperatures and nozzle profiles used in gasdynamic lasers, gradients of the index of refraction may reach $\sim 2 \cdot 10^{-4}$/cm. Such gradients cause maximum deflection of rays of up to ~0.5° on characteristic propagation lengths of ~1 m, which is too small to be taken into account in model calculations. On the other hand, where necessary the refracted radiation that is coupled out can be "improved" by an optical system for transfer to the object.

To get the quantitative characteristics of a gasdynamic laser with additional self-pumping, a solution was found for the self-consistent problem of finding the steady-state value of energy coupled out of the system.

The approximation of an inviscid thermally nonconductive gas was used, and it was assumed that in time $\tau = (x_r - x_1)/\bar{u}$, where x_1, x_r are the zero coordinates of the absorption and cavity regions respectively and $\bar{u} = \left(\int_{x_1}^{x_r} u(x)\,dx\right) \Big/ (x_r - x_1)$ is some average velocity of the flow on segment (x_1, x_r), the intensity of the incident radiation is constant. In this case, when $0 < t < \tau$, the flow can be taken as steady-state, and the system of equations that describes gas motion in the presence of external radiation sources is represented as

$$\hat{A}_k F_k = M. \tag{6}$$

Here $\hat{A}_k = \partial/\partial x_k$ is a differential operator; F_k and M are vectors with components

$$F_k = \begin{Vmatrix} \rho u_k \\ \| \rho u_k u_m + p\delta_{km} \| \\ \rho u_k (h + W^2/2) \\ \| \rho u_k \varepsilon_j \| \end{Vmatrix}, \quad M = \begin{Vmatrix} 0 \\ 0 \\ g \\ \| \rho g_j \| \end{Vmatrix};$$

ρ and p are the gas density and pressure; u_k and u_m are velocity components along the coordinate axes; $W^2 = \sum_{k=1}^{3} u_k^2$; h is the total enthalpy of the mixture; $\| \rho u_k u_m + p\delta_{km} \|$, $\| \rho u_k \varepsilon_j \|$ $\| \rho g_j \|$ are column matrices with m = 1-3, j = 1-n, where n is the number of independent modes of vibrations in the given molecular system; δ_{km} is the Kronecker delta; ε_j is the average number of vibrational quanta of type j per molecule; g and g_j are the specific powers of the sources of luminous and vibrational radiation. System (6) is closed by the equation of state of the gas.

To determine g_j for a CO_2-N_2-H_2O mixture, the generally accepted model of partial vibrational temperature was used, where the temperatures of the symmetric T_1 and deformation modes T_2 in CO_2 due to strong Fermi interaction are the same, while the values of the corresponding vibrational quanta satisfy the condition $2h\nu_2 = h\nu_1$. The energy levels of H_2O due to rapid VT relaxation were considered to be populated with the gas temperature. Thus g_j in (6) are non-zero only for the aggregate of deformational, symmetric (j = 2) and asymmetric vibrations of CO_2 (j = 3) and excited molecules of N_2 (j = 4). With consideration of induced transitions under the action of the resonant radiation field

$$g_j = \left(\frac{d\varepsilon_j}{dt}\right)_{VV'} + \left(\frac{d\varepsilon_j}{dt}\right)_{VT} + \left(\frac{d\varepsilon_j}{dt}\right)_{J}. \tag{7}$$

The first two terms in (7) are responsible for intra- and intermolecular vibrational exchange and VT-relaxation, and the third term is responsible for the change in the number of vibrational quanta in the j-th mode in the inducing

field. In the optical cavity,

$$\left(\frac{dz_j}{dt}\right)_J = (2\delta_{2j} - \delta_{3j})\frac{g\mu}{\rho A h\nu \gamma_{CO_2}}, \tag{8}$$

where $g = k_\nu j_0$; k_ν is the index of amplification of the medium on laser transition P(20) (00^01-10^00) in CO_2; μ is the molecular weight of the mixture; A is Avagadro's number; J_0 is intensity of radiation in the cavity.

The general expression for terms $(d\varepsilon_j/dt)_{VV'}$ and $(d\varepsilon_j/dt)_{VT}$ is given in Ref. 3 and the elementary processes that determine them are taken the same as for example in Ref. 4. The corresponding rate constants for these processes are taken from Ref. 4, 5.

The index of amplification was calculated by a standard formula (e. g. see Ref. 6) with form factor of the vibrational-rotational transition line defined by the Voigt function. The coefficients of impact expansion of the lines by different components of the mixture were considered to be temperature-dependent, and were selected on the basis of Ref. 7, 8. The Einstein coefficient of the working transition was taken as 0.187 s^{-1} [Ref. 7].

For quantitative analysis of the gasdynamic laser with feedback, a flat slit nozzle was selected, designed for undetached gas flow and uniform distribution of parameters in the output section, with contour given in Ref. 9. The height of the critical cross section $a = 1$ mm, degree of expansion $\xi = 20$, dimension of the nozzle in the direction of the Z-axis L = 1 m (see Fig. 1).

The solution of system of equations (6) with sources of form (8) for given chemical composition of the mixture and stagnation conditions (pressure p_0 and temperature T_0) was begun in the subsonic part of the nozzle and was found as in Ref. 9 by an implicit difference method of second-order approximation. In the cavity, the condition of steady-state lasing [Ref. 6]

$$\langle k_\nu \rangle = -\ln(R_1R_2)/2L \equiv k_\nu^{\text{п}} \tag{9}$$

was added to (6), where $\langle k_\nu \rangle = \left(\int_{x_r}^{x_r+l} k_\nu(x)\,dx\right)\Big/ l$, l=20 cm is the length of the cavity in the direction of flow; $R_1 = 0.98$, $R_2 = 0.9$ are reflectivities of the mirrors. The zero coordinate of the cavity was combined with the coordinate of the maximum in distribution $k_\nu(x)$. From the solution of (6), the intensity J_0 in the cavity was found that satisfies condition (9). The power coupled out was determined by the expression [Ref. 6]

$$G = \langle k_\nu \rangle J_0 HLl\left|(1+\sqrt{R_1/R_2})(1-\sqrt{R_1R_2})\right|^{-1}, \tag{10}$$

where H is the height of the cavity, equal to $a\xi = 2$ cm. All this power was injected into the supersonic near-critical part of the nozzle, and the point of injection of radiation corresponded to the maximum index of absorption k. For a given aperture S of the beam coupled out of the cavity, the intensity of radiation introduced into the absorption region was calculated from the ratio J = G/S (in the calculations aperture S was taken as 0.35 cm^2). The cross

section of the absorption region was the field bounded on two sides by the outline of the nozzle (see Fig. 1) and by the dimension (x_1, x_k) along the flow determined (at fixed x_1) from the condition that S be equal to the area of this field. To find the distribution of parameters along the Z-axis, calculation of the flow was done in several cross sections z_n in each of which the acting intensity was determined from the known $\bar{k}$: $J_n = J \exp(-kz_n)$. In doing this, the quantity g in expression (8) for the source was replaced by $(-\bar{k}J_n)$. Using distributions of nonequilibrium parameters found in this way, new boundary conditions at the input to the optical cavity were calculated by averaging with respect to z.

The described cycle of calculations was repeated until transillumination of the working transition was attained in the absorption region, and the intensity in the cavity stopped changing. The unabsorbed part of the incident radiation in region 1 is the output power of the gasdynamic laser with feedback.

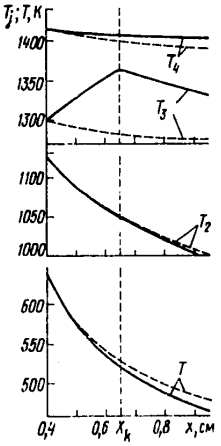

Fig. 2. Distributions of vibrational and gas temperatures in the near-critical region of the nozzle for a mixture of CO_2:N_2:H_2O = 25:74:1; T_0 = 1500 K, p_0 = 2.5 atm

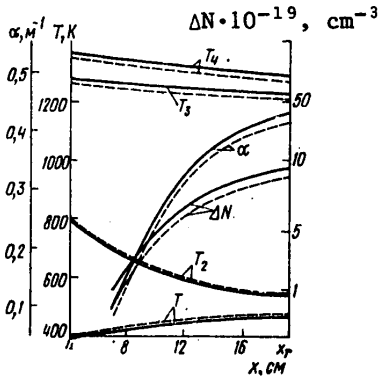

Fig. 3. Distributions of vibrational and gas temperatures, index of amplification α and population inversion ΔN in the cavity region for the same conditions as in Fig. 2

Let us give some results of calculations. Fig. 2 shows typical distributions of vibrational and gas temperatures in the absorption region and somewhat downstream for CO_2-rich mixtures. For comparison, the broken curves show the distributions of these parameters in the absence of additional resonant optical pumping. It can be seen that a rapid drop in T_3 without additional pumping is replaced by a rise when feedback is switched on. The simultaneous increase in T_4 but to somewhat less of an extent can be attributed to the fact that the quasi-resonant exchange of quanta between CO_2 and N_2 does not have time to "track" the change in T_3 accompanying optical pumping. We can also see that due to the strong coupling of T_2 and T and the large capacity

of the energy reservoir of translational degrees of freedom of the molecules, the corresponding reductions in T_2 and T are not so appreciable.

Fig. 3 shows the behavior of vibrational and gas temperatures, the weak-signal amplification index α and population inversion ΔN on transition 00^01-10^00 of CO_2 in a channel of fixed cross section of the nozzle in the cavity region. As in Fig. 2, the broken curves correspond to the behavior of equilibrium parameters in a conventional gasdynamic laser. Since the medium is more nonequilibrium after passing the absorption region in the presence of additional optical pumping, inversion and amplification arise earlier (higher upstream) and reach greater maximum values. The total store of vibrational energy in N_2 and on asymmetric levels of CO_2, and the extracted radiation energy are greater. The part of this power G_1 that is not absorbed in region 1 is greater than G_0--the output power of a gasdynamic laser without feedback with the same stagnation parameters.

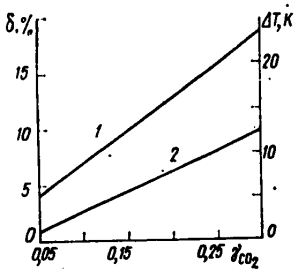

Fig. 4. Curves for δ (1) and ΔT (2) as functions of the mole fraction of CO_2 in CO_2-N_2-H_2O mixture at γ_{H_2O} = 0.01, T_0 = 1500 K, p_0 = 2.5 atm

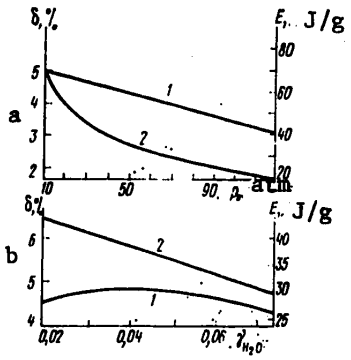

Fig. 5. Curves for δ (1) and E (2) as functions of stagnation pressure p_0 (a) and γ_{H_2O} at $\gamma_{H_2O}+\gamma_{N_2}$ =0.803 and p_0 = 60 atm (b)

Fig. 4 shows the dependence of the quantity $\delta = (G_1/G_0 - 1)\cdot 100\%$ (analog of δ in (3)) on the mole fraction of CO_2 in the mixture. Also given here is the change in depth of cooling of the gas ΔT with increasing γ_{CO_2} ($\Delta T = T^* - T$, where T^* is the gas temperature in the cavity region in a system without additional optical pumping). The data of Fig. 4 show the practically linear relation between δ and ΔT, which confirms the conclusion about the large role of kinetic cooling in gasdynamic lasers with self-pumping.

Calculations show that, an increase in the relative content of water vapor at small p_0 and ξ leads to an increase in ΔT since it is mainly through H_2O that coupling is realized between vibrational and rotational degrees of freedom in the molecular mixture. In the region of low γ_{H_2O} ($\lesssim$1%), δ has a pronounced maximum and falls off due to increasing relaxation losses of energy of the upper level with increasing γ_{H_2O}.

The results given above demonstrate the feasibility of improving efficiency of converting thermal energy to energy of coherent emission in a certain model gasdynamic laser with high carbon dioxide content when the specific vibrational energy converted to radiation is low ($\lesssim 5$ J/g).

To determine δ in real gasdynamic lasers that use combustion reactions for thermal pumping of vibrations of N_2 and CO_2 molecules, calculations of such lasers were carried out in the presence of feedback. Lasers were considered that operate on products of combustion of acetylene in air. The use of acetylene as a fuel gives working mixtures with high stagnation temperature $T_0 \sim 2500$ K at low CO_2 and H_2O content that have a considerable store of vibrational energy (~100 J/g). The calculations were done for a mixture of acetylene with air containing 6.5% C_2H_2. The equilibrium composition and stagnation temperature of the combustion products were calculated in accordance with Ref. 10. It was found that with a change of initial pressure (at air temperature of ~300 K) the composition of the combustion products and the temperature T_0 vary little, and at $p_0 = 10$-150 atm may be taken as equal to $T_0 = 2875$ K, $\gamma_{CO_2} = 0.117$, $\gamma_{N_2} = 0.73$, $\gamma_{O_2} = 0.69$, $\gamma_{H_2O} = 0.073$. It was assumed in the calculations that the vibrational levels of molecules of the mixture are just as effectively deactivated by the presence of trace amounts of O, H and OH in the combustion products as by H_2O molecules. The profile of the expanding part of the nozzle was selected to maximize the power of the extracted radiation for a given mixture composition and given stagnation parameters with simultaneous realization of undetached flow [Ref. 11, 12]. Degree of expansion of the nozzle was $\xi = 140$, height of the critical cross section $a = 0.35$ mm.

Results of calculations of δ and specific energy output E in such a gasdynamic laser are shown in Fig. 5. The drop in δ and E with increasing stagnation pressure (Fig. 5a) can be attributed to an increase in the rates of relaxation processes, reducing the effectiveness of pumping radiation. The low absolute values of δ are due to the low percent content of CO_2 in the mixture and the shorter time that the gas stays in the absorption region for nozzles with high ξ, and consequently lower "kinetic cooling" of the system. The optimum on the curve for $\delta(\gamma_{H_2O})$ (Fig. 5b), in contrast to gasdynamic lasers with lower degrees of expansion and stagnation parameters, shifts toward greater γ_{H_2O} and is determined by competition of two factors: increasing depth of "kinetic cooling" and increasing relaxation losses.

Thus our analysis has shown the feasibility of increasing efficiency of a CO_2 gasdynamic laser by introducing optical feedback. On the standard laser transition 00^01-10^00 this efficiency may be increased by 5-15%. Obviously, the resultant conclusions can be applied in some measure to other gasdynamic lasers using triatomic molecules (N_2O, CS_2, COS).

REFERENCES

1. Gebhardt, F. G., Smith, D. C., APPL. PHYS. LETTS, Vol 20, 1972, p 129.

2. Shmelev, V. M., Margolin, A. D., KVANTOVAYA ELEKTRONIKA, Vol 2, 1975, p 1445.

3. Biryukov, A. S., TRUDY FIZICHESKOGO INSTITUTA IMENI P. N. LEBEDEVA AKADEMII NAUK SSSR, Vol 83, 1975, p 13.

4. Anderson, J., "Gazodinamicheskiye lazery: Vvedeniye" [Gasdynamic Lasers: Introduction], Moscow, Mir, 1979.

5. Biryukov, A. S., Konyukhov, V. K., Lukovnikov, A. I., Serikov, R. I., ZHURNAL EKSPERIMENTAL'NOY I TEORETICHESKOY FIZIKI, Vol 66, 1974, p 1248.

6. Losev, S. A., "Gazodinamicheskiye lazery" [Gasdynamic Lasers], Moscow, Nauka, 1977.

7. Biryukov, A. S., Volkov, A. Yu., Kudryavtsev, Ye. M., Serikov, R. I., KVANTOVAYA ELEKTRONIKA, Vol 3, 1976, p 1748.

8. Volkov, A. Yu., Demin, A. I., Logunov, A. N., Kudryavtsev, Ye. M., Sobolev, N. N., Preprint No 4, Lebedev Physics Institute, Moscow, 1977.

9. Biryukov, A. S., Serikov, R. I., Starik, A. M., Shelepin, L. A., KVANTOVAYA ELEKTRONIKA, Vol 4, 1977, p 787.

10. Smekhov, G. D., Fotiyev, V. A., ZHURNAL VYCHISLITEL'NOY MATEMATIKI I MATEMATICHESKOY FIZIKI, Vol 18, 1978, p 1283.

11. Losev, S. A., Makarov, V. N., KVANTOVAYA ELEKTRONIKA, Vol 3, 1976, p 960.

12. Makarov, V. N., Tunik, Yu. V., ZHURNAL PRIKLADNOY MEKHANIKI I TEORETICHESKOY FIZIKI, No 5, 1978, p 23.

6610
CSO: 1862/114

UDC 621:373.826.038.823

CW LASING OF PHOTODISSOCIATION LASER WITH CYCLIC CIRCULATION OF GASEOUS FLUOROFORMYL IODIDE

Moscow KVANTOVAYA ELEKTRONIKA in Russian Vol 9, No 1(115), Jan 82 (manuscript received 20 Feb 81) pp 20-25

[Article by V. Yu. Zalesskiy, A. M. Kokushkin, and S. S. Polikarpov]

[Text] Continuous stimulated emission is achieved in a photodissociation iodine laser with cyclic recirculation of gaseous fluoroformyl iodide. An estimate is made of the irreversible loss of molecules of working gas per unit of emitted energy for optimum rate of scavenging and optimum extraction of radiation from the cavity. This loss is less than 1% of the gas flowrate for a cw chemical iodine laser.

1. Introduction

Certain possible laser applications -- large-base interferometry for solving geophysics problems, quantum frequency standards, fiber-optics communications -- require stable lasing for a prolonged time from the laser used. The problem of cw lasing duration in the case of the indicated uses for the iodine laser deserves attention since frequency stabilization by an electric-discharge absorbing cell with iodine atoms is of interest in the first and second cases [Ref. 1], and in the second and third cases a wavelength of $\lambda = 1315$ nm may be more preferable.

In Ref. 2, 3, consideration is given to development of a cw photodissociation iodine laser, and development of an iodine laser with purely chemical pumping is considered in Ref. 4-7. In the former research, lasing with power of ~1 W for a period of ~1 s has been attained with photodissociation of $(CF_3)_3CI$ molecules in a stream of gas passing one time through the pumping region 17 cm long at a rate of ~30 m/s [Ref. 2]. Pumping was by PRK-7 high-pressure mercury lamps. Ref. 3 reports on an attempt to achieve cw lasing with pumping by more efficient low-pressure mercury lamps made by the Brown Boveri Company.

The second research area has met with greater success. Continuous action of a chemical iodine laser or an oxygen-iodine laser is based on producing metastable oxygen molecules $O_2(^1\Delta)$ in the reaction $H_2O_2+Cl_2+2NaOH \rightarrow O_2(^1\Delta)+2H_2O+2NaCl$, mixing streams of oxygen and iodine (in argon), dissociating iodine

molecules in processes $2O_2(^1\Delta) \rightarrow O_2(^3\Sigma) + O_2(^1\Sigma)$ and $O_2(^1\Sigma) + I_2 \rightarrow O_2(^3\Sigma) + 2I$, and finally transferring oxygen excitation to iodine atoms in the process $O_2(^1\Delta) + I(^2P_{3/2}) \rightarrow O_2(^3\Sigma) + I(^2P_{1/2})$ [Ref. 8]. A report was given in Ref. 5, 6 on attainment of continuous stimulated emission in chemical iodine lasers with power of 100 and 155 W for several minutes.

Despite such impressive results in development of the cw chemical iodine laser, it may turn out to be more suitable for applications where relatively low power (up to 0.1-0.2 W) is required with duration that is not too short (10-20 minutes) to use the cw photodissociation iodine laser in which it is relatively simple to realize cyclic circulation of the working gas in a closed system. With consideration of this circumstance, it is interesting to compare the expenditure of working fluid per unit of energy of laser emission E in the cw chemical and photodissociation iodine lasers.

As shown in Ref. 7, metastable oxygen at the output of the chemical reactor makes up $\eta_1 \cong 30$-40% of all the oxygen in the cw chemical iodine laser, and the fraction η_2 used for excitation of the laser level is 3% [Ref. 7], i. e. $\eta_1\eta_2 \cong 1\%$ of the expended oxygen.

Under normal conditions, expenditure of the main component of the gas mixture (oxygen) is $E_{chem} = (Lh\nu\eta_1\eta_2)^{-1} = 27$ cm^3/J, where L is the Loschmidt number, and $h\nu$ is the energy of a photon of laser emission ($1.5 \cdot 10^{-19}$ J).

In the cw photodissociation iodine laser with cyclic circulation, the working gas is not consumed upon leaving the lasing region. Moreover, not even that part of the gas with RI molecules subject to photodissociation and used in laser transitions is completely consumed. A fraction η_3 of the iodine atoms formed in photodissociation is recombined with radicals, as a rule in a rapid reverse recombination process

$$R + I \rightarrow RI, \qquad (1)$$

again forming molecules of working gas [Ref. 9, 10]. The other part of the atoms and radicals $(1 - \eta_3)$, which is usually small and depends on the structure of the radical R and other conditions (see below), reacts with formation of final products R_2 and I_2, and is irreversibly consumed.

The consumption of working fluid in the case of the cw photodissociation iodine laser can be evaluated by the formula $E_{phot} = (1 - \eta_3)/(Lh\nu f^*\eta_4)$, where f^* is the quantum yield of excited atoms in an act of photodissociation, and η_4 is the fraction of excited atoms that participate in emission of laser radiation. For working gas CF_3I, $f^* \cong 0.9$, $\eta_3 \cong \eta_4 \cong 0.6$ (see below), and the estimate gives $E_{phot} \cong 0.19$ cm^3/J, which is 140 times less than in the case of the cw chemical iodine laser.

Earlier [Ref. 11] we reported on calculations of amplification and stimulated emission of the iodine laser using fluoroformyl iodide with single-pass flow of working fluid. In the present paper we have set ourselves the task of achieving stimulated emission in a cw photodissociation iodine laser with cyclic circulation of the working gas CF_3I in a closed system, and evaluating

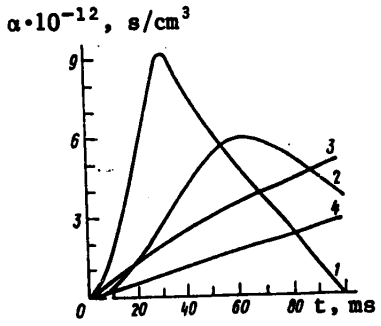

Fig. 1. Calculated time dependences α(t) for CF_3I (1, 2) and $(CF_3)_3CI$ (3, 4). Constants of quenching by working gas $5.5 \cdot 10^{-17}$ (1, 2) and $6 \cdot 10^{-16}$ cm^3/s (3, 4); photodissociation probabilities γ and molecule concentrations n respectively 0.1 s^{-1} and $5 \cdot 10^{17}$ cm^{-3} (1, 3), 0.05 s^{-1} and $2.5 \cdot 10^{17}$ cm^{-3} (2, 4)

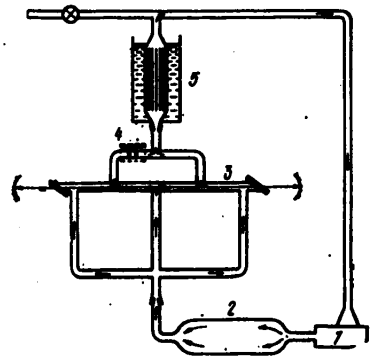

Fig. 2. Diagram of working gas circulation

the feasibility of increasing the lasing duration to levels that would be of practical interest.

Laser iodides are considerably different in their photochemical properties. We are of the opinion that fluoroformyl iodide CF_3I has better prospects than trifluoroformylmethane iodide $(CF_3)_3CI$ for use in cyclic circulation. It is a weak quenchant of iodine atoms, and is relatively ineffective as a third body in the iodine atom recombination process

$$I + I + RI \rightarrow I_2 + RI \qquad (2)$$

(R is a radical) that leads to accumulation of a strong quenchant -- I_2 molecules; thanks to the relatively short-wave working absorption band, CF_3I has a rather large absorption cross section on wavelength $\lambda = 254$ nm for the fundamental radiation of low-pressure mercury lamps ($4.1 \cdot 10^{-19}$ cm^2) and also, thanks to volatility that is highest of all laser iodides, the release of molecular iodine admixture is relatively good. Iodide $(CF_3)_3CI$ used in Ref. 2, despite the absence of radical losses in the process

$$R + R \rightarrow R_2 \qquad (3)$$

(which apparently is not realized in the case of $(CF_3)_3C$ radicals), is most likely unsuitable for this process since it has high self-quenching (according to our data 13-20 times stronger then CF_3I), does not prevent accumulation of I_2 molecules in process (2), has a low absorption cross section for photons

with $\lambda = 254$ nm ($1.3 \cdot 10^{-19}$ cm^2), and almost no I_2 admixture is released by cooling.

For comparison of iodides CF_3I and $(CF_3)_3CI$, Fig. 1 shows some calculated [Ref. 11] time dependences of integral $\alpha(t) = \int_0^t N dt'$ where N is overpopulation of levels. As shown in Ref. 11, amplification (with longitudinal flow of working gas) is proportional to α if gas velocity is assigned, and to α/t if the length of the illuminated part of the laser tube is assigned.

2. Lasing in Cyclically Circulating Working Gas

Cyclic circulation of the working gas was accomplished by using the same facility as in Ref. 11 with certain modifications. The pumping arrangement is shown in Fig. 2. The gas was put into motion by titanium centrifugal blower 1 driven by a 3.5 W GEA-2A electric motor with magnetic clutch.

Fig. 3. Oscillogram of atom luminescence damping with pulsed excitation in two cross sections of the tube 3 cm apart along the flow, observed in a downstream cross section (*1*). The other luminescence oscillograms were taken in stationary gas (blower turned off)
$2_{MC} = 2$ ms

The molecular iodine was absorbed, and condensed on the surface (~2000 cm^2) of cooled (-60°C) copper plates -- the main elements of the working gas regeneration system 4. To increase the reserve of working gas and smooth out the velocity pulsations, a 3.5-liter buffer tank 2 was included in the circulation system preceding the input to the laser tube. The velocity v of the gas in the laser tube measured by the double luminescence pulse method [Ref. 11] at a working pressure of ~4 kPa was only 1.1 m/s (Fig. 3).

Upon entering quartz laser tube 3 with diameter of 16 mm and with Brewster windows, the gas was split into four streams flowing along the tube at equal velocities, and then rejoined first into two and subsequently into one stream at the output from the laser tube before entering cooler 5. The four illuminated sections were in contact with the output orifices to avoid absorption of laser radiation in the uninverted active medium. Stimulated emission was realized with an optical cavity having losses of 3.5% per pass (round-trip) [Ref. 11] consisting of two opaque spherical mirrors with radius of curvature of 1 m separated by 140 cm for total length of the illuminated part of the laser tube $l_\Sigma = bl = 20$ cm (number of branchings $b = 4$).

In contrast to Ref. 11, where $\gamma = 0.05$ s^{-1}, the probability of photodissociation was increased by a factor of about 1.5 by using additional aluminum foil reflectors.

Fig. 4. Recording of laser radiation registered by the terminal photodiode in one of the experiments at CF_3I pressure of 4 kPa, gas velocity of 110 cm/s and total length of illuminated laser tube sections of 20 cm
$1_{мин}$ = 1 minute

Lasing started usually within 2-5 s (sometimes longer) after admission of the working gas CF_3I (4-4.5 kPa). Within about 2 minutes after admission, it began to damp out, and lasted about 4-6 minutes (Fig. 4), i. e. about 30-45 cycles. The duration of one cycle $t_{cyc} = V/(s_t vb) = 8$ s, where V is the volume of the closed circulation system (7 liters), s_t is the cross sectional area of the laser tube (2 cm^2). With a small addition of fresh CF_3I, lasing lasted for 10 minutes.

Fig. 5. Oscillograms of pumping (a) and laser ($б$) emission
$2_{мс}$ = 2 ms

An oscillogram of the lasing signal at the maximum (Fig. 5) with power supply to two mercury (low-pressure) pumping lamps by an alternating current of 8 A shows that the lasing threshold was exceeded by a factor of about 2.

Damping of stimulated emission can be explained by insufficient capacity of the regeneration system. In addition damping was also enhanced by hydrogen-containing quenchant impurities that got into the working gas, apparently from sections of the rubber vacuum hose used to connect components of the gas circulation system. This is evidenced by a reduction in lifetime of excited iodine atoms in the quartz tube with 16 mm diameter from 20 ms right after admission of the CF_3I at pressures up to 2.5 kPa, to 8-10 ms 10 minutes after admission (with the pumping lamps turned off).

3. Laser Power

After replacing the cavity mirrors with a flat opaque mirror and a spherical mirror with radius of curvature of 10 m and transmission of 1.5%, an IMO-2 instrument was used on the side of the spherical mirror to measure the power of laser emission, which was found to be 2 mW at CF_3I pressure of 4.5 kPa.

Radiation power is determined by the formula

$$P = \eta_1 \eta_s f^* h\nu n \gamma V_l,$$

where $\eta_5 = 0.3$ is the fraction of power recorded by the receiver; $V_l = bs_l l = bs_l \nu l$; s_l is the cross sectional area of the laser beam $\varnothing \sim 2{,}5$ mm; $l = 5$ cm; $\gamma = 0.07\ s^{-1}$.

Substitution of numbers gives $P = 1.3\eta_4$ mW, and comparison with the experimental value of P gives us $\eta_4 = 0.6$. The fact that η_4 differs from unity can be attributed both to quenching and to entrainment of excited atoms out of the laser tube.

Analysis of factors that influence the power of the cw photodissociation iodine laser shows that there are at least three reserves of power that could be tapped to increase the power level by two orders of magnitude without appreciable design changes.

A. *An increase in gas velocity.* According to our estimates, the kinematic viscosity of CF_3I gas is ~1 cm^2/s. Tripling gas velocity (to 330 cm/s) while retaining the diameter of the laser tube (16 mm) would not yet turbulize the flow (which would present a hazard due to the increased contribution of quenching on the walls of the tube) since then the Reynolds number would be ~500.

By correspondingly increasing l, we would get a total length of the illuminated part of the laser tube of $l_\Sigma = 60$ cm and coefficient of power increase $k_V = 3$. At the same time, there would be a considerable increase in amplification over the threshold, enabling realization of the following two power reserves.

B. *Increasing the fraction of useful cavity losses (i. e. the transmission of the output mirror).* We would assume that the corresponding coefficient of power increase k_η could be taken as two, which corresponds to $\eta_5 = 0.6$.

C. *Increasing the cross sectional area of the laser beam with large excess over the threshold, and also using longer-focus (or even flat) mirrors with radius of curvature up to 30-40 m.* Apparently, a real increase in beam diameter from 2-3 to 10 mm would give a corresponding coefficient $k_S = (10/2.5)^2 = 16$.

The use of all three reserves ($k_V k_\eta k_S = 96$) we would hope could increase the power to $P \cong 200$ mW.

One could also expect a considerable power increase by using transverse pumping of the working gas as in the cw chemical iodine laser. While leaving the optimum time of illumination and gas velocity essentially unchanged, transverse circulation would appreciably increase the region of optical pumping of the gas stream, and hence the laser power.

REFERENCES

1. Orayevskiy, A. N., KVANTOVAYA ELEKTRONIKA, Vol 5, 1978, p 1850.

2. Andreyeva, T. L., Birich, G. N., Sobel'man, I. I., Sorokin, V. N., Struk, I. N., KVANTOVAYA ELEKTRONIKA, Vol 4, 1977, p 2150.

3. Witte, K. G., Burkhard, K., Luthi, H. R., OPTICS COMMS, Vol 28, 1979, p 202.

4. Benard, D. J., McDermott, W. E., Bousek, R. K., Pchelkin, N. R., J. OPT. SOC. AMER., Vol 68, 1978, p 652.

5. Benard, D. J., McDermott, W. E., Pchelkin, N. R. et al., APPL. PHYS. LETTS, Vol 34, 1979, p 40.

6. Benard, D. J., LASER FOCUS, Vol 15, No 6, 1979.

7. Richardson, R. J., Wiswall, C. E., APPL. PHYS. LETTS, Vol 35, 1979, p 138.

8. Derwent, R. G., Thrush, B. A., CHEM. PHYS. LETTS, Vol 9, 1971, p 591.

9. Andreyeva, T. L., Kuznetsova, S. V., Maslov, A. I., Sobel'man, I. I., Sorokin, V. N., PIS'MA V ZHURNAL EKSPERIMENTAL'NOY I TEORETICHESKOY FIZIKI, Vol 13, 1971, p 631; KHIMIYA VYSOKIKH ENERGIY, Vol 6, 1972, p 418.

10. Yershov, L. S., Zalesskiy, V. Yu., Sokolov, V. N., KVANTOVAYA ELEKTRONIKA, Vol 5, 1978, p 863.

11. Zalesskiy, V. Yu., Yershov, L. S., Kokushkin, A. M., Polikarpov, S. S., KVANTOVAYA ELEKTRONIKA, Vol 8, 1981, p 830.

6610
CSO: 1862/114

UDC 535

LASER PHOSPHATE GLASSES

Moscow LAZERNYYE FOSFATNYYE STEKLA in Russian 1980 (signed to press 28 Nov 80) pp 2-8, 12-15

[Annotation, preface, introduction excerpt and table of contents from book "Laser Phosphate Glasses", by Nikolay Yefimovich Alekseyev, Valentin Pavlovich Gapontsev, Mark Yefremovich Zhabotinskiy, Valeriy Borisovich Kravchenko and Yuriy Petrovich Rudnitskiy, Izdatel'stvo "Nauka", Glavnaya redaktsiya fiziko-matematicheskoy literatury, 2600 copies, 352 pages]

[Text] The book gives a detailed description of the physical properties of new effective laser materials--phosphate glasses activated by rare-earth ions. The possibilities and outlook for using these materials in lasers of various types are demonstrated.

Data are given on the structure of phosphate glasses and on the spectral-luminescence, lasing, thermo-optic and nonlinear optic characteristics of laser phosphate glasses activated with Nd^{3+} ions. An examination is made of processes of energy transport and luminescent quenching in phosphate glasses, and of luminescent sensitization in glasses coactivated by ions of Nd^{3+} and Yb^{3+}, Yb^{3+} and Er^{3+}. Figures 113, tables 47, references 545.

Preface

Phosphate laser glasses, now being more and more extensively used in the major industrialized nations, first made their appearance in the Soviet Union. Phosphate laser glasses are especially important for making high-power and super-powerful lasers, and lasers that operate in the pulse-periodic mode.

At present it can be stated that a certain stage in research and development of phosphate laser glasses has been completed, that their advantages have been recognized, and that a start has been made on industrial production and use in series-produced lasers. This is what makes the proposed book of current interest.

It should be noted that the last systematic survey on laser glasses was published some ten years ago, and like its predecessors it contains practically no information on phosphate laser glasses.

The authors of this book have taken part in research and development of many phosphate laser glasses from the very first, so that a considerable portion of the book is based on their own papers, and the book itself makes no pretense to completeness in coverage of the multifaceted problem of laser glasses.

The book presents the results of physical and spectral-luminescence studies of phosphate laser glasses, investigation of processes of excitation of rare-earth ions, excitation transfer and relaxation processes in laser glasses. These data demonstrate both the advantages of phosphate laser glasses over other glasses, and the potential capabilities that they embody. The book also presents physicochemical and lasing characteristics of these glasses, and gives a comparison with silicate laser glasses.

The book is intended for physicists interested in research on laser materials and processes that take place in lasers, for technologists working on improvement of laser materials and active elements made from them, and for laser designers who need the specific characteristics of active elements without which it would be impossible to design and build lasers.

The book is made up of six chapters.

Chapter 1 examines the requirements for physical parameters of laser glasses that arise from the problem of optimizing the characteristics of lasers of different types and purposes. Among such parameters are for example the spectral-luminescence parameters that determine the energy characteristics of lasers, including efficiency. The corresponding parameters for lasers that operate in the free lasing mode differ appreciably from those necessary for the mode of short and ultrashort pulses.

Particular attention is given to parameters that determine the applicability of glasses in high-power and superpowerful lasers for which nonlinear characteristics, optical and thermal stability and thermo-optic distortions become as important as efficiency.

Chapter 2 deals with the structure of phosphate glasses, which is appreciably different from that of silicate glasses, and in the final analysis is responsible for their advantages. The physicochemical processes that occur as phosphate glasses are being made determine their structure, which has features inherent in inorganic polymers. This in turn determines the near environment of activator ions and the structure of succeeding coordination spheres, thereby determining the excellent spectral-luminescence and lasing characteristics of phosphate laser glasses as well as the capability for controlling their thermo-optic characteristics.

Chapter 3 examines current concepts of the mechanisms and principles of occurrence of processes of non-radiative transfer of the energy of electronic excitation in laser glasses. An analysis is made of different varieties of ion-ion transport, including the process of migration of excitation energy as well as processes of many-photon non-radiative relaxation of excited states of rare-earth ions due to interactions with oscillations of dopant hydroxyl groups and structural elements of the glass proper. The exposition is based

primarily on original results of the authors, most being published here for the first time. For purposes of exhaustive substantiation of the uniqueness of the properties of phosphate glasses, the authors have deemed it necessary to extend the range of objects that are analyzed by including other activators and glass-forming systems, making the results fundamental in nature. The ideas and results of this chapter have played a large part in development of laser phosphate glasses.

Chapter 4 is devoted exclusively to phosphate-neodymium laser glasses and the possibilities for using them in lasers of different types.

The basic content of chapter 5 is made up of data on the thermo-optic properties of phosphate laser glasses; the investigation of such properties has enabled goal-directed synthesis of compositions with characteristics that are optimized for application to specific jobs. In particular, this chapter examines problems that arise in developing glasses for pulse-periodic lasers and high-energy laser systems. In both cases, the advantages of phosphate glass over silicate laser glasses show up with particular clarity.

In chapter 6 an analysis is made of the spectral-luminescence and lasing characteristics of erbium-doped laser phosphate glasses, and an examination is made of the specifics of designing lasers based on these materials. Particular attention is given to erbium lasers stimulated by neodymium laser emission since combined systems of this type can give us sources of emission in the 1.5 μm range that are similar to neodymium lasers with respect to emission characteristics, and in some respects are even superior to them in the mode of amplification of short and ultrashort pulses.

The limited space of the book has precluded examination of the properties of phosphate laser glass coactivated by neodymium and ytterbium, which has good prospects for use in powerful amplifiers. Those interested may refer to the primary sources given in the bibliography.

The list of references, which includes 545 titles, has been brought up to the end of 1979. It contains the most significant papers, but makes no pretense to be complete.

The authors thank all researchers who have given permission to use the graphics from their publications. Appropriate citations are made in the text or in the captions to figures.

The authors thank their colleagues at the Institute of Radio Engineering and Electronics and the Institute of General and Inorganic Chemistry imeni N. S. Kurnakov, and the Rubina Scientific Production Association with whom they have cooperated in research and development of phosphate laser glasses, and also those at the Physics Institute imeni Lebedev and the State Optics Institute imeni Vavilov for constructive criticism.

The materials of the book are distributed among authors as follows: N. Ye. Alekseyev -- §§4.1-4.3, 4.8-4.10; V. P. Gapontsev -- chapters 3, 6;

M. Ye. Zhabotinskiy -- the introduction; V. B. Kravchenko -- §§1.4-1.6, chapter 2, §§5.1, 5.2; Yu. P. Rudnitskiy -- §§1.1-1.3, §§4.4-4.6, §4.7, §5.3.

Introduction

[Excerpt] It was not until 1966 that a collective of workers doing research at the Institute of Radio Engineering and Electronics of the Soviet Academy of Sciences (including the authors) came to the conclusion of the potential capabilities of phosphate laser glasses, if such materials could only be produced. This conclusion came out of research results obtained by this collective in studying luminescence of ions of rare-earth elements and polyphosphoric acids, as well as from known ideas about the structure of phosphate glasses. The work attracted a collective of researchers from the Institute of General and Inorganic Chemistry imeni Kurnakov, among whom a pre-eminent part was played by V. V. Tsapkin and the late G. V. Ellert.

The result of this purposeful research was development of a method of synthesizing phosphate laser glasses based on metaphosphates of alkali and alkali-earth elements. The very next year saw the development of laser elements made of neodymium-activated phosphate glass; these elements had satisfactory physicochemical characteristics and surpassed silicate glass in major laser characteristics. For example, the width of the lasing spectrum of the new glasses was only 4 Å as compared with 80-120 Å for the silicate glass, and efficiency was 1.5-2 times higher under the same conditions of excitation. Soon this glass, designated as grade LGS-40, became the first industrial phosphate laser glass. A disadvantage of the material was relatively low chemical stability.

It should be noted that research on the feasibility of developing phosphate laser glasses was being done independently at the time by Leichbein and his colleagues in France. They published detailed results of spectral-luminescence studies of some phosphate glass compositions activated by neodymium, and reported on attainment of lasing.

Phosphate laser glasses of the Institute of Radio Engineering and Electronics developed jointly with LZOS [expansion not given] -- LGS-40 M, LGS-41 and LGS-42 -- have improved physicochemical characteristics.

The second generation of phosphate glasses of the Institute of Radio Engineering and Electronics was intended especially for use in large industrial and research facilities in which severe requirements arise for both the thermo-optic characteristics of the glass and its efficiency. The athermal characteristics of LGS-I phosphate laser glass have subsequently been reproduced in the corresponding silicate glasses.

Phosphate laser glasses of the second generation should include some neodymium glass compositions developed by the State Optics Institute imeni Vavilov and LZOS, industrially produced as grades GLS-21, GLS-22, GLS-23, GLS-24, LGS-55 and LGS-56.

The next stage in development of phosphate glasses was synthesis of "athermal" phosphate glasses with reduced temperature dependence of thermo-optic characteristics (type LGS-M), with reduced concentration quenching of luminescence, and accordingly with high activator concentration (LGS-K glass developed by the Institute of Radio Engineering and Electronics, and lithium-neodymium phosphate glass developed by the Physics Institute imeni Lebedev). Recently, research on high-concentration glasses has started outside the Soviet Union as well.

Despite the advances that have been made in improving the characteristics of phosphate laser glasses, there is one area where it is no match for yttrium-aluminum garnet, and that it is the mode of rapid pulse recurrence. Of major importance in this mode are the thermomechanical characteristics of the material, especially heat conduction and mechanical strength. Yttrium-aluminum garnet crystals have considerable advantages over glass with respect to both these characteristics.

Conventional methods of hardening glass, such as quenching, have considerable disadvantages, the worst being being the prolonged time for reaching the working state, and impairment of thermo-optic characteristics.

At the Institute of Radio Engineering and Electronics of the Soviet Academy of Sciences, original methods have been developed for hardening active elements made of phosphate laser glass. As a result, elements that operate at a pulse recurrence rate of up to 10 Hz develop nearly the same average power as YAG elements of the same size under identical pumping conditions but at considerably lower cost with more extensive availability.

Two more advantages of phosphate laser glass should be noted.

One of these shows up in large facilities intended for getting short and ultrashort pulses with high energy and high radiation density. The limiting processes here are nonlinear processes that lead to internal damage due to self-focusing. Accordingly, the limiting energy flux densities in phosphate glass are about twice as high as in silicate glass.

The second advantage is due to the more effective energy transfer between rare-earth ions in phosphate glass than in silicate glass. Utilization of this advantage has enabled development of high-quality erbium laser glass sensitized by ytterbium ions. On the basis of this glass the authors succeeded as early as 1969 in being the first to achieve lasing in the 1.54 μm region using free-lasing neodymium glass lasers as the source of excitation. Subsequently, such erbium glass was brought to the state of industrial production (grade LGS-E). This step required in particular that a solution be found for the complicated job of deep desiccation. Sysystematic studies were also done on the spectral-luminescence characteristics of erbium glasses, as well as a number of questions involved in optimizing the emission characteristics of erbium lasers with both laser and lamp pumping. In 1973, one of the authors gave convincing arguments for the feasibility of using erbium re-radiators of neodymium lasers as amplification stages of powerful laser systems intended for a variety of applications.

Another sensitized laser phosphate glass developed and systematically studied in these same years at the Institute of Radio Engineering and Electronics is glass activated by ions of neodymium (sensitizer) and ytterbium (activator) that is promising for use in the final stages of power amplifiers of pulses with average duration from 10^{-6} to 10^{-4} s.

Recently our industry has developed and produced several types of phosphate laser glass that are being used in active elements for different purposes.

Outside the Soviet Union, the leaning has been toward silicate glass, and the development of phosphate glasses has not been taken seriously.

However, quite recently the situattion has changed. Industrial phosphate glasses have been produced in Japan, and more recently in the United States. These glasses are being used in large process lasers and facilities for heating thermonuclear plasma in the United States, Japan and France. Developers of laser systems for other applications have also begun to take a new look at phosphate glasses.

The possibilities of phosphate laser glass are far from exhausted. In many laboratories fundamental research is continuing for further improvement of the characteristics of phosphate glasses and glasses with several vitrifying agents including phosphorus. We should expect a considerable increase in the average power and pulse energy of lasers based on glasses of these types, attainment of lasing on new long waves, a further reduction in the duration of ultrashort pulses, utilization of active fibers and the like.

Contents page

6610
CSO: 1862/129

UDC 537.876.23.029.7:551.510.5

PROPAGATION OF LASER RADIATION IN ATMOSPHERE

Moscow RASPROSTRANENIYE LAZERNOGO IZLUCHENIYA V ATMOSFERE in Russian 1981 (signed to press 6 Apr 81) pp 2-4, 285-288

[Annotation, preface and table of contents from book "Propagation of Laser Radiation in Atmosphere", by Vladimir Yevseyevich Zuyev, Izdatel'stvo "Radio i svyaz'", 3256 copies, 288 pages]

[Text] The book generalizes principal results of theoretical and experimental research on the complex problem of propagation of laser radiation in the atmosphere. The basis of the exposition is research by the author and his students done at the Institute of Optics of the Atmosphere, Siberian Department of the USSR Academy of Sciences, as well as other results published both in the USSR and elsewhere. An examination is made of the major aspects of linear interaction of laser emission with the atmosphere: refraction of laser beams, absorption and scattering of laser radiation, fluctuations of laser beam parameters due to atmospheric turbulence. An analysis is made of nonlinear effects that accompany propagation of intense laser radiation in the atmosphere. The book discusses problems in using lasers to study the atmosphere and the processes that take place there, including processes of pollution by products of man's industrial activity.

The book is intended for scientific workers and specialists working in the field of physics and optics of the atmosphere, meteorology, astronomy, geodesy, optoelectronics and laser technology. Figures 71, tables 20, references 829.

Preface

Although no more than 20 years have passed since the first laser was made, laser technology has found a multitude of applications in science and in practice. Problems of laser radiation propagation in atmosphere have taken a special place in this situation. Successful utilization of laser systems for communication and transmission of information, detection and ranging, surveying and navigation and the like necessitates quantitative data on the influence that atmosphere has on the parameters of a laser beam carrying some useful information. Besides, the totality of data on propagation of laser emission in the atmosphere could be extensively used for solving problems that have nothing to do with the use of lasers. Among such problems is determination of the radiation term in weather forecasting equations, solution

of inverse problems of satellite meteorology, determination of the heat balance of the earth as a planet, getting rid of the aggravating influence of the atmosphere in data of astronomical observations and much more.

Propagation of laser radiation in the atmosphere is accompanied by quite an array of linear and nonlinear interaction phenomena. And not one of these effects shows up by itself. According to purely qualitative features, these phenoemna can be divided into the following major groups: refraction of rays of the laser beam; absorption of laser beam energy by atmospheric gases; scattering of laser beam energy by aerosol particles, fluctuations in air density and the like; fluctuations of laser beam parameters caused by atmospheric turbulence.

Each of the enumerated groups of phenomena of interaction between laser radiation and the atmosphere can show up in regions of both linear and nonlinear optics. On the other hand, each of these groups has clear specific features that must be taken into consideration in corresponding theoretical and experimental studies.

The high monochromatism, spatial boundedness, capability of getting large powers and energies and short durations of laser pulses have occasioned rigid requirements in formulating the corresponding theoretical and experimental studies on the propagation of laser emission in the atmosphere. In most cases, it has turned out that information accumulated over many years of research on propagation of optical waves in the atmosphere does not suffice for the corresponding quantitative evaluations as applied to lasers.

The broad front of research that has developed in the complex program of propagation of laser radiation in the atmosphere has not only advanced the problem itself, but has also been a stimulus to development of new areas in science and engineering, foremost among which are those involving remote laser probing of the atmosphere, and ultrahigh-resolution laser spectroscopy. It is only just and proper to include in such new areas the field of nonlinear optics of the atmosphere that has arisen and taken form over the last 10-12 years.

Progress in solving the problem of propagation of laser radiation in the atmosphere is documented in thousands of articles published in various journals, dozens of surveys, and several monographs dealing with individual aspects of this complex issue. In this connection, it seems topical to attempt a monographic generalization of the problem as a whole. The proposed book is written to do just that.

The monograph generalizes major results of theoretical and experimental research done in the Soviet Union and elsewhere. A considerable portion of the materials appearing in the monograph were obtained by the author and his numerous students and colleagues at the Institute of Optics of the Atmosphere, Siberian Department, USSR Academy of Sciences.

The author considers it his exceptionally pleasant duty to express sincere gratitude to his coworkers A. B. Antipov, Yu. S. Balin, O. K. Voytsekhovskaya,

V. N. Genin, I. I. Ippolitov, B. V. Kaluy, G. M. Krekov, A. V. Kuzikovskiy, V. P. Lopasov, V. P. Lukin, G. G. Matviyenko, I. E. Naats, L. I. Nesmelova, A. A. Pershin, V. V. Pokasov, I. V. Samokhvalov, V. A. Sapozhnikova, S. D. Tvorogov and V. V. Fomin for all kinds of assistance in working on the manuscript of the book. The author is especially grateful to Yu. F. Arshinov, M. V. Kabanov, Yu. D. Kopytin, Yu. S. Makushkin and V. L. Mironov for their effective help in preparing some of the materials, and for constructive criticism of the manuscript on specific chapters, improving the quality of the finished book. The author is greatly indebted to Professor Yu. G. Yakushenkov for valuable critical comments made in reviewing the monograph.

All comments and suggestions on the content of the book can be addressed to: Moskva, 101000, Glavpochamt, a/ya 693.

Contents page

6610
CSO: 1862/132

SPHERICAL MICROTARGET IRRADIATION BY 2-TERAWATT IODINE LASER

Moscow ZHURNAL EKSPERIMENTAL'NOY I TEORETICHESKOY FIZIKI in Russian Vol 82, No 2, Feb 82 (manuscript received 2 Oct 81) pp 459-461

[Article by F. M. Abzayev, N. N. Beznasyuk, V. G. Bezuglov, A. V. Bessarab, A. V. Veselov, L. M. Vinogradskiy, V. A. Gaydash, I. V. Galakhov, A. S. Gasheyev, V. A. Yeroshenko, A. I. Zaretskiy, G. A. Kirillov, S. B. Kormer, G. G. Kochemasov, S. M. Kulikov, Yu. V. Kuratov, V. M. Murugov, V. D. Nikolayev, G. P. Okutin, V. I. Pankratov, V. T. Punin, N. N. Rukavishnikov, A. V. Ryadov, V. A. Samylin, A. Ye. Senik, S. A. Sukharev and A. I. Funtikov]

[Text] The power of the Iskra-IV iodine laser is increased to ~2 TW by shortening the duration of the laser pulse without losses in energy. The authors are the first to attain a neutron yield of 10^5 neutrons in the "exploding shell" state in iodine laser irradiation of DT-filled spherical microtargets.

Experiments on laser irradiation of spherical microtargets 150-170 μm in diameter with wall thickness of 1 μm filled with DT-gas to pressures of 10-40 atm were done on the Iskra-IV single-channel iodine laser [Ref. 1] with emission wavelength of 1.315 μm.

To irradiate the spherical targets, the output beam with diameter of 270 mm was divided by beam splitters into four beams that were focused on the target by parabolic mirrors with F = 270 mm. Accuracy of aiming at the target in these experiments was 10-20 μm. To improve uniformity of irradiation, the target was placed in a plane where spot size was 200 μm.

To prevent self-excitation of the system made up of the master laser, amplification stages and target, optical decouplers were used in the form of bismuth films sputtered on a glass backing, and also saturable shutters based on dyes. This gave an energy contrast of $K_E \gtrsim 10^7$ and power contrast of $K_p \gtrsim 2 \cdot 10^6$ in the output beam. Beam divergence at the output of the facility was $\approx(1\text{-}2) \cdot 10^{-4}$ radian.

In the first experiments, 500 joules of laser energy were injected into the target chamber. At this energy level, the preferred mode for getting high neutron yields is the "exploding shell" state [Ref. 2]. This state can be

realized if the fast electron temperature is sufficiently high: ≥10 keV, which requires a power density of $\geq 10^{15}$ W/cm^2 on the surface of the microtarget. To get such radiation power fluxes at the given energies and target sizes, it is necessary to have a laser pulse duration of ≤0.3 ns. A reduction of pulse duration was achieved both by increasing the steepness of the master laser pulse and by selecting the working conditions of the amplification stages of the iodine laser. As a result of the steps that were taken, a pulse duration of $\tau = 0.3 \pm 0.05$ ns was attained at the laser output, which agrees with results of calculations. It is significant that in contrast to neodymium lasers the energy at the output of the facility did not decrease when pulse duration was shortened from 1 to 0.25 ns.

The energy balance in the laser plasma was determined by specially developed calorimeters. For the experiment in which the greatest neutron yield was registered (~$1.5 \cdot 10^5$ neutrons/pulse), the energy injected into the chamber was 480 J, of which 280 J reached the target, and 50 J was absorbed by the target. Flux density of laser radiation on the target was ≈10^{15} W/cm^2.

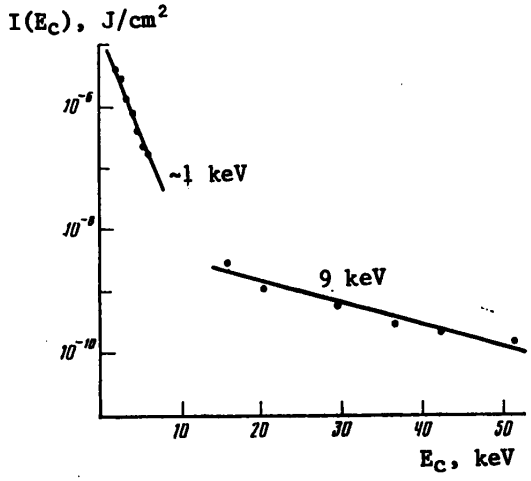

Fig. 1. Plasma x-ray spectrum

The x-ray spectrum measured by the method of filters is shown on Fig. 1. The temperatures corresponding to soft and hard parts of the spectrum were $T \approx 1$ keV and $T_h \approx 9$ keV respectively. The temperature of the corona close to the critical surface as determined from the line spectrum (relative intensities of the resonance lines of helium-like and hydrogen-like silicon ions) was 0.8 keV. The temperature near the surface where electron density was ≈ρ/4 as determined from the distance between spectral maxima $^3/_2\omega$, was 0.9 keV.

The x-ray self-image of the target produced by a camera obscura (see Fig. 2) showed that the DT-gas is comparessed by a factor of about 30.

The results of measuring the neutron yield are shown on Fig. 3, where the experimental values of neutron yield are plotted along the axis of ordinates,

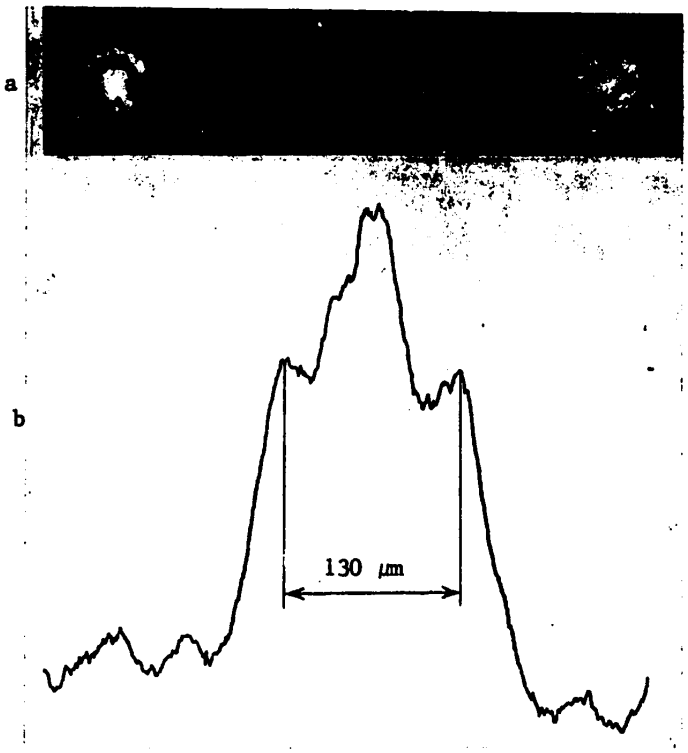

Fig. 2. X-ray self-image of target (a) and characteristic densitometer plot (b)

Fig. 3. Comparison of experimental results on N-yield with Livermore laboratory results: o--experiments on Iskra-IV laser; •--data of Livermore laboratory; the line parallel to the axis of abscissas shows the sensitivity threshold

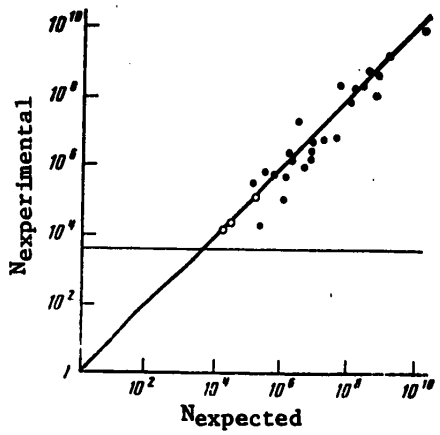

and the expected values are plotted along the axis of abscissas. These values were determined from a semiempirical model [Ref. 2] describing the results of experiments done at Livermore Laboratory in the United States in the "exploding shell" state, which are shown on the same figure. As can be seen, our results are in good agreement with the experimental data of Livermore Laboratory. The fast electron temperature measured in the experiments (≈9 keV) for the given thickness of glass microtargets (≈1 μm) shows that the "exploding shell" state was realized in our experiments as well.

As a result of the research, the power of the Iskra-IV facility has been increased to 2 TW by shortening the duration of the laser pulse from 1 to 0.3 ns with almost no losses of energy. This is the first time that an iodine laser has been used to get a neutron yield of 10^5 and volumetric compression of about 30 times in irradiation of spherical microtargets filled with DT-gas.

REFERENCES

1. Kormer, S. B., IZVESTIYA AKADEMII NAUK SSSR: SERIYA FIZICHESKAYA, Vol 44, 1980, p 2002.

2. Storm, E. K. et al., PHYS. REV. LETT., Vol 40, 1978, p 1570.

6610
CSO: 1862/130

UDC 517.9:621.378.325

RADIATION DIVERGENCE IN POWERFUL LASER AMPLIFIERS USING ACTIVE ELEMENTS OF RECTANGULAR CROSS SECTION

Moscow DOKLADY AKADEMII NAUK SSSR in Russian Vol 261, No 6, Dec 81 (manuscript received 7 Sep 81) pp 1333-1336

[Article by Academician A. N. Tikhonov, V. Ya. Arsenin, V. I. Pavlov and A. Kh. Pergament, Institute of Applied Mathematics imeni M. V. Keldysh, USSR Academy of Sciences, Moscow]

[Text] The investigation of typical singularities of wave fronts of radiation propagating in active elements of laser system amplification stages, and thereby the feasibility of focusing a powerful light beam on a small target is an important job in planning modern laser facilities and solving problems of controlling them.

Due to inhomogeneity of the temperature field, stresses are set up in the volume of the active element that give rise to volumetric thermal distortions of the optical medium (corresponding changes n' in the index of refraction for different polarizations of emission) [Ref. 1] and lead to end surface deformations [Ref. 2-4]. Since there is a considerable difference between the typical times of the laser pulse ($\sim 10^{-9}$ s), the pumping pulse ($\sim 10^{-3}$ s) and elastic wave propagation ($\sim 10^{-5}$ s), end surface deformations and volumetric thermal distortions can be taken as static during pulse emission. Nonlinearity of the medium leads to self-focusing.

Our research shows that when powerful radiation propagates in an active element of rectangular cross section, the combined action of end surface deformation and large-scale self-focusing may lead to a system of appreciable emission intensity maxima in the far zone, which is experimentally confirmed. A statistical approach to description of small-scale self-focusing enables correct calculation of the growth of noise intensity throughout the volume of the active element, as well as evaluation of their characteristic spatial scale.

This paper gives the results of comprehensive calculations of propagation of power laser emission in an active element with consideration of volumetric thermal distortions of the optical medium, end surface deformations, large-scale self-focusing and growth of minor small-scale perturbations of random nature. Calculations were done for an active element of rectangular cross section made of neodymium silicate glass. Such elements were selected because

they are extensively used in present-day laser facilities [Ref. 5, 6], and in addition they are distinguished by considerable end surface deformations on the large side of the cross section [Ref. 3, 4]. Theoretical studies and experimental data [Ref. 3, 4] show that the shape of the distorted end faces is close to a parabolic cylinder, and the amount of flexure may reach several wavelengths, depending on pumping conditions. Calculations of emission are based on the parabolic approximation.

Propagation of powerful emission in an active element in the presence of random small-scale perturbations is preferably described by equations for the statistical moments of the electric field [Ref. 7] derived by averaging the parabolic equation. Calculations have shown that in such an approach the increase in noise intensity is more appreciable than in other approaches; the influence of thermal distortions in this case is slight. Evaluation of the distribution of noise intensity in the far zone (Fig. 1) is in good qualitative agreement with experimental data given in Ref. 8. The position of the maximum values of noise intensity x_0 is determined by the amplitude of the intensity and the spatial distribution of the output radiation. As long as the noise dispersion remains appreciably less than the mean field (isolated spikes in the field may be appreciable), the phase front of the average field at the output of the active element varies insignificantly in dependence on the level of noise dispersion. As a consequence, there is also little variation in the distribution of intensity of the average field in the far zone. Therefore, under these conditions, calculations of the influence that thermal effects and large-scale self-focusing have on the phase fronts can be done without considering the presence of noises.

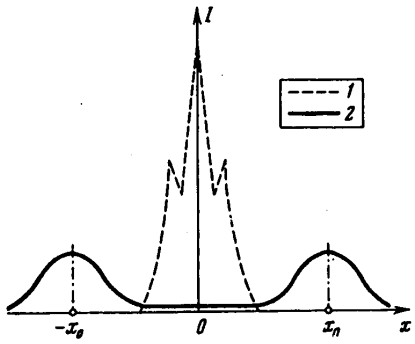

Fig. 1. Central cross section along the x-axis for distribution of average field intensity (1) and noise intensity (2) in the far zone. There are no thermal distortions. Scale is not observed

Let the x-axis be directed along the short side of the cross section of the active element, while the y-axis is directed along the long side, and the z-axis is along the direction of emission propagation. The modification of the conventional quasi-optical equation for complex amplitude of the field polarized along one of the axes (x or y) with consideration of thermal effects in the case of symmetric pumping takes the form

$$2ik\frac{\partial E}{\partial z} + \Delta_\perp E + \frac{k^2}{n_0} n_2 |E|^2 E + \frac{k^2 \cdot 4f}{L} E + \frac{k^2 2n'}{n_0} E - i\beta k E = 0.$$

Here $\Delta_\perp$ is the transverse laplacian; L is the length of the active element; f is a function that describes the distorted end surfaces; the index of refraction of the medium $n_{x,y} = n_0 + \frac{1}{2}n_2|E|^2 + n'_{x,y}$; $k = n_0\omega/c$ is the wave number in the medium with index of refraction n_0; β is gain. The equation is solved

in the region of the rectangular parallelepiped, and end surface deformations are accounted for by the term $\frac{k^2 \cdot 4f}{L}E$. In doing numerical calculations, the boundary conditions were assigned in the form $E|_S = 0$, where S is the lateral surface of the active element excluding the input and output faces. Gaussian beams were assigned on the input face with intensity level of ~1 GW/cm^2. The temperature distribution in the pumping zone was taken as parabolic along the short side of the cross section of the active element [Ref. 9], $n'_{x,y} = (P \pm Q)T(x)$, where P and Q are the thermo-optical constants; the characteristics of the laser glass are taken from Ref. 10. Wavelength $\lambda = 1.06$ μm.

The following was established by numerical calculations. Without end surface deformations, both in the presence and in the absence of volumetric thermal distortions, there is a single maximum in the intensity distribution in the far zone with greatest intensity, and a number of local maxima at which the intensity values are considerably lower. In the presence of end surface deformations, as their magnitude increases there is at first somewhat of a reduction in width of the intensity distribution in the far zone. Then as end surface deformations increase there is an increase in the width of the distribution, and the principal intensity maximum splits into two local maxima of appreciable amplitude with equal intensity situated along the short side of the cross section (Fig. 2. With a further increase in end surface deformations

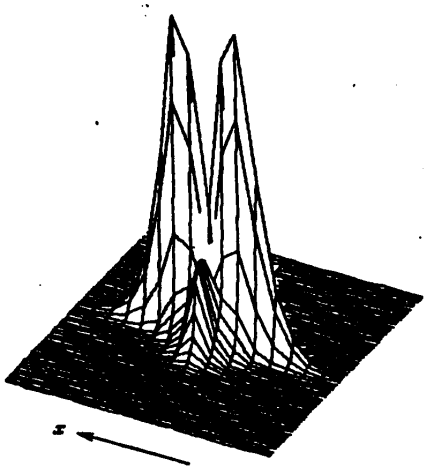

Fig. 2. Calculation of emission intensity distribution in far zone. Magnitude of end surface deformations: $\max|f| \cong 1.4\lambda$; $n' = 0.5 \cdot 10^{-7} T(x)$; $T(x) = 1.82\left[1 + \left(\frac{x}{h/2}\right)^2\right]$; $\beta = 0.025\left[1 + \left(\frac{x}{h/2}\right)^2\right]$; $|x| \leq h/2$; h is the short dimension of active element cross section. Distance between maxima ~200 μm at focal length of 200 cm.

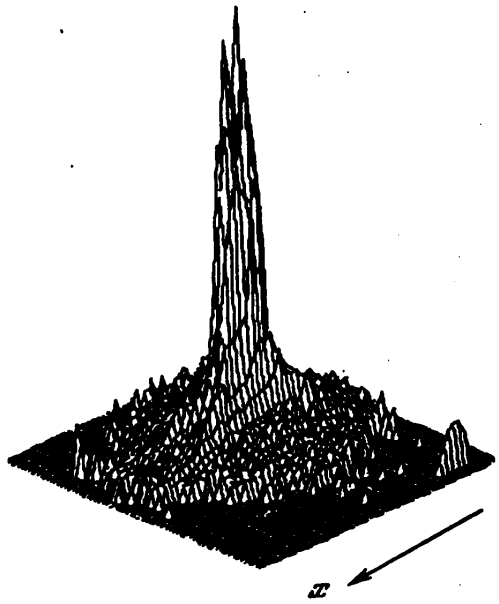

Fig. 3. Emission intensity distribution in far zone (experiment). The angular distance between maxima is in complete agreement with computational results of Fig. 2.

a greater number of local maxima of considerable intensity may show up. Such intensity distribution in the far zone is indicative of considerable radiation divergence.

Bifurcation in the distribution of intensity in the far zone along the short side is confirmed by experimental data (Fig. 3) [Ref. 11].

Within a certain range of variation in their magnitude, volumetric thermal distortions may lead to a reduction in the divergence of powerful radiation, and in this case, bifurcation in the distribution of intensity in the far zone begins at greater magnitude of end surface deformations. Within a certain range of variation in the magnitudes of end surface deformations and volumetric thermal distortions, the reduction of divergence of powerful emission demonstrates some mutual compensation of distortions of the phase front due to large-scale self-focusing and thermal effects.

Appreciable mutual compensation of distortions of the phase front can be realized by selecting spatial distribution of the input beam intensity at certain magnitudes of end surface deformation and volumetric thermal distortions that bring the radiation divergence close to the diffraction limit. In model calculations this is realized by taking the input intensity profile in the form of a paraboloid, and the magnitude of end surface deformations equal to $0.47 \cdot \lambda$ and $n' \approx 7 \cdot 10^{-7} \cdot 1{,}82 \left[1 + \left(\frac{x}{h/2}\right)^2\right]$.

REFERENCES

1. Anan'yev, Yu. A., Grishmanova, N. I., ZHURNAL PRIKLADNOY SPEKTROSKOPII, Vol 12, No 4, 1970, p 668.

2. Anan'yev, Yu. A. et al., Ibid., Vol 5, No 1, 1966, p 51.

3. Pavlov, V. I., Pergament, A. Kh., Ponomarev, A. V., Chernyak, V. M., Preprint, Institute of Problems in Mechanics, USSR Academy of Sciences, No 8, 1978.

4. Pavlov, V. I., Pergament, A. Kh., Ibid., No 64, 1979.

5. Korobkin, V. V. et al., "Tezisy dokladov Vos'moy Vsesoyuznoy konferentsii po kogerentnoy i nelineynoy optike" [Abstracts of Reports to the Eighth All-Union Conference on Coherent and Nonlinear Optics], Tbilisi, Metsniyereba, Vol 2, 1976, p 235.

6. Burdonsky, I. N. et al., APPL. OPT., Vol 15, No 5. 1976, p 1450.

7. Pavlov, V. I., Preprint, Institute of Problems in Mechanics, USSR Academy of Sciences, No 104, 1980.

8. Fleck, J. A. Jr., Morris, J. R., Bliss, IEEE J. QUANT. ELECTRON., Vol QE-14, No 5, 1978, p 353.

9. Ponomarev, A. V., Chernyak, V. M., Preprint, Institute of Atomic Energy, IAE-3079, Moscow, 1979.

10. Avakyants, L. I. et al., KVANTOVAYA ELEKTRONIKA, Vol 5, No 4, 1978, p 725.

11. Tikhonov, A. N., Arsenin, V. Ya. et al., "Thirteenth European Conference on Laser Interaction With Matter", Leipzig, 1979, p 98.

6610
CSO: 1862/96

UDC 621.373.826

USING SOLID FUEL IN GASDYNAMIC LASER

Moscow KVANTOVAYA ELEKTRONIKA in Russian Vol 9, No 1(115), Jan 82 (manuscript received 23 Mar 81) pp 125-129

[Article by M. Syczewski and Cz. Bartoszek, Polish Military Technical Academy, Warsaw]

[Text] Stimulated emission is realized in a gasdynamic laser using solid-state fuel of the ballistic powder type. Thermodynamic calculations are done on the composition of products and the temperature when fuel is burned in different gases. Analogous combustion conditions are realized in an experiment. Based on analysis of the results of the experimental studies and calculations, an interpretation is given for the dependence of laser energy on the N_2/CO_2 ratio and temperature in the combustion chamber, and the role of the CO_2/H_2O ratio is determined.

Previously we had discussed the results of studies of gasdynamic lasers using gaseous fuels [Ref. 1-4]. In this paper we have attempted to achieve lasing by using solid fuel. There have been studies of solid fuels that belong to the class of shock-sensitive initiating explosives [Ref. 5, 6]. Therefore, practical use of these substances involves the hazard of uncontrolled explosions. Also, it is impossible to use large charges of such substances that would enable prolonged laser operation. It is our opinion that the solid fuel studied in our research is free of these disadvantages.

Ref. 7 reported on use of nitro compounds to fuel gasdynamic lasers, but unfortunately it is not known which nitro compounds they were. If the definition is taken literally, the authors of Ref. 7 were not studying the organic nitrates treated in our paper. Since the mechanisms of combustion of organic nitrates and aromatic nitro compounds are different, as are the conditions of the experiment, our results are not comparable with those of Ref. 7.

In addition to achieving lasing on combustion products of fuel of the ordinary smokeless powder type, we investigated the influence that the time of stay of the products in the combustion chamber, gas composition and temperature of the gas mixture have on the energy characteristics of the laser. The results allow us to optimize the conditions of gasdynamic laser operation for

a variety of energy characteristics and fuel compositions. In our opinion, most of the observed patterns can be attributed to chemical causes: composition, properties and interaction of combustion products.

Experimental Technique

The experiments were done on a facility described in Ref. 1, with the exception that a glowing wire was used in place of spark ignition. The laser operated in the pulse-periodic mode. The solid fuel was injected into the combustion chamber with 30-liter volume through an orifice covered by a door. After closing, the chamber was filled with the appropriate gas mixture.

The combustion chamber was connected via an electromagnetic valve to a two-dimensional flat nozzle (200 mm wide with critical cross section 0.7 mm high). The optical cavity was placed at the end of the nozzle, and beyond the cavity was a low-pressure chamber ($p \cong 2$ kPa). After fuel ignition (charge of ~30 g) in a plate 1 mm thick, the pressure in the chamber rose until the instant of total combustion (duration of the process ~1.2 s). The valve was opened at the required instant after ignition (before or after completion of combustion). The generated signal was recorded by a semiconductor (mercury-cadmium telluride) radiation sensor, energy was measured by calorimeter, and pressure by a strain-gage sensor (Fig. 1).

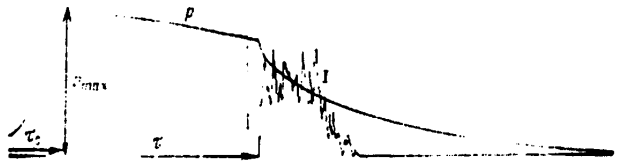

Fig. 1. Typical oscillogram of laser operation: τ_c--powder combustion time; τ--valve opening delay time (relative to time of powder ignition); p--pressure in combustion chamber; I--intensity of laser emission

Results of Thermochemical Calculations and Status of the Question

According to thermochemical calculations, combustion of the investigated fuel (40% nitroglycerin, 60% nitrocellulose) is described by the equation (for 1 kg)

$$C_{18.74}H_{25,98}O_{37,60}N_{10,56} \rightarrow 7{,}36\,CO_2 + 11{,}37\,CO + 10{,}77H_2O + 2{,}21H_2 + \\ +0{,}29\,O_2 + 0{,}15\,NO + 5{,}20\,N_2.$$

The temperature of the combustion products is ~3100 K. To attain the appropriate composition and temperature of combustion products, the fuel must be heated in the proper gas atmosphere. The table gives some results of calculations.

Product composition and combustion temperature of principal investigated mixtures

Products	Composition 1	Composition 2	Composition 3	Composition 4
CO_2, %	19,7	7,0	8,8	16,3
N_2, %	13,9	51,8	81,6	75,0
CO, %	30,4	14,1	0,5	0,3
H_2O, %	28,9	14,4	6,3	5,9
H_2, %	5,9	—	—	—
O_2, %	0,8	12,7	2,8	2,5
NO, %	0,4	—	—	—
N_2/CO_2	0,71	7,38	9,28	4,50
CO_2/H_2O	0,68	0,50	1,42	2,85
$\frac{CO + N_2}{CO_2}$	2,24	9,59	9,29	4,50
T, K	3100	3720	2500	2280

Composition 1 corresponds to burning 1 kg of powder without air. Composition 2 corresponds to combustion of powder in a quantity of air that exceeds the stoichiometric amount by 20%. Composition 3 is obtained like composition 2, but with the addition of nitrogen to reduce the temperature of the gas mixture to 2500 K.

Composition 4 is similar to composition 3; however, some of the nitrogen is replaced by carbon dioxide (in the same molar quantity) to give a ratio of $N_2/CO_2 = 4.5$. According to research that we did using acetylene [Ref. 3] such a ratio is optimum. Experiments done with compositions 2-4 were carried out in various versions.

Results of Experiments and Discussion

Since solid fuel burns more slowly than gas, the question arises of when the valve should be opened during combustion of the charge to trigger the laser so that stimulated emission is maximized.

Fig. 1 shows an oscillogram in which the valve is opened after completion of combustion within time τ_c relative to the instant of ignition.

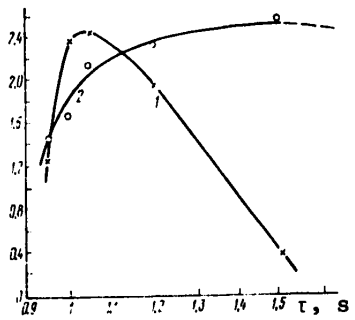

Fig. 2. Integrated laser emission energy (1) and maximum pressure in combustion chamber (2) as functions of delay of valve opening relative to the instant of powder ignition

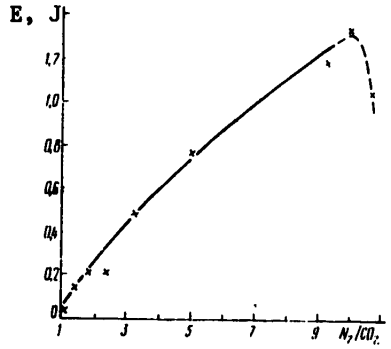

Fig. 3. Integrated energy of laser emission as a function of ratio of N_2/CO_2 in the combustion products

Fig. 2 shows the way that radiation energy (throughout the time of laser operation) depends on the delay of valve opening relative to the instant of powder ignition. This curve was obtained for composition 4 with the position of points averaged from three measurements. Maximum pressures in the chamber P_{max} were determined for the same points.

It is not quite clear why there is a sharp drop in laser energy at $\tau > \tau_c$. In all probability, such an abrupt fall-off of laser energy cannot be attributed to heat transfer from the combustion products to the walls of the chamber. Apparently consideration must be taken of the kinetics of reactions of additional combustion of gases that arise on the first stage of gasification of the powder (dissociation processes, formation of H_2O instead of H_2 and so on).

Major emphasis is given to the investigation of optimum ratios of N_2/CO_2 and CO_2/H_2O in the combustion products (working gases).

The principal composition that was studied was №4 in which the N_2/CO_2 ratio was varied without changing the total number of moles of the gases. This caused only a slight change in temperature of the products (2250-2500 K) due to the different specific heats of N_2 and CO_2.

The curve for $f(N_2/CO_2)$ (Fig. 3) is surprising in view of results found with gas fuel [Ref. 3]. When acetylene is being burned, the optimum ratio of $N_2/CO_2 = 4.5$, while in the investigated solid fuel it is 10. We assume that the reason for this difference is larger water content in the powder combustion products ($CO_2/H_2O = 2.84$) than in combustion products of the optimum composition of an acetylene mixture ($CO_2/H_2O = 4.5$). An increase in the relative amount of water increases the optimum N_2/CO_2 ratio. This is indirectly confirmed by the results of Ref. 8, although the values of the given ratios differ.

The practical value of these studies is that the heat released in burning of powder is sufficient not only for heating the combustion products, but also for heating an additional quantity of gas (N_2-CO_2 mixture). Under such

conditions it will be more advantageous if nitrogen is used as the dopant gas, and an additional amount of CO_2 in the cold state is mixed into the supersonic flow in the nozzle.

In addition to the investigation of composition 4, studies were also done on composition 2 and similar high-temperature compositions. In place of some of the N_2 of composition 2, an amount of CO_2 was added such as to compensate for its dissociation, giving a ratio $N_2/CO_2 = 4.5$ (as in composition 4).

Since under corresponding conditions CO may act in the same role as N_2 [Ref. 9], in this case it is advisable to consider the ratio $(CO+N_2)/CO_2$. When a high-temperature mixture is used, the given ratios assume an optimum value of 3.0-3.5.

Thus it has been established that with increasing temperature of the combustion products, the optimum ratios N_2/CO_2 and $(CO+N_2)/CO_2$ decrease, while $CO_2/H_2O \cong 1.0$ (with consideration of the dissociation of H_2O). Putting it briefly, the detrimental effect of water on laser emission decreases with increasing temperatures. High-temperature compositions are interesting in that in optimum compositions the level of the generated energy is equal to the energy obtained in low-temperature optimum compositions (see Fig. 3), whereas in the latter case the gas expenditure is more than double that in the former (in composition 4, 1.442 kg of air and 3.212 kg of N_2 are added per kg of powder, while only 1.442 kg of air is added in composition 2).

Let us try to explain theoretically why water does not deactivate CO_2 molecules as the temperature of the gases increases. In accordance with references cited in Ref. 11, we know that relatively strong interaction of a chemical nature takes place between molecules of H_2O and CO_2. There is a certain deformation of CO_2 molecules in this process:

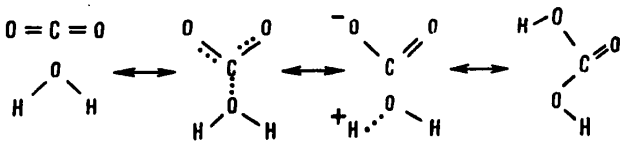

The energy of vibrational excitation of carbon dioxide molecules is dissipated in this interaction, the reaction energy being of the order of 33.44 J/mole (8 kcal/mole). At high gas temperature, when the energy of translational motion (kT) approaches the indicated value, the molecules cease to interact. In the sudden cooling in the nozzle, there is no time for interaction to be restored. The result is high inversion of vibrational levels of CO_2 molecules despite the large water content in the working gases.

The authors thank V. K. Konyukhov for constructive criticism during preparation of the manuscript.

REFERENCES

1. Syczewski, M., ARCHIWUM TERMODYNAMIKI I SPALANIA, Vol 6, 1975, p 586.

2. Syczewski, M., Ibid., Vol 8, 1977, p 287.

3. Syczewski, M., Rutkowski, J., Ibid., p 459.

4. Bartoszek, Cz., Syczewski, M., BIULETYN WOJSKOWEJ AKADEMII TECHNICZNEJ, Vol 28, 1979, p 2.

5. Yellin, N., Gabai, A., J. APPL. CHEM. BIOTECHNOL., Vol 25, 1975, p 103.

6. Dzhidzhoyev, M. S., Korolev, V. V., Mirkov, V. N., Plotonenko, V. T., Khokhlov, R. V., PIS'MA V ZHURNAL EKSPERIMENTAL'NOY I TEORETICHESKOY FIZIKI, Vol 13, 1971, p 73.

7. Beletskiy, A. K., Vazyulin, V. A., Gavrikov, V. F., Didyukov, A. I., Dronov, A. P., Orlov, V. K., Piskunov, A. K., Cherkasov, Ye. M., KVANTOVAYA ELEKTRONIKA, Vol 1, 1974, p 439.

8. Meinzer, R. A., AIAA J., Vol 10, 1972, p 388.

9. Kozlov, I., Ivanov, V. N., Selezneva, I. K., FIZIKA GORENIYA I VZRYVA, Vol 18, No 4, 1979, p 88.

10. Kondrat'yev, N., Nikitin, Ye. Ye., "Kinetika i mekhanizm gazofaznykh reaktsiy" [Kinetics and Mechanism of Gas-Phase Reactions], Moscow, Nauka, 1974.

6610
CSO: 1862/114

OPTICS AND SPECTROSCOPY

UDC 543.42:621.375.9:535.375.5:537.228.5:539.184.22

LASER-INDUCED NONLINEAR RESONANCES IN CONTINUOUS SPECTRA

Novosibirsk LAZERNOYE INDUTSIROVANIYE NELINEYNYKH REZONANSOV V SPLOSHNYKH SPEKTRAKH in Russian 1981 (signed to press 1 Jul 81) pp 2-4, 156-180

[Annotation, preface and table of contents from book "Laser Induction of Nonlinear Resonances in Continuous Spectra", by Yuriy Isayevich Geller and Aleksandr Kuz'mich Popov, Institute of Physics imeni L. V. Kirenskiy, Siberian Department, USSR Academy of Sciences, Izdatel'stvo "Nauka", 1700 copies, 160 pages]

[Text] This monograph is devoted to development of the theoretical principles of nonlinear laser spectroscopy and resonant nonlinear optics for the case of transitions to a continuous spectrum (continuum) and to auto-ionization states. The authors give methods of using laser emission to form narrow nonlinear resonances similar to artificial auto-ionization levels in arbitrary sections of continuous spectra. An investigation is made of the effect that laser emission has on actual auto-ionization states. The book discusses the use of these effects in nonlinear spectroscopy, for generating coherent vacuum ultraviolet and soft x-radiation by methods of resonant nonlinear optics, for selective action of radiation on matter.

The book is intended for scientific workers interested in current problems of laser physics, nonlinear spectroscopy and nonlinear optics, as well as for instructors and students.

Figures 20, tables 2, references 130.

Preface

Lasers that can be tuned with respect to frequency of quasimonochromatic radiation have opened up extensive possibilities for studying and using resonant nonlinear processes that accompany interaction of intense optical emission with atomic-molecular systems. These processes are actively used in studying matter by methods of nonlinear spectroscopy [Ref. 1, 2], in selective action on matter to initiate controlled chemical reactions and to separate isotopes [Ref. 3, 4], for nonlinear conversion of laser emission frequencies to the pioneering vacuum ultraviolet and soft x-ray bands of coherent radiation [Ref. 5-8]. Transitions between discrete levels and the continuum play an important part in solution of this class of problems. The basic theory of

nonlinear spectroscopy and nonlinear conversions of laser radiation with participation of transitions to the continuum has been developed to a much lesser extent than the theory of corresponding effects for the discrete spectrum.

This book is the first monograph that has been specially devoted to the principles of the theory of nonlinear resonances and nonlinear-optics transformations of radiation with the participation of transitions to the continuum. Considerable attention is devoted to the influence of strong resonant laser emission on the spectral characteristics of auto-ionization resonances in absorption, ionization and generation of sum frequencies by methods of nonlinear optics of gaseous media. Of considerable importance are the prospects that have been opened up for selective action on spectral characteristics of the continuum. The monograph describes possibilities for inducing nonlinear resonances similar to artificial auto-ionization levels in arbitrary sections of the continuous spectrum (continuum), as well as capabilities for continuous control of their characteristics. Uses are pointed out for these phenomena in optics and nonlinear spectroscopy of the vacuum ultraviolet and soft x-ray bands, for generating coherent radiation in these bands of the spectrum, for producing polarized electrons and for selective ionization of isotopes.

The authors are grateful to coworkers of the laboratory of coherent optics and the theoretical division of the Institute of Physics imeni L. V. Kirenskiy of the Siberian Department, USSR Academy of Sciences for constructive discussion of the material of the monograph.

REFERENCES

1. Letokhov, V. S., Chebotayev, V. P., "Printsipy nelineynoy lazernoy spektroskopii" [Principles of Nonlinear Laser Spectroscopy], Moscow, Nauka, 1975, 280 pp.

2. Rautian, S. G., Smirnov, G. I., Shalagin, A. M., "Nelineynyye rezonansy v spektrakh atomov i molekul" [Nonlinear Resonances in Spectra of Atoms and Molecules", Novosibirsk, Nauka, 1979, 312 pp.

3. Letokhov, V. S., "Selective Action of Laser Radiation on Matter", USPEKHI FIZICHESKIKH NAUK, Vol 125, No 1, 1978, pp 57-96.

4. Letokhov, V. S., Mur, S. B., "Lazernoye razdeleniye izotopov" [Laser Separation of Isotopes], KVANTOVAYA ELEKTRONIKA, Vol 3, No 2, 1976, pp 248-287; No 3, pp 485-545.

5. Sorokin, P. P., Wynne, J. J., Armstrong, J. A., Hodgson, R. T., "Resonantly Enhanced Nonlinear Generation of Tunable Coherent Vacuum Ultraviolet (VUV) Light in Atomic Vapors", Annals N. Y. Acad. Sci., Vol 267, 1976, pp 30-50.

6. Popov, A. K., "Resonant Nonlinear Optics of Gaseous Systems and Generation of XUV Radiation" in: "Primeneniye lazerov v atomnoy, molekulyarnoy i yadernoy fizike" [Using Lasers in Atomic, Molecular and Nuclear Physics], Moscow, Nauka, 1979, pp 131-147.

8. Reintjes, J., She, C. Y., Eckhardt, R. C., "Generation of Coherent Radiation in the XUV by Fifth- and Seventh-Order Frequency Conversion in Rare Gases", IEEE J. QUANT. ELECTRON., Vol QE-14, No 8, 1978, pp 581-596.

Contents page

6610
CSO: 1862/121

UDC 681.513.6

LOCAL DEFORMATIONS OF CONTINUOUS MIRRORS AND THEIR FREQUENCY DEPENDENCES

Leningrad OPTIKO-MEKHANICHESKAYA PROMYSHLENNOST' in Russian No 11, Nov 81 (manuscript received 13 Nov 80) pp 11-13

[Article by V. G. Taranenko, G. P. Koshelev and N. S. Romanyuk]

[Text] Of considerable interest at the present time in connection with the growth of adaptive optics is research and development of mirrors with controllable profile. Such mirrors, called active mirrors, enable improvement of the characteristics of large-scale astronomical systems [Ref. 1], and dynamic compensation for random phase distortions of the wave field [Ref. 2]. An adaptive mirror can be made in the form of a reflecting surface synthesized from individual segments, or as a continuous reflective plate whose surface acquires a predetermined shape under the action of special drives.

The main complication in controlling the surface shape of a continuous mirror is the necessity for taking consideration of mechanical interaction of adjacent points of the reflecting surface due to the finite rigidity of the reflective plate. This gives rise to the problem of studying the mechanical properties of a continuous active mirror.

This article gives the results of measurements of the principal characteristics of continuous mirrors over a wide band of controlling signal frequencies. A mirror 140 mm in diameter was made for the research, with seven piezoelectric drives controlling the position of surface points. Each drive was made in the form of a stack of piezoceramic disks. One drive was placed at the center, and the other six were situated at the vertices of a regular hexagon inscribed in a circle 70 mm in diameter. The entire structure was put together with epoxy cement. The experimental data are the results of studies of a series of mirrors of the described design with deformable plates of various thicknesses made of materials with different elastic properties: aluminum, copper and steel. The thickness of the deformable mirror surface was 3-12 mm. Local deformations were measured by an interferometric method. Selected as the measured parameters were the amplitude of deformation, i. e. displacement of the mirror surface under the action of the controlling voltage at the maximum point, the function of surface response to the action of the drive, and the frequency response curve.

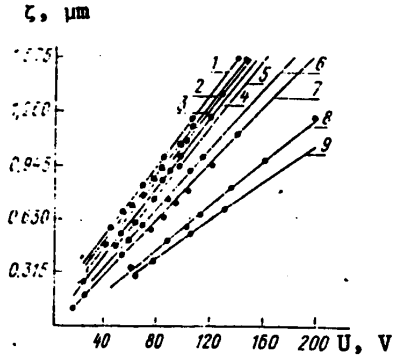

Fig. 1. Amplitude of reflective plate deformation as a function of controlling voltage: 1--displacement of piezodrive; 2, 3, 4 --deflection of reflective surface of plates 3 mm thick made of aluminum, copper and steel respectively; 5, 6, 8--same for plates 6 mm thick; 7, 9--for aluminum plates 9 and 12 mm thick respectively

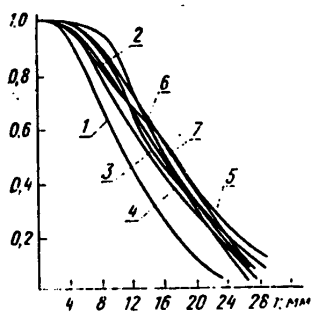

Fig. 2. Response function of active mirrors with drive 20 mm in diameter made of copper 3 mm thick (curve 1) and 6 mm thick (curve 2), of aluminum 6 mm thick (curve 3), 9 mm (curve 4) and 12 mm thick (curve 5), and of steel 3 mm (curve 6) and 6 mm thick (curve 7)

The experimental dependence of deformation amplitude as a function of controlling voltage with drive diameter of 20 mm is shown in Fig. 1. The mean square error of measurement was 1.026 μm. It can be seen that the amplitude of deformation is linearly dependent on the size of the controlling signal at voltages up to 200 V. The coefficient of proportionality in this case depends both on properties of the metal used and on the thickness of the reflective plate. Analysis of the results shows that within an error of no more than 10% the deformation amplitude can be expressed by the empirical formula

$$\zeta \approx k_0 U\left[1-\frac{10^{-7} Eh^2}{2(1-\sigma^2)}\right], \qquad (1)$$

where k_0 is the drive sensitivity in μm/V; U is the controlling voltage in V; E is Young's modulus in N/m^2; σ is the Poisson ratio of the material used; h is the thickness of the plate in m. Expression (1) implies that the amplitude of local deformation decreases linearly with increasing ratio D/h, where D is the bending stiffness of the plate. The formula enables selection of the stiffness and thickness of the plate during development of an active mirror, and evaluation of the amplitude of the phase shift at a predetermined drive sensitivity. Measurements were done in the frequency band of 0-1 kHz. The experimental data show absence of frequency dependence of deformation amplitude in this band.

Results of measurements of the response function are shown in Fig. 2. Distance r was reckoned from the center of the drive toward the center of the adjacent drive. The mean square error did not exceed 0.02. The curves are plotted for active mirrors with drive 30 mm in diameter. Mirrors of materials with relatively low Young's modulus (aluminum, copper) have a response function close to the Gauss function. In particular, for a copper plate 3 mm thick, the response function can be represented with accuracy of 5% by an expression of the form

$$f(r) = \exp\left(-\frac{r^2}{191}\right),$$

and for a 9-mm aluminum mirror with the same accuracy in the form

$$f(r) = \exp\left(-\frac{r^2}{304}\right).$$

The response function of an active steel mirror is approximated by the curve $\exp(-ar^{2 \cdot 5})$ or, according to the terminology of Ref. 2, a "supergaussian" curve. For example, when the plate thickness is 3 mm, the dependence

$$f(r) = \exp\left(-\frac{r^{2,5}}{1464}\right)$$

approximates the experimental results with accuracy of 5%.

The cemented molybdenum active mirror described in Ref. 2, despite its appreciable differences from mirrors of the investigated series, also had a "supergaussian" response function. Apparently, gaussian and "supergaussian" curves are typical of plate active mirrors with rigid securing of drives.

From the standpoint of controlling the surface, it is preferable to use an active mirror with narrow response function that precludes interaction of drives. The value of the response function on the edge of the adjacent drive will be called the engagement factor. The value of this factor correlates with the value of the response function at r equal to half the distance between centers of the drives. Analysis of Fig. 2 shows that the mutual correlation coefficient is 0.79.

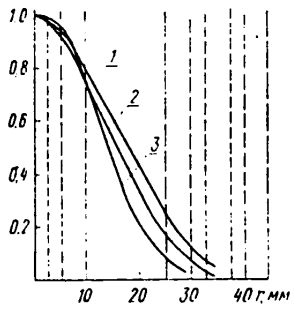

Fig. 3. Response function of aluminum mirror with reflective plate 3 mm thick for drive diameter of 5 mm (curve 1), 100 mm (curve 2) and 20 mm (curve 3); drive boundaries are indicated by the broken lines

Fig. 3 shows the response functions of mirrors with drives of different diameters. The measurements were made with an aluminum plate 3 mm thick. As a result of reduction in drive diameter, the distance to the edge of the adjacent drive increases, and the response function widens. As can be seen from the figure, there is actually no resultant change in the engagement factor.

The frequency properties of active mirrors were studied in the 0-12 kHz band. In this study, the amplitude of the controlling voltage sent to the piezodrive corresponded to low values of the deformation amplitude (~0-15 μm). During the investigation, resonances of the 3-mm copper mirror were observed on a frequency of 10.5 kHz, and of the steel mirror of the same thickness on a frequency of 11.2 kHz. The frequency response curve for these mirrors in the resonance region is shown in Fig. 4. Calculation of natural oscillations of a plate fastened at drive locations is a complicated problem. For a rough estimate of the resonant frequencies of a mirror, we can use the formula [Ref. 3]

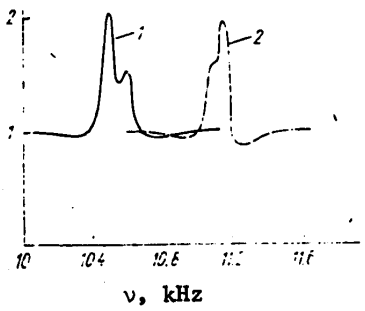

Fig. 4. Frequency response of active mirrors in the resonance region: 1--copper mirror; 2--steel mirror

$$\nu = \frac{10{,}21\,h}{2\pi R^2}\sqrt{\frac{E}{12\rho(1-\sigma^2)}}, \qquad (2)$$

derived for a circular plate secured around the edges. Here R is the distance to the edge of the adjacent drive; ρ is the density of the material. Calculated values of $\nu = 9.1$ kHz for a copper mirror, and $\nu = 11.5$ kHz for a steel mirror are close to the experimentally found values (Fig. 4).

The following conclusions can be drawn:

1. For controlling voltages reaching hundreds of volts applied to the piezodrive of an active mirror, the amplitude of mirror deformation is a linear function of the controlling signal.

2. The amplitude of deformation of an active mirror decreases linearly with increasing ratio of plate stiffness to its thickness, and may be approximately calculated from formula (1). For comparatively thin plates of soft metal (e. g. aluminum plates 3 mm thick), the deformation amplitude is practically no different from the amplitude of motion of the free drive, while for stiff plates (e. g. for aluminum 12 mm thick or for steel 6 mm thick) the deformation amplitude falls to about half.

3. The response function of active mirrors can be approximated by a gaussian curve (for "soft" metal) or by a "supergaussian" curve (for "stiff" metal).

4. An increase in the width of the response function at fixed drive diameter as a rule is accompanied by an increase in the engagement factor, the value for mirrors of the given series changing over limits of 0.01-0.2.

5. The width of the response function at a fixed distance L between centers of the drives increases with decreasing drive diameter, and may be approximately 0.3-0.4L on a level of e^{-2}, whereas the engagement factor practically does not change.

6. Deformation of an active mirror in the frequency range up to 1 kHz does not depend on the frequency of the controlling signal sent to the piezodrive.

7. Typical values of resonant mechanical frequencies of active mirrors in accordance with experiment are in a region above values of the order of 10 kHz, and may be approximately estimated by formula (2).

In conclusion, it should be noted that the investigated range of parameters of active mirrors covers typical values characteristic of systems for correcting atmospheric phase distortions, and for adaptive optical cavities of IR lasers, i. e. the given conclusions are valid for an extensive group of metallic active mirrors with piezodrive that realize dynamic phase front correction.

REFERENCES

1. Vanyushkin, Yu. A., Denisyuk, G. V., OPTIKO-MEKHANICHESKAYA PROMYSHLENNOST', No 1, 1975, p 55.

2. Pearson, J. E., Hansen, S., JOSA, Vol 67, No 3, 1977, p 325.

3. Filippov, A. P., "Kolebaniya deformiruyemykh sistem" [Oscillations of Deformable Systems], Moscow, Mashinostroyeniye, 1970.

6610
CSO: 1862/115

OPTOELECTRONICS

UDC 522.24

DETERMINING ANGULAR COORDINATES OF ASTRONOMICAL OBJECTS WHEN USING OPTOELECTRONIC MEASUREMENT SYSTEMS

Leningrad OPTIKO-MEKHANICHESKAYA PROMYSHLENNOST' in Russian No 12, Dec 81 (manuscript received 8 Oct 79) pp 1-3

[Article by B. N. Avsenin and Yu. A. Seliverstov]

[Text] Among known methods of determining angular coordinates of astronomical objects we can single out for example Turner's method based on statistical processing of data with $k \geqslant 3$ reference stars, and (orthogonal) methods of four constants using two reference stars and traditionally taken as approximate [Ref. 1, 2].

Optoelectronic systems with high penetrating capacity and comparatively narrow fields of view ($2\beta < 1°$) are being extensively used in astronomical practice [Ref. 3]. This situation enhances the topicality of methods for determining angular coordinates that minimize the number of reference (catalog) stars. Under these conditions, it makes sense to re-examine our attitude toward orthogonal methods that may be improved in accuracy by statistical processing at $k > 2$, especially if steps are taken to ensure equality of scales along the axes, and perpendicularity of axes of the system of measured coordinates. Differential effects have insignificant influence for narrow-field systems [Ref. 1, 4].

This paper suggests a method of determining angular coordinates of astronomical objects generalized to number of stars $k \geqslant 2$, and computing coordinates of the object by the method of least squares.

The relation between ideal and measured coordinates when using orthogonal methods can be expressed by the formulas [Ref. 1, 2]

$$\begin{aligned} \xi_l &= ax_l + by_l + c, \\ \eta_l &= -bx_l + ay_l + f. \end{aligned} \qquad l = 1, k,$$

where x, y are the measured coordinates, and ξ, η are the ideal coordinates of reference stars.

If these are rewritten in the form

$$v_{1,i} = x_{1,i}a_1 + x_{2,i}a_2 + 1a_3 + 0a_4 + \xi_{1,i},$$
$$v_{2,i} = x_{2,i}a_1 - x_{1,i}a_2 + 0a_3 + 1a_4 + \xi_{2,i}$$

or in matrix form

$$\vec{v} = X\vec{a} + \vec{\xi},$$

where X is the matrix composed by rwos

$$\vec{x}_{1,i}\{x_{1,i}, x_{2,i}, 1,0\} \text{ and } \vec{x}_{2,i}\{x_{2,i}, -x_{1,i}, 0,1\},$$

then the solution of the system of equations will be

$$Q = X'X,\ K = Q^{-1},\ \vec{L} = X'\vec{\xi},\ \vec{a} = -K\vec{L};$$

where $\vec{a}$ is the vector of estimates of frame constants; Q is the matrix of normal equations that takes the form

$$Q = \begin{vmatrix} [x_1^2] + [x_2^2] & 0 & [x_1] & [x_2] \\ 0 & [x_1^2] + [x_2^2] & [x_2] & -[x_1] \\ [x_1] & [x_2] & k & 0 \\ [x_2] & -[x_1] & 0 & k \end{vmatrix}.$$

Use of the cellular method of matrix inversion [Ref. 5] with consideration of symmetry and other characteristic peculiarities of matrix Q enabled us to find a successful form of transition from the measured coordinates to elements of the matrix K, bypassing stages of formation and transposition of matrix X, as well as formation and inversion of matrix Q. Leaving out intermediate transformations, we give the final form of matrix K:

$$K = Q^{-1} = (X'X)^{-1} =$$
$$= \frac{1}{W}\begin{vmatrix} k & 0 & -[x_1] & -[x_2] \\ 0 & k & -[x_2] & [x_1] \\ -[x_1] & -[x_2] & R & 0 \\ -[x_2] & [x_1] & 0 & R \end{vmatrix},$$

where $R = [x_1^2] + [x_2^2]$ $W = k \cdot R - [x_1]^2 - [x_2]^2$.

For elements of the vector of free terms of the normal equations we find

$$\vec{L} = X'\vec{\xi} = \begin{vmatrix} [x_1\xi_1] + [x_2\xi_2] \\ [x_2\xi_1] + [x_1\xi_2] \\ [\xi_1] \\ [\xi_2] \end{vmatrix}.$$

Then the ideal coordinates of the object to be determined are obtained from the expressions

$$\vec{a} = -K\vec{L},\ \xi_{1,ob} = \vec{x}_{1,ob}\vec{a},\ \xi_{2,ob} = \vec{x}_{2,ob}\vec{a},$$

while the equatorial coordinates of the object are calculated from known formulas [Ref. 1]

$$\alpha_{o6} = \operatorname{arctg}\left(\frac{\xi_{1,o6}}{\cos D - \xi_{2,o6}\sin D}\right) + A,$$
$$\delta_{o6} = \operatorname{arctg}\left[\frac{(\sin D + \xi_{2,o6}\cos D)\cos(\alpha_{o6} - A)}{\cos D - \xi_{2,o6}\sin D}\right],$$

where A, D are equatorial coordinates of the center of the frame.

The error of the resultant coordinates of the objects $\mathring{\Delta}_\alpha$, $\mathring{\Delta}_\delta$ is comprised of the error of reduction $\mathring{\Delta}_\xi$ and the error of measured coordinates of the object $\mathring{\Delta}_x$:

$$\mathring{\Delta}_\alpha = \mathring{\Delta}_{\xi_1} + M\mathring{\Delta}_{x_1} \text{ and } \mathring{\Delta}_\delta = \mathring{\Delta}_{\xi_2} + M\mathring{\Delta}_{x_2},$$

where the scale factor $M = \sqrt{a_1^2 + a_2^2}$ [Ref. 1]. The error of reduction in solving a system of 2k equations with four unknowns by the method of least squares is defined by the variance [Ref. 6]

$$\sigma^2\left(\mathring{\Delta}_{\xi_1}\right) = \frac{[v_1^2]}{2(k-2)}P_1,\ \sigma^2\left(\mathring{\Delta}_{\xi_2}\right) = \frac{[v_2^2]}{2(k-2)}P_2,$$

where the weighting factors P_1 and P_2 of functions $\xi_{1o6} = \vec{x}_{1,o6}\vec{a}$ and $\xi_{2,o6} = \vec{x}_{2,o6}\vec{a}$ of balanced elements $\tilde{a}$ are found from the formulas [Ref. 6]

$$P_1 = \sum\left(\frac{\partial\xi_{1,o6}}{\partial a_j}\right)^2 K_{jj} + 2\sum\left(\frac{\partial\xi_{1,o6}}{\partial a_i}\right)\left(\frac{\partial\xi_{1,o6}}{\partial a_j}\right)K_{ij};$$
$$P_2 = \sum\left(\frac{\partial\xi_{2,o6}}{\partial a_j}\right)^2 K_{jj} + 2\sum\left(\frac{\partial\xi_{2,o6}}{\partial a_i}\right)\left(\frac{\partial\xi_{2,o6}}{\partial a_j}\right)K_{ij}.$$

Considering that $\partial\xi_{o6}/\partial\vec{a} = \vec{x}_{o6}$, P_1 and P_2 can be represented as quadratic forms corresponding to vectors $\vec{x}_{1,o6}$ and $\vec{x}_{2,o6}$ and matrix K [Ref. 7]:

$$P_1 = \vec{x}'_{1,o6}K\vec{x}_{1,o6},\ P_2 = \vec{x}'_{2,o6}K\vec{x}_{2,o6}.$$

The final appearance of formulas for evaluating accuracy will be

$$\tilde{\sigma}\left(\mathring{\Delta}_\alpha\right) = \sqrt{\frac{[v_1^2]}{2(k-2)}P_1 + M^2\sigma^2\left(\mathring{\Delta}x_1\right)\cos D},$$
$$\tilde{\sigma}\left(\mathring{\Delta}_\delta\right) = \sqrt{\frac{[v_2^2]}{2(k-2)}P_2 + M^2\sigma^2\left(\mathring{\Delta}_{x_2}\right)}.$$

As an example, we give the results of processing of a frame with field of 1 x 1° and center coordinates $A = 3^h48^m$ and $D = 25°33'$. The coordinates of the reference stars and of the luminaries to be determined, for which catalog stars were selected, are given in Table 1, while the results of calculating the positions of the luminaries and their errors are given in Table 2.

TABLE 1

	Catalog coordinates		Measured coordinates	
	α_{1978}	δ_{1978}	X	Y
	Reference stars			
1	$3^h46^m52^s,185$	25°29'47,53"	+0,348600	—0,380834
2	3 47 18,312	25 25 45,32	+0,447351	—0,447187
3	3 48 07,167	25 15 30,74	+0,632701	—0,616310
4	3 48 56,665	25 51 00,28	+0,811030	—0,023124
5	3 49 00,524	25 11 33,74	+0,834426	—0,680108
6	3 50 01,147	25 14 33,27	+1,062296	—0,627544
7	3 50 22,263	25 29 41,52	+1,138440	—0,374332
8	3 50 28,828	25 47 17,06	+1,159164	—0,080873
9	3 50 31,247	25 34 57,50	+1,170311	—0,288126
10	3 50 33,505	35 32 08,69	+1,180155	—0,332873
	Luminaries being determined			
1	$3^h48^m20^s,683$	25°29'09,11"	+0,681437	—0,388567
2	3 48 44,296	25 42 13,09	+0,767959	—0,170005
3	3 49 42,531	25 29 39,29	+0,989073	—0,376844

TABLE 2

	α_{1978}	$\sigma(\Delta\alpha)$	δ_{1978}	$\sigma(\Delta\delta)$
	Proposed method			
1	$3^h48^m20^s,683$	$0^s,0008$	25°29'09,13"	0,010"
2	3 48 44,494	0,0008	25 42 13,03	0,011
3	3 49 42,529	0,0007	25 29 39,28	0,010
	Turner's method			
1	$3^h48^m20^s,683$	$0^s,0008$	25°29'09,13"	0,011"
2	3 48 44,295	0,0010	25 42 13,03	0,014
3	3 49 42,529	0,0007	25 29 39,28	0,010

The calculation time by the proposed method on the BESM-4 computer was about 0.1 s, and by the Turner method -- about 0.18 s. While the question of comparative efficacy of one method or the other might be a topic for independent study, we can assume a priori that the orthogonal method is more efficient for optoelectronic systems, if only because the probability that two stars will appear in the field of such systems is higher than for the appearance of three stars [Ref. 8].

REFERENCES

1. Bugoslavskaya, Ye. Ya., "Fotograficheskaya astrometriya" [Photographic Star Measurements], Moscow-Leningrad, Gostekhizdat, 1947.

2. Deych, A. N., ASTRONOMICHESKIY ZHURNAL, Vol 25, No 1, 1948, pp 44-58.

3. Abramenko, A. N. et al., "Televizionnaya astronomiya" [Television Astronomy], Moscow, Nauka, 1974.

4. Mozhzherin, V. M., IZVESTIYA KRYMSKOY ASTROFIZICHESKOY OBSERVATORII, Vol 1, 1974, pp 126-132.

5. Vergasov, V. A. et al., "Vychislitel'naya matematika" [Computer Mathematics], Moscow, Nedra, 1976.

6. Chebotarev, A. S., "Sposob naimen'shikh kvadratov s osnovami teorii veroyatnostey" [Method of Least Squares With Principles of Probability Theory], Moscow, Geodezizdat, 1958.

7. Bellman, R., "Vvedeniye v teoriyu matrits" [Introduction to Matrix Theory], Moscow, Nauka, 1976.

8. Seliverstov, Yu. A. et al., OPTIKO-MEKHANICHESKAYA PROMYSHLENNOST', No 3, 1980, p 10.

6610
CSO: 1862/116

NEW IMAGE CONVERTERS

Moscow PRIRODA in Russian No 2(798), Feb 82 pp 15-24

[Excerpts from article "New Class of Image Converters", by Doctor of Physical and Mathematical Sciences Igor' Nikolayevich Kompanets, senior science worker, Physics Institute imeni P. N. Lebedev, USSR Academy of Sciences]

[Excerpts] PROM and PRIZ

Another well known type of image converter that belongs in the class of space-time light modulators is the PROM, so called from the first letters of the words "Pockels-Readout Optical Modulator". In contrast to the photototitus, here the photosemiconductor and electro-optical properties have been combined in one crystal, necessitating design changes in the structure. Usually thin transparent dielectric layers are produced on both surfaces of the crystal plate (which has a thickness of the order of hundreds of micrometers), and transparent electrodes are sputtered on these layers. In this way, a metal-dielectric-semiconductor-dielectric-metal (MDSDM) structure is formed. As before, in this structure the intensity distribution in the input image is converted to spatial distribution of the photoproduced electron-hole pairs. As a result of the drift of electrons and holes in the external electric field, the carriers settle on the surface traps on interfaces with the dielectric, so that the space charge set up compensates the field on illuminated sections of the semiconductor crystal. As a result, the space-charge surface relief is converted to corresponding distribution of changes in the index of refraction of the crystal, modulating the light beam transmitted through the crystal with wavelength lying outside the region of photosensitivity of the semiconductor.

The high resistivity of the bismuth silicate and germanate crystals used in the PROM (of the order of 10^{13} $\Omega \cdot cm$) and the presence of dielectric films on the one hand enables charge accumulation whereby weak luminous fluxes can be registered, and on the other hand ensures slow relaxation of the space charge after exposure, i. e. image storage for prolonged periods (up to one hour in darkness). Erasure is by intense illumination of the structure with shorted electrodes. The minimum time of a modulation cycle, i. e. energizing, readout and erasure of the converted image, lies in the millisecond range.

TABLE

Characteristics of optically controllable space-time light modulators

Light modulation characteristics	Phototitus	PROM	PRIZ	Liquid crystal		
				with polycrystal CdS-ZnS	with single crystal $Bi_{12}SiO_{20}$	with single crystal Si
Region of sensitivity, μm	0.4-0.5	0.3-0.45	0.3-0.5	0.3-0.5	0.3-0.45	0.4-1.1
Sensitivity, J/cm^2	10^{-5}	10^{-4}	$5 \cdot 10^{-6}$	10^{-6}	$5 \cdot 10^{-7}$	10^{-9}
Optical contrast	100	1000	1000	100	100	100
Efficiency	0.8	0.8	0.01	0.8	0.8	0.8
Resolution, Lines/mm	6	6	70	350	250	8
Supply voltage, V	200	$7 \cdot 10^3$	10^3	30	100	100
Turn-on time, ms	0.03	1	1	0.1	0.1	0.1
Turn-off time, ms	1-2	1-2	1-2	1-2	1-2	1-2
Cycle time, ms	1	20	20	1-3	1-3	1-3
Storage time	1 hr (in darkness	1 hr (in darkness)	0.5 min (in darkness)	1 s	1 s	1 s
Erasure method	— — — — by light — — — —			— — by rf electric field — — —		

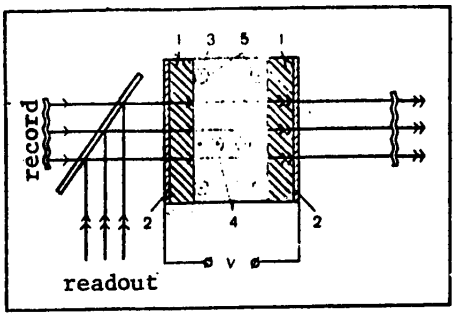

Diagram of PROM structure: 1--dielectric; 2--transparent electrodes; 3--photosemiconductive electro-optic crystal; 4--light-generated charge carriers; 5--charge carriers on traps

Other characteristics of converters of the PROM type are given in the Table. Also given there are the spatial light modulation parameters of a very successful Soviet modification of the PROM--the PRIZ [from the letters of the Russian words for image converter (PReobrazovatel' IZobrazheniy)]. This device differs in the direction of the optical axis in the semiconductor plate, and as a result it has greater sensitivity and spatial resolution.

Liquid Crystal Image Converters

Selection of the electro-optic effect in liquid crystals is determined by the specific problem to be solved by the image converters. For example, devices based on controllable birefringence enable modulation of both the phase and intensity of the light (when polaroids are used) in converted images. They are distinguished by the greatest sensitivity to input signal, but require greater care in manufacture, and feedback compensation for temperature drifts of the phase of the light. While devices based on other effects in liquid crystals enable for practical purposes only amplitude conversions of images, they are characterized by greater stability, the twist structure providing high optical contrast (greater than 100), and light-scattering cells providing a wider angular aperture of the modulated input flux (tens of degrees).

Liquid crystal image converters have the same working principles as the representatives of the class of space-time modulators that have already been considered--phototitus and PROM (PRIZ). Two converter arrangements are used that have their own design and other peculiarities associated with the presence of a liquid electro-optic medium and the chosen type of photosemiconductor. For example, both arrangements have glass substrates and spacers that determine the thickness of the liquid crystal layer (usually 1-30 μm). Contact of the liquid crystal with the electrode or photoconductor is often via a thin (about 10 nm) specially treated dielectric layer to ensure a certain orientation of the molecules in the layer. To maintain the temperature interval within which the liquid crystal state of the substance can exist (usually chosen in a range that includes room temperature), the devices may be thermostatically controlled, including by passing current through auxiliary transparent electrodes on the substrates.

In the liquid crystal image converter arrangement that is similar to the phototitus, high-resistivity polycrystalline or amorphous layers of cadmium sulfide, arsenic sulfide and other materials produced by sputtering to a thickness of a few μm are used as the photosemiconductor. Therefore the range of sensitivity of such converters lies in the blue-green or red region of the spectrum. The greatest percentage modulation at maximum efficiency approaching

100% is attained as soon as the energy of the exposing radiation has reached a value of the order of 10^{-6} J/cm^2. The resolution of an image converter with liquid layer thickness of the order of 1 μm and with low dielectric anisotropy exceeds 100 lines/mm. Time parameters are mainly determined by the properties of the liquid crystals used; a frame frequency close to the television standard of 25 Hz can be attained fairly simply.

Still higher paramters are realized in image converters which, like the PROM or PRIZ, use a single-crystal semiconductor plate, but with a liquid crystal layer as one of the dielectrics of the MDS structure. In this case, the semiconductor is only a few tens of μm thick.

In the MDS structure with liquid crystal, the photosensitive and electro-optic parts of the device are once more separate. Nevertheless, the working principle of the MDS structure with electro-optic data readout is not disturbed as a result. It retains the property of accumulating charge carriers formed during exposure (photoproduction) until they compensate the external field in the body of the semiconductor. As a result, the image is converted to a potential relief on the interface of the semiconductor with the dielectric. There is a voltage differential in both these layers, and in one of them (in the given case in the liquid crystal), an optical response is produced.

The sensitivity of the image converter to the exposing radiation depends on the parameters of the semiconductor (quantum yield, carrier concentration and so on), and the liquid crystal (on the type of electro-optic effect, the threshold voltage of reorientation of molecules, dielectric anisotropy), and it increases when the total resistivities of both layers are matched. In a structure based on gallium arsenide and a liquid crystal with positive dielectric anisotropy, a threshold sensitivity of 10^{-11}J/cm^2 with respect to energy and $5 \cdot 10^{-8}$ W/cm^2 when converted to radiation intensity is reached even in the red region of the spectrum. The maximum optical contrast that is realized upon reorientation of the liquid crystal molecules through a small angle corresponding to phase modulation of the light by π, exceeded 100:1. For a structure based on cadmium sulfide in the green region of the spectrum the sensitivity exceeded 100 GOST units (about 10^{-10} J/cm^2). Of importance is the fact that using different semiconductor crystals enables coverage of a spectral range of sensitivities of converters from the ultraviolet to the near infrared (see Table), some of the devices being quite wide-band, e. g. those based on silicon.

Another important advantage of the MDS structure with liquid crystal is the capability for attaining short times of turn-on and turn-off of the optical response of the order of 10^{-3}-10^{-4}. It is also possible to register light signals of duration 10^{-6} s or less with subsequent visualization with the response time of the liquid crystal. The resolution of such structures with high-resistivity semiconductor crystals reaches 300 lines/mm.

If we now compare the parameters of optically controllable space-time light modulators (laboratory prototypes) with those of the simpler but currently more widely used representatives of image converters--photographic film--

we can notice that spatial modulators of light with the same sensitivity band and resolution not only have the capability for operational data storage (in the range of seconds for liquid crystal converters, and minutes for the PROM and phototitus), but they also enable image conversion with a frame frequency of hundreds of hertz or more in the dynamic mode in the same (single) section of a stationary recording medium, with the implied additional functional capabilities. They can be used for visualizing ultraviolet and infrared images, for displaying information in the form of two-dimensional blocks of optical signals and images, for carrying out dynamic conversions of images (for example contrast inversion, color change, converting images from "incoherent" to "coherent" and the like), including television and aerospace photographic images, and for intensifying brightness and large-screen projection of signals and images.

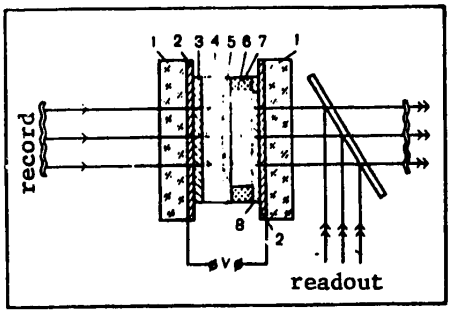

Diagram of image converter based on a photosensitive MDS structure with liquid crystal: 1--glass substrate; 2--transparent electrode; 3--dielectric layer; 4--semiconductor crystal; 5--dielectric mirror; 6--liquid crystal layer; 7--spacer; 8--orienting cover

Particular mention should be made of the capabilities for image handling with such converters in coherent-optics systems of analog information processing. Image converters are the principal functional components of the systems, since in addition to image input (including from CRT and image converter tube screens), they can perform some of the operations already mentioned above on the images, carry out spectral analysis and dynamic filtration (in particular outlining and the like) by an algorithm dictated by an external optical signal (image), add, subtract, compare and recognize images.

Space-time light modulators fit best with parallel processing of information in large blocks, i. e. in the form of images. The ease and high productivity with which conversions are made by converters of the given class is often striking (computers carry out conversions in series with respect to individual points of an image). For example, image adding is a consequence of simple parallel summation in the device of the spatial potential reliefs that arise from each image. Subtraction obviously requires the reverse action--in the phototitus and PROM it is done with shorted electrodes (after recording the first image), and in the liquid crystal structure it is handled by transmitting rf voltage that changes the conditions of molecule orientation and ensures forced relaxation. Comparison of input images with a standard, or in other words recognition is accomplished when the input image is passed through a hologram of the standard (including dynamic holograms registered by the converter)--in accordance with a correlation light signal in the output plane of the corresponding device. The intensity and position of the signal characterize the coordinates and the measure of closeness of the image to the standard, and when feedback is present, these parameters enable control of input images or automation of image processing.

Experimental models of the image converters are now being made, and organization of industrial production has begun. At the same time, intense developmental work is in progress on a variety of opto-electronic systems that use these converters. Thus it can be stated with confidence that the new class of image converters -- optically controlled spatial light modulators -- will take an important place in technology of the near future.

REFERENCES

1. Mustel', E. R., Parygin, V. N., "Metody modulyatsii i skanirovaniya sveta" [Light Modulating and Scanning Methods], Moscow, Nauka, 1970.

2. "Prostranstvennyye modulyatory sveta" [Spatial Light Modulators], Leningrad, Nauka, 1977.

3. Sonin, A. S., "Kentavry prirody" [Centaurs of Nature], Moscow, Atomizdat, 1980.

4. Blinov, L. M., "Elektro- i magnitooptika zhidkikh kristallov" [Electro- and Magneto-Optics of Liquid Crystals], Moscow, Nauka, 1978.

6610
CSO: 1862/118-A

UDC 535.2

DENSE PLASMA PARAMETERS, HIGH-PRESSURE AND INTENSE RADIATION PULSES THAT ARISE WHEN POWERFUL PROTON FLUXES INTERACT WITH OBSTACLES

Moscow DOKLADY AKADEMII NAUK SSSR in Russian Vol 261, No 6, Dec 81 (manuscript received 27 Apr 81) pp 1337-1339

[Article by A. V. Dobkin, T. B. Malyavina and I. V. Nemchinov, Institute of Physics of the Earth imeni O. Yu. Shmidt, USSR Academy of Sciences, Moscow]

[Text] As intense fluxes of radiation or fast particles vaporize the surface layers of a barrier material, they heat these layers to high temperatures and cause dispersal at high velocities. In this situation, high-pressure pulses arise on the barrier. This effect is currently attracting attention in connection with the problem of inertial nuclear fusion. However, it is also of interest for simulating explosions and impact of micrometeorites against an obstacle, acceleration of microscopic objects to high velocities, studying equations of state of matter under extreme conditions, as well as a number of other scientific and technological purposes (formation of holes and the like). In connection with the rapid development of powerful ion sources (see for example Ref. 1-5), we give the results of some calculations of the parameters of a dense plasma heated by intense ion fluxes, and also of the resultant high-pressure pulses upon the obstacle. These calculations supplement the estimates of Ref. 6-8 aimed at determining the feasibility of initiating fusion reactions. We will show that impact of an ion beam against an obstacle may also give rise to powerful pulses of intense radiation in the ultraviolet and x-ray bands emitted by hot plasma.

On the initial stage of the interaction process the thickness x of the plasma layer is small compared with beam radius R or radius of curvature of the obstacle r_0. Calculations were done on one-dimensional (plane) unsteady radiation-gasdynamic processes that occur when protons with energy of 0.1-10 MeV interact with an aluminum obstacle. The method of calculation is similar to that used previously in an analogous problem concerning the action of laser radiation [Ref. 9]. The calculations were done with detailed consideration of the spectral makeup of the radiation, and detailed tables of optical and thermodynamic properties of an aluminum plasma were used [Ref. 10]. To accelerate the calculations, a method of frequency-averaging radiation transport equations was used [Ref. 11] that was quite effective. In determining the law of release of proton energy in the material, consideration was taken of the interaction of protons with bound and free plasma electrons [Ref. 12].

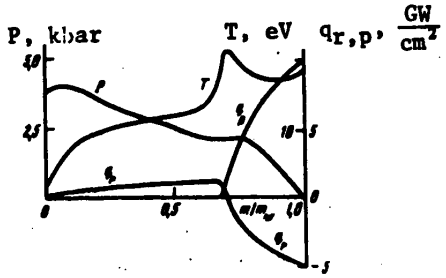

Fig. 1. Typical distribution of plasma parameters with respect to mass in the two-dimensional case

Fig. 1 shows the distribution of plasma parameters -- temperature T, pressure P, and also the flux densities of protons q_p and self-radiation of the plasma q_r with respect to the mass m of the vapor at time $t = 1$ μs (when the total vaporized mass $m_w = 4.8$ mg/cm^2) for the case where the energy of protons incident from the outside $\varepsilon_0 = 1$ MeV, and their energy flux density $q_0 = 10$ GW/cm^2. As can be seen, the protons penetrate to only $\frac{1}{3}$ of the mass, the remaining cool part of the mass being heated by radiation of the hot layer. In accordance with estimates of Ref. 13, the density of the radiation flux emitted into vacuum reaches 50% of the q_0.

After the quantity x becomes comparable with R or r_0, effects of lateral spreading of the vapor jet begin to have an influence, leading to increased transparency of their peripheral layers, and to penetration of the particles into deeper layers of the material. A quasi-steady mode of heating and vaporization arises that was considered for the case of laser radiation in Ref. 14 and 15. Analogous solution of the system of equations for steady-state radially symmetric flow from a spherical target of radius r_0 can be used to find the distribution of all parameters with respect to radius r. This distribution is shown in Fig. 2 for the case $q_0 = 11.5$ GW/cm^2, $\varepsilon_0 = 1$ MeV, $r_0 = 1$ cm, when $T_* = 15$ eV. All quantities (radius r, pressure P, velocity u, temperature T and proton energy ε) are normalized to their values in the "critical" cross section, where the Jouguet rule is met (these values are denoted by the asterisk). As can be seen, a narrow cool layer of dense vapor of the substance arises at the surface of the barrier, and far from the surface there is little change in temperature. The proton energy in the critical cross section ε_* is about half the value of ε_0. Pressure on the barrier $P_0 = 10.6$ kbar, and pressure in the critical cross section $P_* = 0.4P_0$. The same ratio between ε_* and ε_0, P_* and P_0 is observed for other variants as well. The distribution of parameters with respect to r is similar.

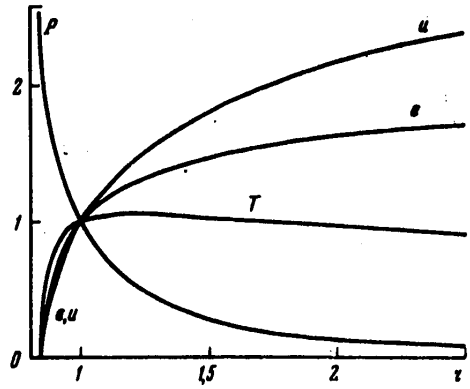

Fig. 2. Distribution of parameters with respect to radius of spherically symmetric steady-state plasma corona

Choice of the "combustion" rate in the quasi-steady state takes consideration of the fact that in the acoustic cross section a certain condition is satisfied between work performed during expansion of the dispersing gas and the energy release. In the given case, it can be written as

$$(1)\quad \frac{\varepsilon_*}{r_*} = \lambda\left(\frac{d\varepsilon}{dr}\right)_*$$

where the dimensionless constant λ is of the order of unity.

Results of systematic calculations of different variants of such a problem can be represented in the form of the following relations:

$$(2)\quad \begin{aligned} P_0 &= 2{,}3\, q_0^{0,6} r_0^{-0,4} \varepsilon_0^{0,75}, \\ T_* &= 5{,}6\, q_0^{0,4} r_0^{0,4} \varepsilon_0^{-0,6}, \end{aligned}$$

where the dimensionalities of the quantities are: P_0--kbar; q_0--GW/cm^2; r_0--cm; ε_0--MeV; T_*--eV.

Comparison of the resultant calculated temperatures and pressures with those for the case of a neodymium laser [Ref. 15] shows that at the same q_0 and radius $r_0 = 1$ cm they are similar if proton energy $\varepsilon_0 = 200$ keV. For protons with energy $\varepsilon_0 = 1$ MeV, the temperature is nearly an order of magnitude higher, and the pressure an order of magnitude lower than for a neodymium laser. Let us note that under the action of radiation of the contiuous spectrum of a high-temperature source, quasi-steady flow and heating of vapor may arise; the pressure in this case is somewhat higher than for protons with $\varepsilon_0 = 1$ MeV (for radius $r_0 = 1$ cm).

Calculations show that as temperature rises, such factors as electronic heat conduction may have an effect. For example, at $q_0 = 5 \cdot 10^4$ GW/cm^2, $\varepsilon_0 = 10$ MeV and $r_0 = 0.4$ cm, when $T_* = 100$ eV, energy fluxes due to electronic heat conduction are about 30% of the q_0, being of the same order of magnitude as energy losses to radiation from the plasma. The amount of pressure P_0 on the barrier reaches ~10 Mbar, and the density in the critical cross section is $\rho_* \approx 0.1$ g/cm^3.

Thus the action of an ion beam on an obstacle enables attainment of high densities of hot plasma and creation of high-pressure pulses on a barrier, as well as producing radiation pulses with a spectrum that extends up to the ultraviolet and soft x-ray region.

REFERENCES

1. Olson, K. D., FIZIKA PLAZMY, Vol. 3, No 3, 1977, p 465.

2. Greenspan, M. A., Hammer, D. A., Sudan, R. N., J. APPL. PHYS., Vol 50, No 5, 1979, p 3031.

3. Filippov, N. V., Filippova, T. I., PIS'MA V ZHURNAL EKSPERIMENTAL'NOY I TEORETICHESKOY FIZIKI, Vol 29, No 12, 1979, p 750.

4. Humphries, S., NUCLEAR FUSION, Vol 20, No 12, 1980, pp 1549-1612.

5. Gribov, V. A., Krokhin, O. N., "Kratkiye soobshcheniya po fizike" [Brief Reports on Physics], Moscow, Vol 6, 1980, p 45.

6. Winterberg, F., PLASMA PHYSICS, Vol 17, No 1, 1975, p 69.

7. Shearer, J. M., NUCLEAR FUSION, Vol 15, No 5, 1975, p 952.

8. Ivanov, B. I., Kalmykov, A. A., Lavrent'yev, O. A., PIS'MA V ZHURNAL TEKHNICHESKOY FIZIKI, Vol 2, No 3, 1976, p 129.

9. Bergel'son, V. I., Nemchinov, I. V., KVANTOVAYA ELEKTRONIKA, Vol 7, No 11, 1980, p 2356.

10. Buzdin, V. P., Dobkin, A. V., Kosarev, I. B., article deposited in All-Union Institute of Scientific and Technical Information, No 370-79 dep.

11. Nemchinov, I. V., PRIKLADNAYA MATEMATIKA I MEKHANIKA, Vol 34, No 4, 1970, p 706.

12. Gott, Yu. V., "Vzaimodeystviye chastits s veshchestvom v plazmennykh issledovaniyakh" [Particle Interaction With Matter in Plasma Research], Moscow, 1978.

13. Dobkin, A. V., Kosarev, I. B., Nemchinov, I. V., ZHURNAL TEKHNICHESKOY FIZIKI, Vol 49, No 7, 1979, p 1405.

14. Nemchinov, I. V., PRIKLADNAYA MATEMATIKA I MEKHANIKA, Vol 31, No 2, 1967, p 300.

15. Malyavina, T. B., Nemchinov, I. V., ZHURNAL PRIKLADNOY MEKHANIKI I TEKHNICHESKOY FIZIKI, No 5, 1972, p 58.

6610
CSO: 1862/96

END